

Granzyme B in Skin Aging, Injury and Repair

by

Paul Ryan Hiebert

B.Sc. (Hons.), Simon Fraser University (2007)

A THESIS SUBMITTED IN PARTIAL FULFILMENT OF THE
REQUIREMENTS FOR THE DEGREE OF
DOCTOR OF PHILOSOPHY

in

The Faculty of Graduate Studies

(Pathology and Laboratory Medicine)

THE UNIVERSITY OF BRITISH COLUMBIA

(Vancouver)

April 2013

© Paul Ryan Hiebert, 2013

Abstract

Granzyme B (GzmB) is a serine protease that can be released into the extracellular spaces by immune cells during chronic inflammation where it is capable of degrading several components of the extracellular matrix (ECM). Several chronic inflammatory skin diseases have demonstrated elevated levels of GzmB however the exact role of GzmB in the skin remains poorly understood. Apolipoprotein E (ApoE) is a protein highly expressed in the skin, where it can regulate inflammation through its anti-oxidative and anti-inflammatory properties. Mice deficient in ApoE develop an inflammatory skin phenotype when fed a high fat diet indicative of premature aging featuring ECM remodeling, hair graying, hair loss and frailty. I therefore hypothesized that GzmB contributes to skin aging, injury and impaired healing in ApoE knockout (ApoE-KO) mice through the degradation of ECM proteins. In the present dissertation, I identified the high fat diet-fed ApoE-KO mouse as a model that displays several characteristic features of skin aging including skin thinning and collagen disorganization. Further investigations also identified that high fat diet-fed ApoE-KO mice show defects in cutaneous wound healing such as delayed wound closure, reduced contraction and altered collagen content. These changes became worse with age and high fat diet. To test the role of GzmB in this process, GzmB/ApoE double knockout (DKO) mice were generated. These DKO mice were protected from skin thinning and collagen disorganization even when fed a high fat diet, suggesting that GzmB plays a role in ECM remodeling during aging of the skin in ApoE-KO mice. Further investigation revealed that GzmB-mediated degradation of the proteoglycan decorin is likely to be a key mechanism by which GzmB contributes to collagen disorganization and skin aging in ApoE-KO mice. Furthermore, DKO mice showed improved wound healing compared to ApoE-KO mice featuring faster wound closure, increased contraction and reduced fibronectin

degradation. *In vitro* cleavage assays revealed that fibronectin fragments generated by GzmB matched those identified in non-healing ApoE-KO mouse wounds. In summary, my findings suggest that extracellular GzmB contributes to skin aging and impaired healing in ApoE-KO mouse skin through the degradation of ECM components such as decorin and fibronectin.

Preface

Figures 1 and 2 and portions of text from chapter 1 were adapted from a published review article entitled, “Intracellular versus Extracellular Granzyme B in Immunity and Disease: Challenging the Dogma.” Boivin WA, Cooper DM, Hiebert PR and Granville DJ. *Lab Invest.* 2009 89(11): 1195-220. Figures 3, 4 and 5 and additional portions of text from chapter 1 are adapted from a published review article entitled, “Granzyme B in Injury, Inflammation and Repair.” Hiebert PR and Granville DJ. *Trends Mol Med.* 2012 18(12): 732-41.

Chapters 4 and 5 contain content published in a manuscript entitled, “Granzyme B Contributes to Skin Aging and Extracellular Matrix Degradation in Apolipoprotein E Knockout Mice.” Hiebert PR, Boivin WA, Abraham T, Pazooki S, Zhao H, Granville DJ. *Exp Gerontol.* 2011 46(6): 489-99. *In vitro* experiments demonstrating GzmB-mediated decorin cleavage were performed by Wendy Boivin. Experiments in chapter 7 involving the analysis of fibronectin by western blotting were performed by Dan Wu.

Table of Contents

Abstract.....	ii
Preface.....	iv
Table of Contents.....	v
List of Tables	viii
List of Figures.....	ix
List of Acronyms and Abbreviations.....	xii
Acknowledgements.....	xiv
1. Introduction.....	1
1.1 Granzymes.....	1
1.2 Granzyme B.....	1
1.3 Granzyme B in apoptosis	3
1.4 Extracellular granzyme B.....	7
1.5 Aging theories	10
1.5.1 Programmed theories	10
1.5.2 Stochastic theories	10
1.5.3 The molecular inflammation theory of aging	11
1.6 Anatomy of the skin	12
1.7 Functional and structural changes in aging skin	15
1.8 The extracellular matrix in skin	17
1.9 Extracellular granzyme B during age-related skin injury	19
1.10 Granzyme B in inflammation.....	23
1.11 Wound healing	25
1.11.1 Acute wound healing	25
1.11.2 Chronic wound healing.....	26
1.12 Potential consequences of granzyme B activity in chronic wound healing	27
1.13 Apolipoprotein E in aging and inflammation.....	36
1.14 Apolipoprotein E knockout mice	37
2. Rationale, hypothesis and aims.....	39
3. Materials and methods	42
3.1 Animals and diets.....	42
3.2 Wound healing surgical procedure.....	43
3.3 Tissue collection and processing.....	43

3.4	Contraction measurements	44
3.5	Histology and immunohistochemistry	45
3.6	Histological analysis and measurements	46
3.7	Multi-photon microscopy	46
3.8	Histological quantification of collagen	47
3.9	Skin homogenization and analysis of fibronectin fragments	48
3.10	Decorin cleavage assay	49
3.11	Mouse fibronectin cleavage assay	49
3.12	Statistical analyses.....	49
4.	Accelerated skin aging in high fat diet-fed apolipoprotein E knockout mice.....	50
4.1	Introduction	50
4.2	Results	52
4.2.1	Morbidity and skin pathology	52
4.2.2	Weight gain.....	55
4.2.3	Skin thickness	57
4.2.4	Collagen disorganization	60
4.2.5	Collagen and elastin abnormalities in diseased skin.....	64
4.3	Discussion	67
5.	Granzyme B contributes to skin aging and extracellular matrix remodeling in apolipoprotein E knockout mouse skin.....	70
5.1	Introduction	70
5.2	Results	72
5.2.1	Granzyme B deficiency reduces morbidity and weight loss.....	72
5.2.2	Granzyme B deficiency protects against skin thinning in apolipoprotein E knockout mice.....	75
5.2.3	Granzyme B deficiency increases skin collagen density in apolipoprotein E knockout mice.....	78
5.2.4	Decorin remodeling and granzyme B expression in the skin of apolipoprotein E knockout mice.....	80
5.2.5	Granzyme B localization and expression by mast cells.....	83
5.3	Discussion	85
6.	Impaired wound healing in apolipoprotein E knockout mice.....	88
6.1	Introduction	88
6.2	Results	90
6.2.1	Impaired wound closure in apolipoprotein E knockout mice fed a high fat diet.....	90

6.2.2 Age and a high fat diet delay contraction in apolipoprotein E knockout mice.....	93
6.2.3 Re-epithelialization.....	96
6.2.4 Inflammation following wounding in apolipoprotein E knockout mice.....	99
6.2.5 Collagen.....	103
6.3 Discussion.....	105
7. Granzyme B contributes to impaired wound healing in apolipoprotein E knockout mice.....	109
7.1 Introduction.....	109
7.2 Results.....	110
7.2.1 Granzyme B deficiency improves wound closure in apolipoprotein E knockout mice.....	110
7.2.2 Contraction and re-epithelialization.....	113
7.2.3 Extracellular matrix remodeling.....	116
7.2.4 Granzyme B-mediated fibronectin degradation in non-healing wounds.....	118
7.3 Discussion.....	124
8. Major findings, study limitations and future directions.....	127
8.1 Major findings.....	127
8.2 Study limitations.....	130
8.3 Future directions.....	133
9. Conclusions.....	136
Bibliography.....	138

List of Tables

Table 1. Age related changes in skin structure and function.....	16
Table 2. Extracellular granzyme B substrates and potential impact of substrate cleavage in a chronic wound.....	34
Table 3. Summary of xanthoma/skin pathology incidence.....	74
Table 4. Summary of age-related phenotypes displayed by all groups of mice at 30 weeks.....	129

List of Figures

Figure 1. Granzyme B in apoptosis.....	6
Figure 2. Potential consequences of extracellular granzyme B activity	9
Figure 3. Skin anatomy	14
Figure 4. Possible mechanisms of granzyme B-mediated injury and inflammation	22
Figure 5. Potential mechanisms of granzyme B-mediated damage during wound repair	32
Figure 6. Granzyme B activity in fibrosis and scarring	33
Figure 7. Increased morbidity in apolipoprotein E knockout mice fed a high fat diet	53
Figure 8. Representative images of wild type and apolipoprotein E knockout mice at the 30 week time point	53
Figure 9. Normal and diseased skin in apolipoprotein E knockout mice	54
Figure 10. Age-related weight gain in wild type versus apolipoprotein E knockout mice.....	56
Figure 11. Skin histology of wild type versus apolipoprotein E knockout mice at 30 weeks	58
Figure 12. Age-related change in skin thickness of wild type versus apolipoprotein E knockout mice.....	59
Figure 13. Reduced dermal collagen in apolipoprotein E knockout mice fed a high fat diet.....	62
Figure 14. Accelerated loss of dermal collagen density in apolipoprotein E knockout mice fed a high fat diet	63
Figure 15. Collagen remodelling in diseased skin from apolipoprotein E knockout mice.....	65
Figure 16. Abnormal elastin deposits in diseased skin from apolipoprotein E knockout mice....	66
Figure 17. Delayed morbidity in granzyme B deficient apolipoprotein E knockout mice fed a high fat diet	73

Figure 18. Weights of wild type, apolipoprotein E knockout and double knockout mice at 30 weeks.....	73
Figure 19. Granzyme B contributes to skin thinning in apolipoprotein E knockout mice	76
Figure 20. Analysis of skin layer thickness	77
Figure 21. Loss of dermal collagen density in apolipoprotein E knockout mice rescued by knocking out granzyme B.....	79
Figure 22. Granzyme B cleaves decorin <i>in vitro</i>	81
Figure 23. Granzyme B deficiency protects against loss of decorin in apolipoprotein E knockout mouse skin	82
Figure 24. Mast cells express granzyme B in apolipoprotein E knockout mouse skin	84
Figure 25. Potential consequences of granzyme B-mediated decorin degradation	87
Figure 26. Delayed wound closure in high fat diet-fed apolipoprotein E knockout mice	91
Figure 27. Wounded skin histology 16 days post-wounding.....	92
Figure 28. Delayed contraction in old apolipoprotein E knockout mice fed a high fat diet.....	95
Figure 29. Histological representations of re-epithelialization at 2, 8 and 16 days.....	97
Figure 30. Re-epithelialization distance at 2, 8 and 16 days	98
Figure 31. Inflammation in young wild type mouse skin at 2, 8 and 16 days post-wounding ...	101
Figure 32. Inflammation at Day 16 in wild type versus apolipoprotein E knockout mice	102
Figure 33. Collagen content at Day 16	104
Figure 34. Granzyme B deficiency improves wound healing in apolipoprotein E knockout mice	111
Figure 35. Granzyme B deficiency improves wound closure in apolipoprotein E knockout mice	112

Figure 36. Improved contraction in granzyme B deficient apolipoprotein E knockout mice.....	114
Figure 37. Re-epithelialization over 16 days in old mice fed a high fat diet.....	115
Figure 38. Collagen and decorin content at Day 16.....	117
Figure 39. Fibronectin content during wound healing.....	120
Figure 40. Mouse granzyme B cleaves mouse fibronectin.....	121
Figure 41. Fibronectin content at Day 16	122
Figure 42. Granzyme B expressing cells in a non-healed wound from an apolipoprotein E knockout mouse	123

List of Acronyms and Abbreviations

ANOVA: Analysis of variance

AP-1: activator protein-1

APAF-1: Apoptosis activating factor-1

ApoE: Apolipoprotein E

ApoE-KO: Apolipoprotein E knockout

Asp: Aspartate

ATF: AMP-responsive element-binding protein

Bak: Bcl-2 homologous antagonist/killer

Bax: Bcl-2 associated X protein

BHK cells: Baby hamster kidney cells

Bid: BH3 interacting-domain

Bim: B-cell lymphoma 2 interacting mediator of cell death

CAD: Caspase-3-activated DNase

Caspase: Cysteine-aspartic protease

CBF: Core-binding factor

CD: Cluster of differentiation

DAMPs: Damage-associated molecular patterns

DKO: Granzyme B/apolipoprotein E double knockout

DNA: Deoxyribonucleic acid

DTT: Dithiothreitol

ECM: Extracellular matrix

EDA: Extra domain A

FGFR1: Fibroblast growth factor receptor 1

GEM: Genetically engineered models

gtBid: Granzyme B-truncated Bid

Gzm: Granzyme

HCl: Hydrochloric acid

H&E: Hematoxylin and eosin

ICAD: Inhibitor of caspase-3-activated DNase

IGF-1: Insulin-like growth factor 1

IL: Interleukin

LPS: Lipopolysaccharide

MAPK: Mitogen activated protein kinase

Mcl-1: Myeloid cell leukemia sequence 1

MMP: Matrix metalloproteinase

mRNA: Messenger ribonucleic acid

NF- κ B: Nuclear factor κ B

NK cell: Natural killer cell

TBS: Tris buffered saline

RGD: Arginine-Glycine-Aspartate

SDS: Sodium dodecyl sulfate

SHG: Second harmonic generation

TGF: Transforming growth factor

Th1: T helper cell type 1

TLR: Toll-like receptor

TNF: Tumor necrosis factor

Treg: Regulatory T cells

UV: Ultraviolet

vWF: von Willebrand factor

WT: Wild type

Acknowledgements

I am very fortunate to have had such tremendous support and guidance throughout my degree. I would like to thank my supervisor, Dr. David Granville for his excellent mentorship, guidance and feedback over the years. Thank you also to all of the wonderful people I have had the pleasure of working with as part of the Granville Lab: Dr. Arwen Hunter and Rani Cruz for supervising my co-op term and undergraduate honours semester. Dr. Wendy Boivin, Lisa Ang and Dr. Ciara Chamberlain for welcoming me into the lab and for their help and guidance especially as I began my degree. To Alon Hendel, Dr. Dawn Cooper and Dr. Sarah Williams, all people I have very much enjoyed working with and have learned a lot from. Thank you also to the most recent Granville Lab members, Ivy Hsu and Dr. Leigh Parkinson for your help in brainstorming, insight into my project and general good times. I would also like to thank our lab manager, Hongyan Zhao for her help with countless techniques and experiments.

Thank you to all of my supervisory committee members: Dr. Gordon Francis, Dr. Bruce McManus, Dr. Darryl Knight and Dr. Chun Seow for all their help, guidance, ideas and interest in my degree. Thank you to the Natural Sciences and Engineering Council of Canada for supporting me in my degree and also to the CIHR Skin Research Training Centre and its members for their teaching, mentorship and financial support. A special thank you as well to the co-op and summer students I have been fortunate to work with over the years: Sara Pazooki, Megan Burns and Dan Wu. Thank you to the GEM animal facility and its staff for their help and assistance with animal models and training. Thank you also to Thomas Abraham for his expertise and training with the 2-photon experiments. Finally, I would like to thank my family,

my parents Don and Elli Hiebert, and my wonderful wife, Hayley, for their endless encouragement and support over the years and throughout my degree.

1. Introduction

1.1 Granzymes

Granzymes are a family of serine proteases with a wide range of intracellular and extracellular activities. First characterized in the 1980s, granzymes were found to be stored in the granules of CD8⁺ T cells and natural killer (NK) cells and secreted upon recognition of a target cell [1-6]. These granule-associated enzymes were then found to play a major role in programmed cell death (apoptosis) of virally infected cells through caspase-dependant and independent mechanisms [reviewed in 7, 8, 9]. Five granzymes exist in humans: granzyme A, B, H, K and M. While very little is known about granzymes H, K and M, granzyme A (GzmA) and granzyme B (GzmB) have been intensively studied. GzmA was originally thought to be cytotoxic, acting as an inducer of apoptosis in target cells, however recent studies suggest it may instead function primarily as a mediator of cytokine release, thereby serving to regulate inflammation [10]. GzmB, like GzmA, was once thought to function purely intracellularly to induce apoptosis, and while that remains an important function of GzmB, researchers are now beginning to discover a number of extracellular functions of this enzyme resulting from its capacity to cleave and degrade extracellular matrix (ECM) proteins and proteoglycans [11-13]. Because of this, granzymes are no longer considered to be just cytotoxic enzymes, but rather a family of proteases with many diverse and widespread activities both in and outside the cell.

1.2 Granzyme B

GzmB was one of the first granzymes to be discovered when Hatcher et al first isolated the cytotoxic protease from human lymphocytes in a report published in 1978 [14]. Also known

as cytotoxic T-lymphocyte-associated serine esterase 1 or granzyme 2, GzmB is a 32 kDa serine protease resembling chymotrypsin, and has homologues expressed in a number of different species. The gene product encoding GzmB is approximately 3,500 bp long, contains 5 exons and 4 introns, and maps to chromosome 14 on the human genome [15]. Similar to caspases, GzmB has a preference for cleaving peptides immediately adjacent to aspartate (Asp) residues [16, 17]. This specificity is due to the structure of the GzmB active site, which contains an arginine (Arg) residue positioned at the side of the active site pocket [18]. An interaction between an Asp residue at the P1 position of the substrate and the Arg residue within the active site is key for enzyme-substrate interaction [18].

Although once thought to be expressed exclusively by natural killer (NK) cells and CD8+ cytotoxic T cells, reports have shown that GzmB can be expressed by a variety of additional cell types. CD4+ T cells, B cells, mast cells, activated macrophages, neutrophils, basophils, dendritic cells and regulatory T cells (Tregs) have all been shown to express GzmB [19-28]. During certain pro-inflammatory conditions, there is even evidence of GzmB expression by non-immune cell types such as smooth muscle cells, chondrocytes, keratinocytes, type II pneumocytes, Sertoli cells, primary spermatocytes, granulosa cells, and syncytial trophoblasts [19-22, 24, 29-34].

Cells regulate GzmB expression and secretion through a number of different mechanisms. GzmB transcripts are constitutively expressed in most lymphocytes and upon activation can increase expression even further. This is regulated by a number of different transcription factors including AMP-responsive element-binding protein (ATF/CREB), activator protein-1 (AP-1), Ikaros and core-binding factor (CBF/PEBP2) [35-38]. GzmB expression is also induced in keratinocytes stimulated with ultraviolet (UV) radiation. UVA was shown to trigger release of migration inhibitory factor in human keratinocytes, stimulating GzmB expression

through a p38 MAPK transcriptional mechanism [39]. Treatment with UVB stimulated keratinocytes to express GzmB through a signaling pathway involving the epidermal growth factor receptor and mitogen activated protein kinase [33]. Both UVA and UVB-mediated GzmB expression pathways were also shown to be redox dependant. Translational regulation of GzmB is also observed in many cell types upon activation where protein levels increase without a noticeable difference in mRNA levels [20, 27, 40]. The specific mechanisms of GzmB regulation at the translational level however are not well known.

Following protein translation, GzmB is trafficked to the cytolytic granules within the cell and stored until it is exocytosed [41]. Once inside the granules, the full length GzmB protein (a zymogen) requires the removal of an N-terminal peptide (Gly-Glu) by the action of converting enzymes such as cathepsin C for it to become active [42]. Although GzmB is cleaved into its active form once it is inside the lytic granules, GzmB activity is suppressed until exocytosis and release during the immunological synapse. This is due to the acidic pH of the granules as well as the storage of GzmB on a proteoglycan scaffold within the granules made up of serglycin [43]. The intracellular GzmB inhibitor, protease inhibitor-9, also prevents GzmB from becoming active inside the cytoplasm prior to exocytosis, protecting the effector cell from accidental GzmB-mediated cytotoxicity [44, 45].

1.3 Granzyme B in apoptosis

Before GzmB can induce apoptosis, it must gain access to the cytoplasm of the target cell. Once inside the cell, it can begin cleaving multiple known substrates initiating the apoptotic cascade. GzmB can only gain access to the cytoplasm with the assistance of perforin, a membrane-disrupting protein also expressed by many GzmB-expressing cells and released along

with GzmB during the immunological synapse. While details regarding perforin-mediated GzmB entry into cells are still under debate, it is generally accepted that GzmB and perforin are endocytosed by the target cells while GzmB entry into the cytoplasm is achieved by endosomal membrane disruption by perforin. Once inside the cell, active GzmB can induce apoptosis by cleaving a number of different substrates belonging to multiple signaling pathways, leading to programmed cell death [reviewed in 9].

A major group of intracellular GzmB substrates are the caspases. Several lines of evidence suggest that GzmB can cleave and activate many different caspases including caspase-2, 3, 6, 7, 8 and 10 [46-48]. Pro-caspase cleavage and activation by GzmB leads to further cleavage of downstream targets ultimately resulting in nuclear DNA fragmentation and apoptosis. Another important substrate of GzmB is the protein Bid [49]. GzmB-mediated Bid cleavage results in the formation of the truncated gtBid, which travels to the mitochondria and interacts with Bax and Bak, resulting in disruption of mitochondrial membrane integrity [50, 51]. This results in the release of cytochrome c from the mitochondria and promotes the formation of the apoptosome, which activates caspase-9 and further downstream caspases leading to nuclear DNA fragmentation and cell death [52, 53]. GzmB can also cleave anti-apoptotic proteins like Mcl-1, rendering them inactive and further promoting apoptotic signaling pathways [54].

Although there are no records of any individuals with GzmB deficiency, several reports have documented the presence of a triple-mutated GzmB allele in humans in which Q⁴⁸P⁸⁸Y²⁴⁵ is mutated to R⁴⁸A⁸⁸H²⁴⁵ [55]. Conflicting reports exist as to the effect of this mutation on the ability of GzmB to induce apoptosis [55, 56]. More recent studies have identified GzmB polymorphisms that are associated with diseases such as breast cancer [57]. Polymorphisms in the GzmB gene have also been implicated in heart and bone marrow transplants [58, 59]. Unlike

GzmB, perforin deficient individuals do exist and suffer from a disease called familial hemophagocytic lymphohistiocytosis [60]. These patients suffer from out of control macrophage and T cell activation leading to excessive pro-inflammatory cytokine production and hypercytokinemia, suggesting perforin also has additional roles in regulating the immune response [61].

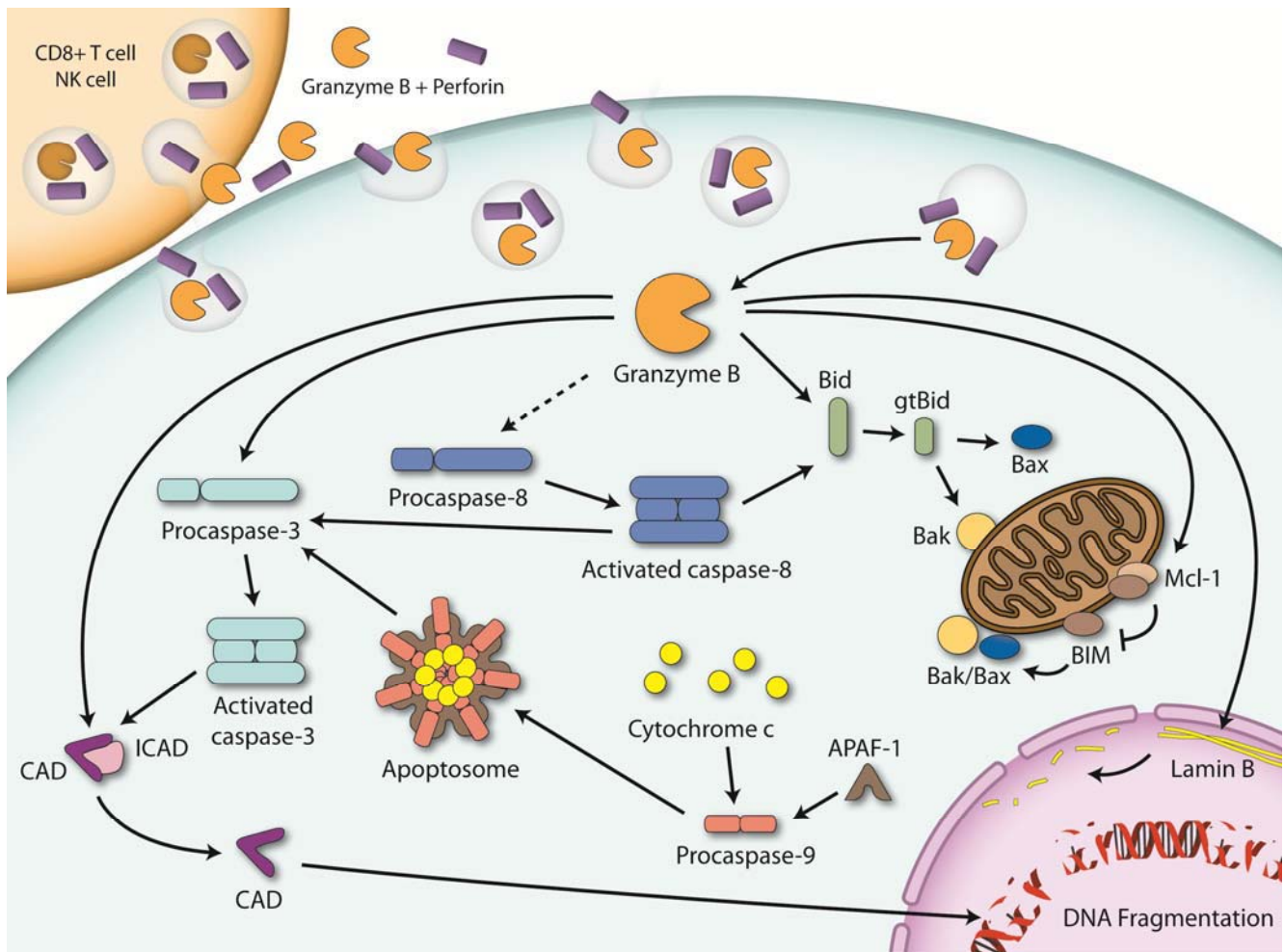


Figure 1. Granzyme B in apoptosis. Granzyme B (GzmB) internalization is facilitated by perforin. Upon internalization, GzmB initiates apoptosis primarily through the cleavage of Bid into a truncated form (gtBid) that triggers mitochondrial cytochrome c release and apoptosome formation leading to caspase activation and manifestation of the apoptosis phenotype. GzmB can also bypass the mitochondrial pathway and initiate caspase activation directly and/or cleave caspase substrates such as the inhibitor of caspase activated deoxyribonuclease (ICAD) thereby allowing CAD to translocate to the nucleus to fragment DNA. GzmB also cleaves the nuclear membrane protein lamin B, resulting in a loss of integrity of the nuclear membrane.

1.4 Extracellular granzyme B

It is now known that a proportion of GzmB can escape from the immunological synapse into the extracellular spaces even in the presence of perforin and in situations where perforin is absent or not expressed, act entirely outside the cell to cleave extracellular substrates [62]. GzmB is therefore capable not only of initiating apoptosis via intracellular mechanisms, but can perform a number of non-cytotoxic actions extracellularly by cleaving different substrates including ECM proteins and proteoglycans [11, 12, 63-65]. Recent reports have also demonstrated the ability of GzmB to process and activate pro-inflammatory cytokines such as IL-18 and IL-1 α .

Several extracellular GzmB substrates have been identified including ECM proteins, proteoglycans, cell surface receptors and cytokines [reviewed in 9]. Fibronectin, vitronectin, laminin and fibrillin-1 are all important ECM proteins critical for structural and functional integrity in tissues and are susceptible to GzmB-mediated degradation [12, 13]. Many extracellular proteoglycans have also been identified as GzmB substrates such as decorin, aggrecan, betaglycan and biglycan [11, 64, 66]. In addition to different ECM components, GzmB has been shown to cleave extracellular domains of certain cell receptors including Notch1, FGFR1, acetylcholine receptor, and neuronal glutamate receptor [67-69].

Recent reports have also uncovered roles for extracellular GzmB in cytokine processing and activation. To date, IL-18 and IL-1 α have been shown to be processed and activated by GzmB through either intracellular and/or extracellular mechanisms [70, 71]. GzmB may also act exclusively in a perforin-independent, extracellular manner in certain diseases such as abdominal aortic aneurysm [13, 72]. Using a mouse model of abdominal aortic aneurysm, it was found that

GzmB-mediated degradation of fibrillin-1 and decorin were likely key mechanisms by which aortic destabilization and aneurysm rupture and dissection occurred.

Extracellular GzmB activity therefore can potentially have a number of potential consequences during chronic inflammatory disease. As outlined in Figure 2, GzmB-mediated degradation and processing of extracellular substrates can lead to cell death by anoikis, have implications for cell migration, signaling, clotting and cytokine processing. ECM fragments themselves have also been shown to be active in recruiting inflammation and signaling through cell receptors (eg. fibronectin), although GzmB-generated fragments have not yet been investigated in this regard. Overall, one or more of these extracellular actions of GzmB could lead to tissue damage and/or a loss of structural integrity and in the context of chronic inflammation, play a major role in disease pathogenesis.

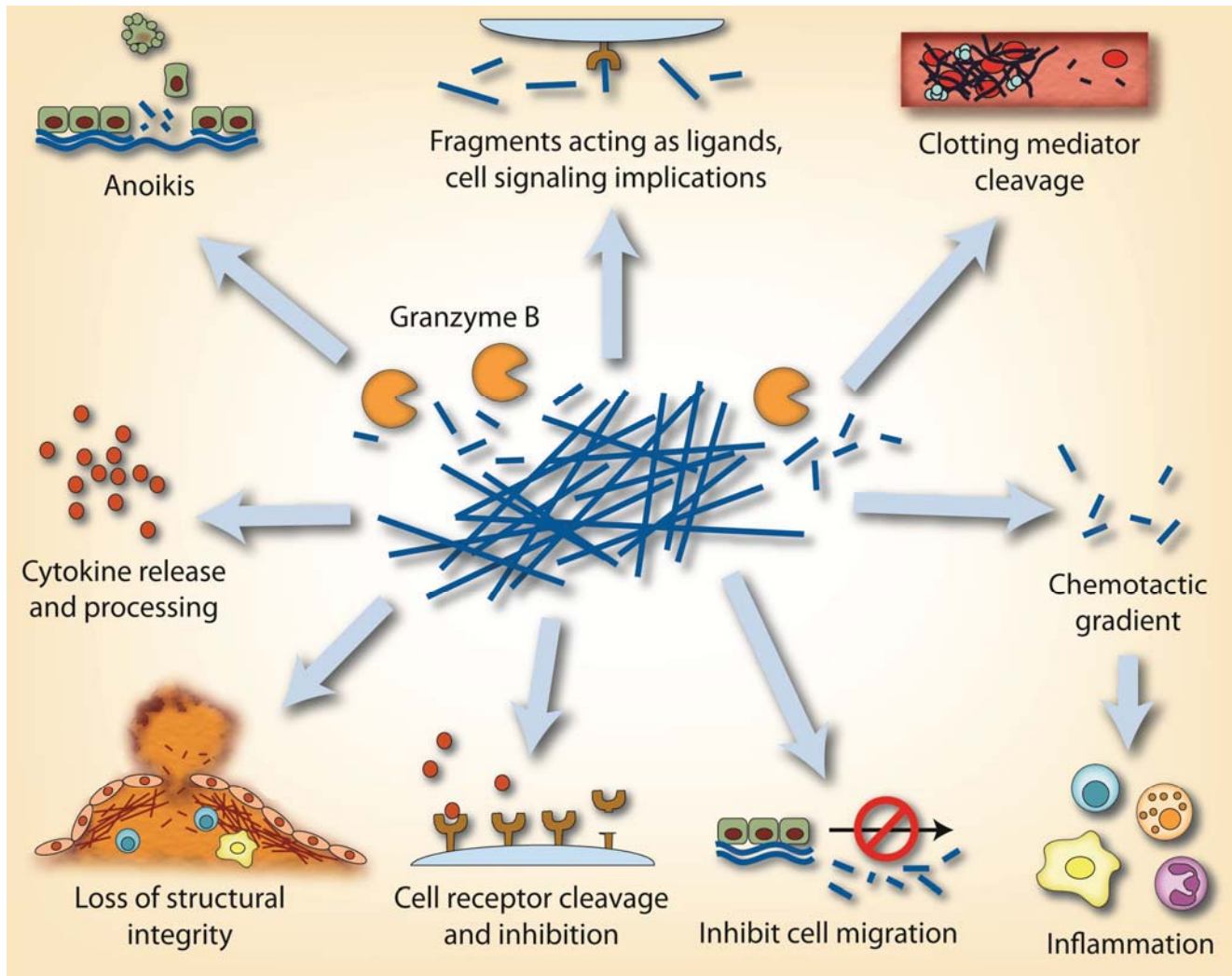


Figure 2. Potential consequences of extracellular granzyme B activity. During a number of chronic inflammatory conditions, Granzyme B (GzmB) accumulates extracellularly in the tissues, blood stream and other bodily fluids. GzmB retains its activity in the blood suggesting that, unlike MMPs and cathepsins, extracellular mediators of GzmB activity may be limited. GzmB can cleave proteins involved in structural integrity and wound healing such as fibronectin. GzmB can also cleave proteins related to clotting (fibrinogen, vWf, plasminogen). GzmB can induce detachment-mediated cell death (anoikis) via the cleavage of ECM. Although yet to be shown for GzmB, MMP-mediated fragments of fibronectin and elastin exhibit chemotactic properties and may enhance the immune response in atherosclerosis. Fragments may also exhibit bioactive properties and may be able to release cytokines from the matrix. GzmB may also play a role in the cleavage of cell surface receptors as seen with Notch1 and FGFR1 [9].

1.5 Aging theories

1.5.1 Programmed theories

Efforts to explain the biology of aging has traditionally been divided into two classes of theories: programmed theories and stochastic (or non-programmed) theories. Programmed theories reflect the view that our genes are what drives the aging process and that age-related changes occur because of a programmed, evolutionarily beneficial mechanism. August Weissman was among the first to propose that aging was an evolutionarily advantageous trait, suggesting that the removal of aged and unfit individuals was beneficial to the society as a whole [73]. This theory however was eventually rejected by Weissman himself due to a lack of an evolutionary mechanism to explain how these mutations would arise. In 1952, Peter Medawar published a new theory in a paper entitled, "An Unsolved Problem of Biology" and pointed out that during evolution individuals rarely survived long enough to have natural selection act on attributes that arise only late in life [74]. His newly proposed theory was called mutation accumulation and stated that only over multiple generations could negative mutations accumulate and cause detrimental "aging" effects to any individual who was somehow able to bypass common mortality causes like predation or infection, and live to old age.

1.5.2 Stochastic theories

The stochastic theories can be generalized as "wear and tear" theories that explain aging as the natural consequence of damage to the body as a function of time, resulting in cell damage, vulnerability to disease and ultimately death. Several researchers today believe that biological aging is not programmed, but rather the consequence of wear and tear and molecular fidelity. Leonard Hayflick, citing Medawar's original work, describes aging as "no longer an unsolved

problem", stating that random events contributing to general wear and tear is the main explanation for why we age [75]. Each individual stochastic theory of aging is not necessarily exclusive, but rather tends to provide overlapping explanations and mechanisms by which aging occurs. Among those theories often cited are the somatic mutation theory, telomere shortening, mitochondrial theory, waste accumulation and others [reviewed in 76]. One of the most well known theories was proposed in 1956 by Denham Harman as the free radical theory of aging [77]. The free radical theory describes an increase in the accumulation of reactive oxygen species with age as a byproduct of cellular metabolism. This gradual increase in reactive species results in an accumulation of oxidative stress, leading to tissue damage and functional decline over time. More recently, the molecular inflammation theory of aging was proposed [reviewed in 78], stating that unresolved, chronic inflammation represents the major mechanism underlying aging and age-related pathologies.

1.5.3 The molecular inflammation theory of aging

The molecular inflammation theory of aging was first coined over a decade ago as the underlying mechanism behind aging and age-related diseases [79]. Several lines of evidence suggests that pro-inflammatory mediators and cytokines increase in our bodies over time, leading to persistent, chronic inflammation causing tissue damage and age-related diseases [reviewed in 78]. Based on the initial observation that reactive oxygen species accumulate over time with age, subsequent redox-dependant upregulation of factors such as NF- κ B, IL-6, IL-1 β and TNF- α can serve to promote chronic inflammation. Persistent, low-grade inflammation can be detrimental to the structural integrity of tissues, resulting in tissue damage, functional decline and ultimately aging and age-related diseases. Examples of this are found in several age-related diseases

[reviewed in 78] including lesion formation and rupture in atherosclerosis [80] and localized damage to the brain in Alzheimer's disease [81].

The immune system itself also undergoes age-related changes over time. Our immune system becomes dysfunctional as we age, featuring changes in both the innate and adaptive branches of immunity [82, 83]. For example, an age-related decrease in the total number of circulating B and T lymphocytes is accompanied by an increase in the number of activated T lymphocytes with increased effector activity [84]. With this comes a reduction in the ability to fight new infections, and an increased risk of chronic inflammatory disease. This phenomenon, often referred to as "inflammaging", has implications for GzmB in the aging process, as several reports have demonstrated increased GzmB expression among activated immune cells, particularly during chronic inflammation [reviewed in 9]. The potential for excessive GzmB activity to contribute to tissue damage through both cell death and ECM degradation make GzmB an interesting candidate as an important mediator of age-related functional decline and disease.

1.6 Anatomy of the skin

The skin is the largest organ in the body. The skin not only provides a protective mechanical barrier to the outside world but also serves to regulate body temperature and acts as an important sensory organ. Human skin contains different layers and a number of anatomical structures that contribute to its proper function (Figure 3A). The outermost layer of the skin is called the epidermis and contains epidermal skin cells (keratinocytes). At the surface of the epidermis lies the stratum corneum, which is made up of flat, dead keratinocyte cells that

eventually fall off and are replaced. New keratinocytes originate at the basal layer of the epidermis where cells are capable of dividing and forming new cells. These newly formed keratinocytes gradually move upward becoming squamous cells and eventually develop into part of the stratum corneum, replacing previously shed cells. Other cells such as melanocytes and Langerhans' cells also occupy the epidermis however keratinocytes are the dominant cell type [85].

Below the epidermis lies the dermis which is composed primarily of collagen and other ECM. Other structures such as hair follicles, sebaceous glands, sweat glands, blood vessels and nerves can be found in the dermis as well. The junction between the dermis and the epidermis is composed of important ECM components including collagen IV, laminin and fibronectin that are important for anchoring the 2 skin layers to one another. The epidermal and dermal layers in healthy skin often contain epidermal invaginations into the dermis called rete ridges that serve to increase surface area of the dermal-epidermal junction. Subcutaneous fat underlies the dermis (also called the hypodermis or panniculus adiposus) and helps regulate body temperature while home to additional blood vessels and nerves.

Some differences exist between human and mouse skin. Unlike humans, mice have an additional layer below the hypodermis made up of striated muscle called the panniculus carnosus (Figure 3B). As shown in Figure 3B, mouse skin in also features a thin epidermis without obvious rete ridges.

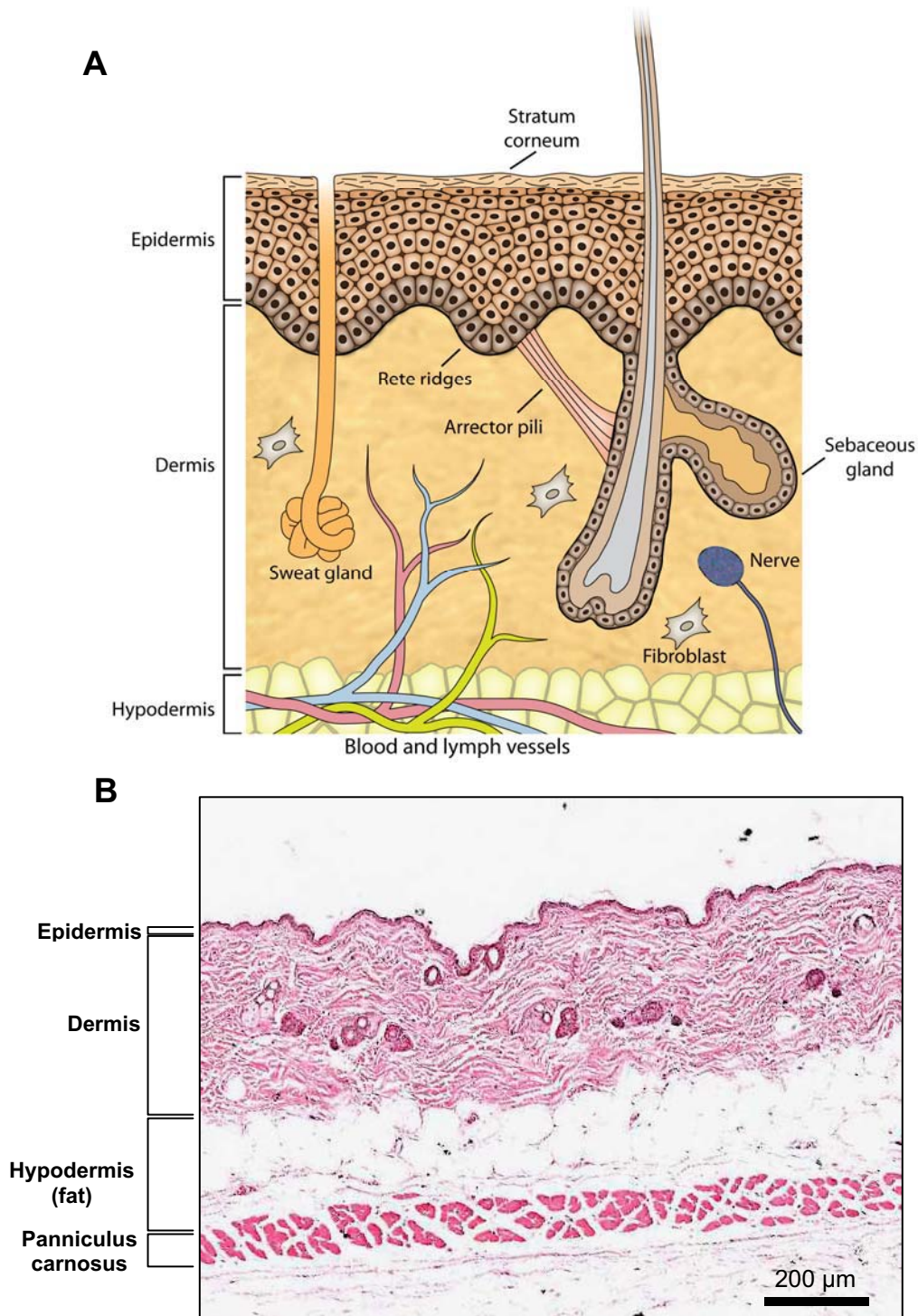


Figure 3. Skin anatomy. (A) Cartoon of basic human skin anatomy, comprised of 3 main layers: epidermis, dermis and hypodermis. The epidermis is comprised mainly of keratinocytes that divide in the basal layer and gradually move upward, becoming squamous and eventually flat dead cells forming the stratum corneum. Rete ridges increase the surface area between the epidermis and dermis facilitating strong adhesion and nutrient exchange. The dermis is comprised mainly of collagen and contains hair follicles associated with sebaceous glands and the arrector pili muscle responsible for erecting the hair during cold temperatures. Fibroblasts, nerves, sweat glands, lymph and blood vessels also reside in the dermis. The hypodermis contains adipocytes, vessels and nerves as well. (B) Mouse skin cross-section stained with hematoxylin and eosin showing a thin epidermis with no obvious rete ridges and the panniculus carnosus muscle layer below the hypodermis.

1.7 Functional and structural changes in aging skin

Several characteristics of skin make it a suitable model for studying aging. As previously suggested [86], the well studied cell-cell and cell-matrix interactions, as well as the accessibility of the skin make it an ideal model organ for aging research. Aging skin undergoes a number of structural and functional changes in humans. Typically, these changes are described as the result of either intrinsic or extrinsic aging mechanisms. Intrinsic, or chronological aging, refers to the random, wear and tear changes that take place in skin as a result of time while extrinsic aging refers to age-related changes/damage caused by environmental factors such as cigarette smoking, poor diet and UV radiation. Because UV radiation is often the greatest contributor to this process, extrinsic aging is often used synonymously with photoaging, a term used to describe the effect of chronic exposure of the skin to UV radiation.

Intrinsic aging of the skin is evident in sun-protected areas in the elderly. Hallmarks of intrinsically aged skin include skin thinning (featuring a flattening of the rete ridges), collagen disorganization and a loss of tensile strength. Studies have shown reduced collagen synthesis and increased proteolytic activity with age in sun-protected skin [87]. Photoaging on the other hand, can result in skin thickening (including increased collagen synthesis), abnormal collagen and elastin deposition and organization as well as increased inflammation and protease activation [87, 88]. Exposure to sunlight has also been suggested to play a role in the onset of age-related skin diseases such as melanoma skin cancer [89] or benign lesions such as seborrheic keratosis [90]. These functional and structural changes that accompany aging skin can present major health challenges for the elderly. Increased susceptibility to injury, chronic inflammation and impaired wound healing often result. Skin thinning, collagen disorganization and the loss of tensile strength can dramatically increase susceptibility to skin tearing and chronic skin ulcers.

Table 1 summarizes the age-related changes in the skin during intrinsic and extrinsic aging and their impact on chronic wound healing.

Table 1. Age related changes in skin structure and function.

	Intrinsic aging	Extrinsic aging	Wound healing
Structural changes	<ul style="list-style-type: none"> skin becomes thinner disorganized collagen flattening of rete ridges reduced melanocytes reduced fibroblasts reduced sebaceous glands redistribution of subcutaneous fat 	<ul style="list-style-type: none"> skin thickening disorganized collagen abnormal elastin deposits course wrinkles 	<ul style="list-style-type: none"> susceptible to chronic ulcer formation can have reduced scarring
Functional changes	<ul style="list-style-type: none"> loss of tensile strength susceptibility to injury loss of elasticity reduced nutrient exchange less moisture reduced microvasculature 	<ul style="list-style-type: none"> hyperproliferating keratinocytes skin stiffening 	<ul style="list-style-type: none"> reduced wound strength healing time is longer reduced angiogenesis
Immune system changes	<ul style="list-style-type: none"> loss of Langerhans cells decreased number of properly functioning lymphocytes thymus involution smaller lymphocyte repertoire increased effector cells increased pro-inflammatory cytokines (IL-1β, IL-6, TNF-α) increased NF-κB activity 	<ul style="list-style-type: none"> General increase in innate immunity, with suppression of adaptive immunity 	<ul style="list-style-type: none"> impaired neutrophil function impaired macrophage function reduced macrophage phagocytosis increased proteases

1.8 The extracellular matrix in skin

Collagen is the most abundant protein in the skin, making up the majority of the matrix-rich dermal layer. Collagen functions to provide an important physical scaffold and framework critical for maintaining structural integrity, tensile strength and proper elasticity. Collagen provides the backbone of the ECM component of skin offering a structure for cells and additional ECM proteins and proteoglycans to bind to. In normal adult skin, collagen content is made up primarily of collagen type I and III (approximately 85% and 15%, respectively) [87]. Several cells including keratinocytes and fibroblasts interact with and signal either directly or indirectly through collagen interactions. Additionally, several other ECM components interact with collagen to influence its organization and structure, helping to form the final, mature fiber. Aging of the skin is associated with increased collagen-degrading proteases and reduced collagen synthesis resulting in an alteration of collagen structure and function resulting in skin thinning and reduced tensile strength [87, 91].

Fibronectin is an abundant glycoprotein that can be found in the circulation (plasma fibronectin) as well as in tissues (cellular fibronectin). Plasma fibronectin is produced by hepatocytes and, due to alternative splicing, contains some sequence/structural differences compared to cellular fibronectin, which is produced by multiple cell types including fibroblasts [92]. Fibronectin makes up an important component of the basal lamina that lines the junction between the dermis and the epidermis. Structural and functional integrity of the basal lamina is crucial for maintaining proper nutrient exchange between the two skin layers, and for protecting the skin from mechanical trauma. Damage to this basement membrane can increase susceptibility of skin tearing and the separation of the epidermis from the dermis during injury. Fibronectin functions as an anchoring protein, helping to secure epidermal keratinocytes to the ECM-rich

dermal layer. Fibronectin is also present in the dermis, where it interacts with several different matrix components, integrins, growth factors and cell types and serves to mediate cell adhesion and migration during wound healing. Fibronectin also plays an important role in wound contraction. *In vitro* studies using collagen gel contraction experiments have demonstrated a critical role for cellular fibronectin in successful gel contraction while plasma fibronectin, on the other hand, was found to be dispensable in this process [93]. While the exact mechanisms of wound contraction still require further investigation, integrin binding sites on fibronectin may be critical for both recruiting and anchoring fibroblasts to collagen, which can then serve to contract the wound.

The presence of proteoglycans in the skin serve as important mediators of tissue health and integrity. One of the most abundant proteoglycans in the skin is decorin, a small leucine-rich proteoglycan that strongly interacts with collagen. Decorin interacts with collagen at the fibril level where it binds and facilitates proper collagen organization and spacing [94, 95]. The importance of decorin in maintaining collagen organization and tensile strength is made clear through the use of decorin knockout mice [95]. When decorin knockout mouse skin was examined by transmission electron microscopy, collagen fibers demonstrated considerable variation in size and spacing compared to wild type (WT) mice [95]. The result is a drastic loss in tissue tensile strength as demonstrated by a susceptibility to skin tearing. Keloid and hypertrophic scarring of the skin, which features remodeled and disorganized collagen, have reduced decorin compared to normal skin [96, 97]. Decorin is also known to bind to and sequester active TGF- β [98]. Therefore, a loss of decorin could also result in an insufficient reservoir for active TGF- β , resulting in increased TGF- β activity that can promote fibrosis [99, 100].

1.9 Extracellular granzyme B during age-related skin injury

The discovery that GzmB can act outside the cell and degrade components of the ECM has given rise to renewed investigations into the role of GzmB in disease onset and progression. An ever increasing list of extracellular GzmB substrates has made investigation into the role of GzmB in tissue injury an emerging area of research. As many of these substrates play important structural and functional roles in the skin, there is potential for GzmB to contribute to skin injury and aging during chronic inflammation.

The ECM protein fibronectin was identified as an extracellular substrate of GzmB in a report showing that GzmB could kill smooth muscle cells in the absence of perforin [63]. GzmB-mediated degradation of fibronectin induced smooth muscle cell detachment, resulting in detachment-mediated cell death (anoikis). GzmB-mediated fibronectin degradation was also observed in a study that added vitronectin and laminin to the list of extracellular GzmB substrates [12]. The latter study also demonstrated that GzmB cleaves vitronectin at the RGD (Arganine-Glycine-Aspartate) integrin-binding site, potentially impacting important cell signaling pathways.

Rete ridges along the dermal-epidermal junction flatten with age, reducing the surface area for nutrient uptake and crosstalk between the dermis and the epidermis. Additionally, this flattening of the rete ridges predisposes the skin to injury such as skin tearing (ie. separation of the epidermis from the dermis). Laminin and fibronectin are abundant near the dermal-epidermal junction and are critical for epidermal cell attachment to the dermis and promote crosstalk between the two skin layers [101]. GzmB-mediated damage of these proteins would therefore compromise the integrity of aged skin, reduce nutrient exchange and promote skin tearing

(Figure 4). In support of this concept, GzmB staining is abundant in the dermal-epidermal junction in a mouse model of skin aging, suggesting GzmB-mediated matrix degradation along the dermal-epidermal junction does occur *in vivo* [64]. Increased GzmB levels are also correlated with disease severity in Stevens-Johnson syndrome/toxic epidermal necrolysis, a skin disease that involves the abrupt separation of the epidermis from the dermis [102].

Many proteoglycans are susceptible to GzmB-mediated degradation including aggrecan, decorin, biglycan and betaglycan [11, 64, 65, 72]. As the skin is a rich source of such proteoglycans, GzmB activity could exert a dramatic impact during aging and disease of the skin. For example, we have shown that decorin, an abundant skin proteoglycan, is degraded by GzmB, and its cleavage contributes to collagen disorganization and aging in mouse skin [64]. In this study, apolipoprotein E knockout mice exhibited significantly thinner skin compared to WT controls when fed a high fat diet for 30 weeks. Skin thinning was associated with reduced dermal thickness, a loss of collagen organization and a reduction in the amount of subcutaneous fat. Knocking out GzmB attenuated skin thinning and resulted in a thicker dermal layer, featuring organized, dense collagen with increased decorin content, suggesting GzmB contributes to collagen disorganization in aging skin through the degradation of decorin. Further, decorin knockout mice exhibit skin thinning, reduced tensile strength and susceptibility to skin tearing due to a lack of proper collagen organization and spacing [95]. Interestingly, decorin degradation and the accumulation of a protease-generated decorin fragment are observed in aged human skin [103]. Whether this fragment can be produced by GzmB requires further elucidation.

GzmB is implicated in ultraviolet (UV)-induced photoaging of the skin. Increased GzmB expression is observed in human skin exposed to UVA compared to non-irradiated skin [39]. Interestingly, a major source of this GzmB was suggested to be derived from epidermal

keratinocytes. Importantly, GzmB released from UV-exposed keratinocytes in culture is active, and capable of degrading fibronectin [33, 39]. Details on how keratinocyte-derived GzmB might act on fibronectin or other ECM in the skin during photoaging *in vivo* remains to be investigated.

While there are several possible cellular sources of extracellular GzmB during injury, mast cells are of particular interest to the skin as they do not express perforin [26]. GzmB expression in the absence of perforin suggests a purely extracellular role for mast cell-derived GzmB and could be an important source of extracellular GzmB during immune mediated injury. In support of this, GzmB-expressing mast cells are abundant in the aged skin of apolipoprotein E knockout mice undergoing decorin and collagen remodeling and xanthomatosis [64]. Human mast cells, including those derived from skin, also express GzmB without perforin and release GzmB into the extracellular environment following stimulation [27]. Interestingly, basophils also express GzmB without perforin when stimulated with supernatant from activated mast cells or IL-3, providing another source for extracellular GzmB [24].

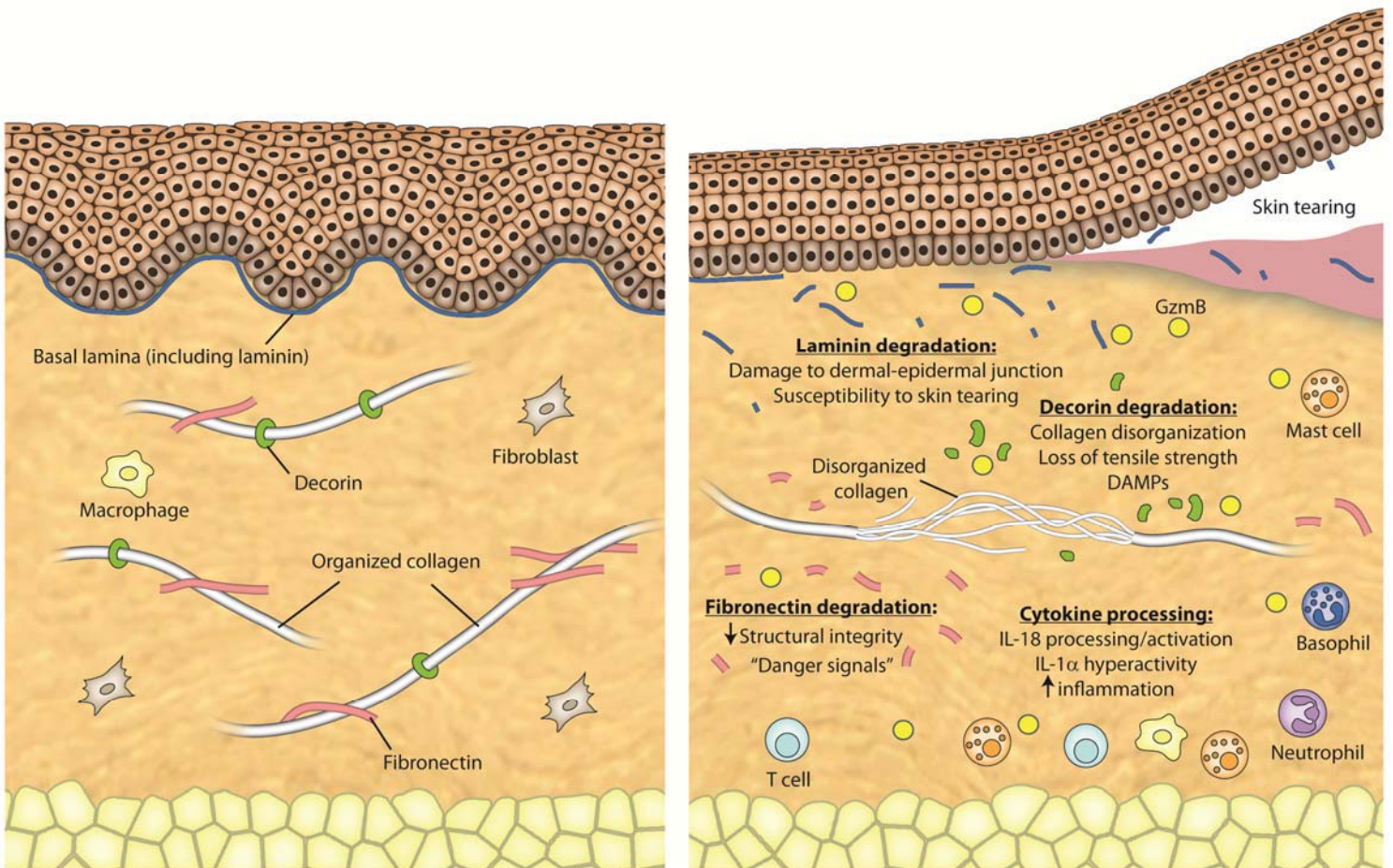


Figure 4. Possible mechanisms of granzyme B-mediated injury and inflammation. Active granzyme B (GzmB) can be released into the extracellular environment by different immune cells, such as lymphocytes, NK cells, mast cells, and basophils. Degradation of GzmB substrates including laminin, fibronectin, and decorin can reduce the structural integrity of the skin and increase susceptibility to injury. GzmB activity can also increase inflammation through the activation and processing of proinflammatory cytokines such as IL-18 and IL-1 α [182].

1.10 Granzyme B in inflammation

GzmB is used directly by immune cells when exerting their effector functions, however new advances have also uncovered roles for GzmB in regulating inflammation itself. Although the immune-regulating functions of granzymes were first considered decades ago [reviewed in 104], interest in the role of granzyme-mediated immune regulation has now been renewed. Discoveries made over the last decade have demonstrated the ability of GzmA, B, K and M to influence cytokine expression and processing, thereby promoting inflammation [10, 70, 71, 105-108]. Additionally, a role for GzmA and GzmB has been proposed in regulatory T cells (Tregs), whereby granzyme-mediated killing of effector cells may act as an important mechanism to control inflammation [109]. These two seemingly opposite functionalities highlight the complexity of immune-regulating granzyme activity, with each being context and cell type-dependent.

Both GzmA and GzmB can influence cytokine production and processing in a number of different cell types. IL-1 β , a cytokine known to be processed by the inflammasome, can also be processed by GzmA [107]. Furthermore, GzmK can induce processing and release of IL-1 β by macrophages in mice [110]. Other reports suggest that GzmA induces the expression of IL-6 and IL-8 in the lung, skin and intestine [10, 106] while GzmK activates protease-activated receptor-1 leading to IL-6, IL-8 and monocyte chemoattractant protein-1 release in human lung fibroblasts [105].

New evidence suggests that GzmB is also an effective mediator of cytokine processing. GzmB was first reported to influence cytokine activity when it was discovered to cleave IL-18, processing it from its inactive form to its active form [71]. Subsequent studies demonstrated that

GzmB processes IL-1 α into a significantly more potent pro-inflammatory fragment [70]. Further, GzmB-mediated cleavage of IL-1 α can occur extracellularly during NK-mediated killing due to the non-specific leakage of GzmB into the extracellular milieu. Of note, IL-1 α fragments similar to those produced by GzmB are observed in the bronchoalveolar lavage from patients with chronic obstructive pulmonary disease, cystic fibrosis and bronchiectasis. When mutant forms of IL-1 α lacking the GzmB cleavage site were injected into mice, IL-1 α bioactivity was reduced compared to when the native protein, which is susceptible to GzmB processing, was used. Similarly, when GzmB knockout mice were injected with IL-1 α , there was a reduced immune response when immunized with ovalbumin compared to WT mice, suggesting that GzmB-mediated cleavage of IL-1 α could also contribute to sustained inflammation *in vivo*.

An immunosuppressive role for GzmB in Tregs has also been proposed. Following the discovery of GzmB mRNA upregulation in activated Tregs [111], some postulated that GzmB could be responsible for a cytotoxic mode of suppression by Tregs *in vivo*. In 2005, researchers provided the first evidence that Tregs act using a cytotoxic, GzmB-dependant mechanism [112]. This study found that upon Treg activation with anti-CD3, GzmB expression was induced. Furthermore, when effector T cells were co-cultured with Tregs from GzmB knockout mice, their ability to suppress effector T cell activity was reduced compared to that of WT mice.

Degradation of the ECM by GzmB may also indirectly regulate inflammation. Fibronectin fragments exhibit chemotactic potential and promote recruitment of monocytes [113, 114], fibroblasts [115] and endothelial cells [116]. Fibronectin fragments also stimulate trans-endothelial migration of mononuclear leukocytes by promoting the production of TNF- α [117] and function as “danger signals” that promote inflammation and injury by stimulating toll-like receptors (TLRs). For example, fibronectin produced in response to injury contains a domain

referred to as extra domain A (EDA). Once cleaved, EDA signals through TLR-4 on human macrophages, leading to the production of MMP-9 [118]. Additionally, proteoglycans such as decorin and biglycan can promote inflammation. As these proteoglycans are normally buried within the ECM, their release and exposure during injury would cause them to be recognized as damage-associated molecular patterns, or DAMPs, which can signal via TLRs and stimulate the production of proinflammatory cytokines [119, 120].

1.11 Wound healing

1.11.1 Acute wound healing

Wound healing is a complex process often described in terms of four overlapping phases: (1) hemostasis, (2) inflammation, (3) tissue formation/proliferation and (4) tissue remodeling. Normal wound healing takes place quickly, allowing the body to recover from injury and restoring the injured tissues close to their original form. This type of wound healing is often termed acute wound healing, reflecting the ability to efficiently repair the wound, avoiding extended health problems. Hemostasis is the key initiating event, required to stop bleeding, recruit inflammatory cells and provide a temporary provisional matrix composed of fibronectin and fibrin. The recruitment of inflammatory cells then occurs beginning with neutrophils, which serve to fight infectious agents and break up damaged tissue. Macrophages also infiltrate and help to phagocytose apoptotic cells and other debris. The role of macrophages in acute wound healing is known to be important also for mediating the behavior of other cell types through the release of different cytokines and growth factors [121]. T cells appear later during the inflammatory phase, and may assist in fighting off infection and other tissue remodeling events. As the tissue proliferation phase occurs, keratinocytes and fibroblasts proliferate to close the

wound and new collagen and blood vessels are formed. The final remodeling stage involves the remodeling of collagen into mature, strong collagen fibres, returning the skin to a normal, healthy state.

1.11.2 Chronic wound healing

While advances in our understanding of chronic wounds have improved prevention and treatment options, there is much regarding the pathogenesis that remains undefined. Wound healing is complex, involving numerous interacting and overlapping phases, cell-matrix interactions and a properly regulated immune response. Chronic wounds fail to undergo the normal phases of wound healing and adopt a state of persistent, chronic inflammation. The result is increased cytokine production, protease secretion, and additional immune cell invasion into the wound leading to further damage and impaired healing. Researchers have therefore explored the role of proteases such as matrix metalloproteinases (MMPs) [122, 123] and serine proteases [124] in this context as potential antagonists of healing during persistent inflammation in a chronic wound.

Conditions such as diabetes increase susceptibility to injury and contribute to impaired wound healing. According to the World Health Organization, the worldwide prevalence of diabetes is expected to rise from 177 million in 2000 to 366 million in 2030, largely due to aging demographics [125]. Approximately 15% of diabetics will develop chronic wounds in the form of diabetic foot ulcers [126], making diabetic foot ulcers alone a major health burden among the elderly. Likewise, skin tears in elderly patients continue to pose a considerable burden. It is estimated that over 18% of patients residing in nursing homes suffer from skin tears [127].

Similarly, decubitus (pressure) ulcer prevalence is on the rise due to an increase in elderly patients. One study found that approximately one third of patients undergoing treatment for hip-fracture developed pressure ulcers following surgery [128].

1.12 Potential consequences of granzyme B activity in chronic wound healing

Several components of the ECM that are critical for skin health and wound healing have been identified as GzmB substrates and are outlined in Table 2. GzmB cleaves important mediators of hemostasis including von Willebrand factor, plasminogen and fibrinogen. GzmB also delays ristocetin-induced platelet aggregation when added to plasma samples from healthy donors [129]. Further experiments demonstrated that GzmB-mediated cleavage of von Willebrand factor and possibly fibrinogen were responsible for preventing aggregation in these samples. Plasminogen, an important mediator of cell migration and angiogenesis, can also be cleaved by GzmB. Normal processing of plasminogen (which can be performed by a number of enzymes including factor XII, tissue plasminogen activator and urokinase plasminogen activator), converts it to plasmin, which serves as a pro-angiogenic factor. Other proteases however can cleave plasminogen or plasmin at a different site causing the production of an anti-angiogenic fragment called angiostatin. GzmB was found to cleave plasminogen and plasmin thereby assisting in the production of the angiostatin fragment, contributing to impaired angiogenesis and delayed wound healing observed in patients with scleroderma [130].

GzmB not only causes damage directly during chronic inflammation, but can indirectly promote inflammation through the activation of cytokines such as IL-18 and IL-1 α . Of interest,

IL-1 α is elevated in chronic wound fluid compared to acute wound fluid [131] and primes neutrophils, a prominent cell type in the chronic wound environment [132].

Keratinocyte proliferation and migration are essential for wound closure. The presence of a provisional matrix scaffold is critical to allow keratinocyte migration across the wound bed. This provisional matrix is composed of several different ECM proteins including fibronectin and vitronectin. Fibronectin is deposited beneath the migrating epidermis while migrating keratinocytes express receptors for fibronectin [133]. The altered inflammatory profile in the chronic wound along with excessive GzmB-mediated degradation of fibronectin and vitronectin could hinder the formation of this provisional matrix, delaying the re-epithelialization process.

Chronic wound fluid contains fragments of fibronectin and vitronectin that are not observed in acute wound fluid [134-136]. Wound fluid from chronic leg ulcers of 11 patients exhibited clear degradation of both fibronectin and vitronectin compared to fluid obtained from patients going through surgical mastectomy or acute blister fluid, both of which showed only the full length proteins [134]. This study also demonstrated that chronic wound fluid containing degraded fibronectin and vitronectin prevented BHK (baby hamster kidney) cells from adhering to gelatin-coated plates while cells readily adhered when fluid containing the full length fragments was used. Full length fibronectin was also found to be rapidly degraded when added to wound fluid from stasis ulcers [135]. Interestingly, fibronectin mRNA is increased in chronic wounds [137] and fibroblasts isolated from venous ulcers can produce as much fibronectin as normal fibroblasts [138], suggesting that these well-described GzmB substrates are degraded in chronic wounds due to high protease activity as opposed to reduced synthesis.

In addition to providing a physical scaffold that facilitates cell migration, the provisional matrix can encourage cells to migrate through signaling via its integrin binding sites and interactions with growth factors. For example, insulin-like growth factor-1 (IGF-1) interacts with vitronectin through intermediate IGF binding proteins. Cell interaction with both vitronectin-bound IGF-1 and the RGD integrin binding site on vitronectin promotes proliferation and migration. Because of the importance of these growth factors in cell proliferation and migration, the addition of soluble growth factors to chronic wounds has been attempted as a strategy to promote wound closure. Unfortunately, such attempts have been met with little success, possibly due to the lack of a synergistic signal arising from interactions between matrix-bound IGF-1/IGF-1 receptor and matrix-facilitated integrin signaling. Indeed, evidence is emerging that the addition of growth factors in complex with vitronectin is a more effective strategy than growth factors alone [139].

As mentioned, GzmB cleaves vitronectin at RGD integrin binding sites, potentially disrupting synergistic integrin/growth factor signaling and preventing proliferation/migration by keratinocytes and fibroblasts. Excessive GzmB activity in the chronic wound could therefore present an obstacle to successful matrix:growth factor therapy. In addition, vitronectin and/or fibronectin degradation by GzmB could have implications for proper hemostasis and angiogenesis as both proteins are important during these processes as well [140, 141].

Laminin degradation by GzmB could also have a considerable impact on wound healing. Laminin is important for facilitating keratinocyte and fibroblast migration and plays a crucial structural role at the dermal-epidermal junction. Studies have demonstrated that reduced levels of laminin at the dermal-epidermal junction is a feature of diabetic ulcers as opposed to acute

excisional wounds [142]. Disruption of proper laminin deposits at the basal lamina could also hinder timely keratinocyte migration and wound closure.

Proteoglycans also have an important role to play in wound healing. Studies using decorin knockout mice have shown decorin to be an important component of strong skin and timely wound healing [95, 143]. Decorin knockout mice heal slower than WT controls when given full thickness excisional skin wounds [143]. Decorin knockout mice also demonstrate an increase in the number of mast cells in wounded skin. Although GzmB was not assessed in this study, mast cells are an important source of extracellular GzmB during skin inflammation [26, 64].

Several other aspects of wound healing such as scarring and fibrosis may also be affected by GzmB activity (Figure 6). Decorin, for example, is thought to be predominately an anti-fibrotic proteoglycan and may inhibit excessive collagen production by fibroblasts [144]. Gene transfer of decorin into mice reduces fibrosis in the lung [145] while over expression of decorin can reduce TGF- β -induced fibrosis *in vitro* and *in vivo* [99, 100]. Reports have also demonstrated reduced levels of decorin in keloid scars and hypertrophic scars compared to normal tissues [96, 97]. As decorin is critical for proper collagen organization and tensile strength, GzmB-mediated decorin degradation would result in collagen spacing and organizational defects leading to reduced tensile strength. Numerous studies have shown that decorin is reduced in fibrotic tissues in the skin and other organs leading to the disorganized collagen that characterizes these lesions. We have demonstrated that disorganized collagen in the skin is associated with reduced decorin levels in mice and that inhibition of decorin prevents this phenomenon [64]. Interestingly, some have reported an increase in endogenous decorin mRNA production by fibroblasts from fibrotic patients compared to healthy controls [146]. Increased decorin mRNA along with decreased

decorin protein in fibrosis and scarring would be explained by increased proteolytic degradation of decorin during these processes.

In addition to decorin, other GzmB substrates such as biglycan, betaglycan and fibrillin-1 act as reservoirs for different growth factors and cytokines. Cleavage of these respective matrix components would be predicted to disrupt this tightly regulated interaction thereby promoting the dysregulated release of sequestered cytokines and growth factors. In support of this concept, it was recently shown that TGF- β is sequestered by several proteoglycans that are susceptible to GzmB-mediated cleavage [65]. Furthermore, GzmB cleavage of decorin, biglycan and betaglycan promoted the release of active TGF- β from the proteoglycans resulting in increased SMAD signaling. As such, GzmB activity could potentially contribute to impaired wound healing and fibrosis through the aberrant and untimely release of sequestered TGF- β .

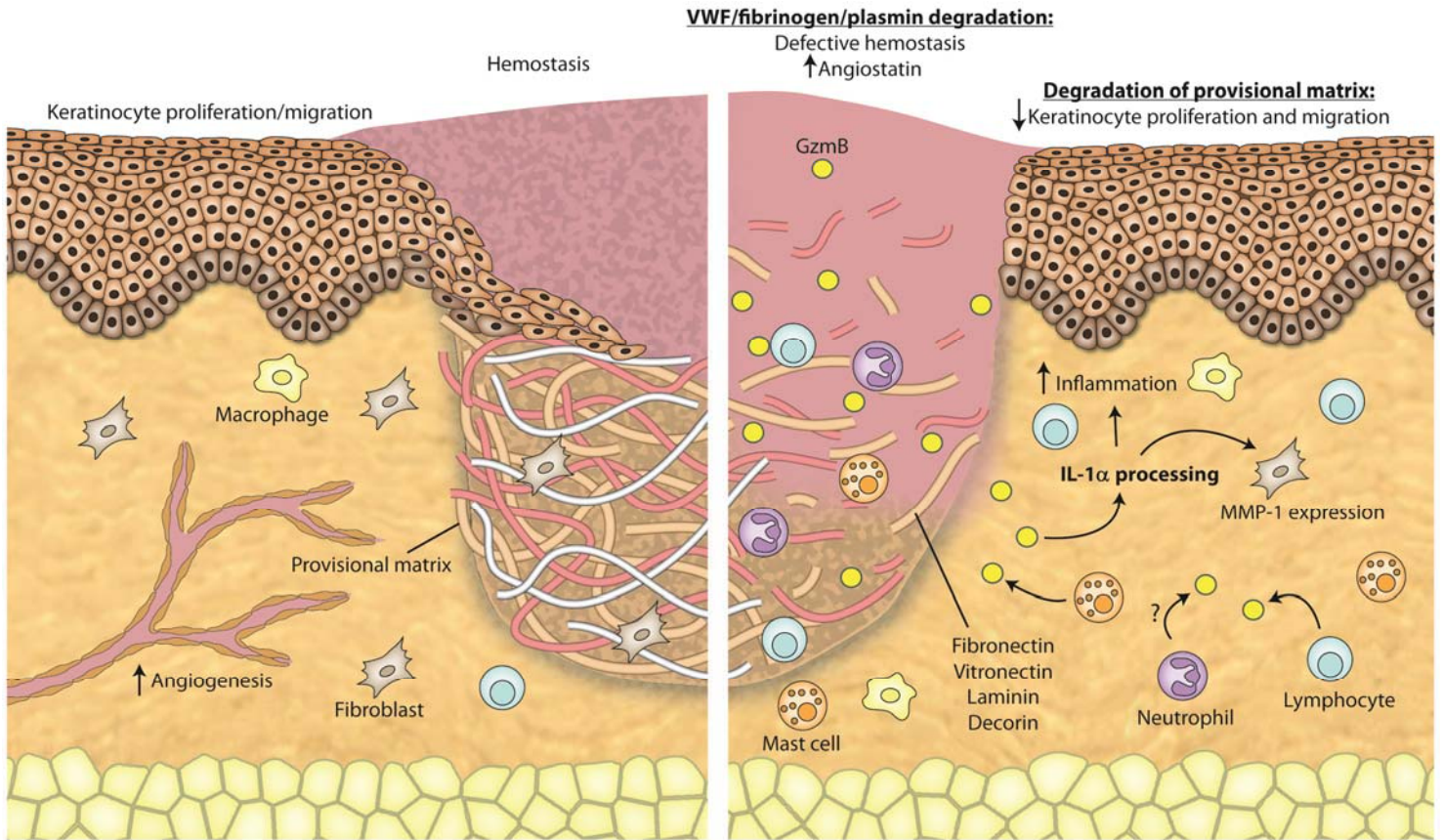


Figure 5. Potential mechanisms of granzyme B-mediated damage during wound repair. Normal wound healing (left) versus impaired wound healing (right), featuring increased granzyme B (GzmB) activity. GzmB-mediated degradation of von Willebrand factor and fibrinogen can delay hemostasis. Cleavage of plasminogen by GzmB increases the levels of angiostatin, preventing proper angiogenesis. GzmB can cleave components of the provisional matrix (fibronectin, vitronectin, laminin, and decorin) preventing proliferation and migration of keratinocytes and fibroblasts. GzmB-mediated activation of IL-1 α can also lead to an increased inflammatory response and can stimulate fibroblasts to produce more matrix metalloproteinase 1 (MMP-1) [182].

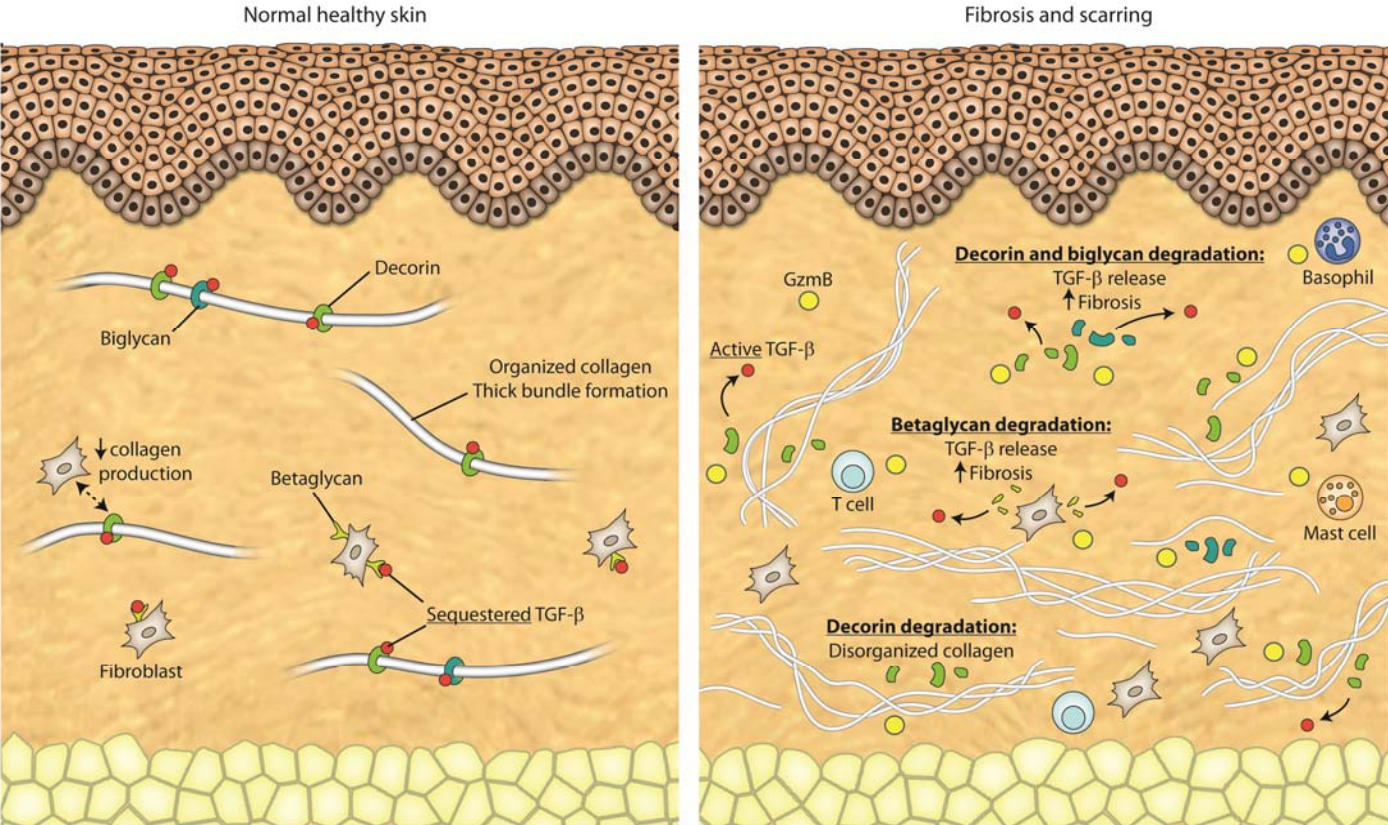


Figure 6. Granzyme B activity in fibrosis and scarring. Degradation of decorin by granzyme B (GzmB) can be pro-fibrotic by promoting disorganized collagen. Fibroblasts may also be encouraged to produce more collagen in the absence of inhibitory signals from the decorin proteoglycan. GzmB-mediated degradation of decorin, biglycan, and betaglycan can also result in the release of active TGF-β, potentially increasing the fibrotic response [182].

Table 2. Extracellular granzyme B substrates and potential impact of substrate cleavage in a chronic wound (182).

Protein	Role in wound healing	Potential consequence of cleavage by GzmB	Status in impaired wound healing and/or fibrotic diseases	References
Decorin	Regulates collagen fibrillogenesis, spacing, organization and tight bundle formation. Sequesters active TGF- β , reduces excessive cell proliferation.	Lack of collagen organization during scar formation leading to reduced tensile strength of scar. Impaired regulation of TGF- β release, fibroblast proliferation and angiogenesis.	Reduced or absent in chronic skin ulcers, sun-damaged skin, hypertrophic scarring and is cleaved to a truncated size consistent to that which is produced by GzmB in keloid scar tissue. Decorin-deficient mice exhibit pronounced skin fragility, impaired wound healing.	[95, 143, 147-150]
Fibronectin	Essential for keratinocyte migration and wound closure.	Impaired wound closure.	Degraded in ulcers. Fragmented in wound fluid from patients with chronic non-healing wounds. Fragments are not observed in acute wound fluid.	[134]
Von Willebrand Factor	Platelet adhesion and clotting.	Impaired platelet adhesion, spreading, clotting.	Increased plasma levels observed in diabetics with foot ulcers. Observed deficiency in patients with non-healing pressure ulcers. Ulcer cured when treated for von Willebrand disease.	[151, 152]
Plasminogen	Converted to plasmin. Plasmin degrades ECM allowing keratinocyte migration and endothelial migration to form new blood vessels.	Angiostatin production, defective clot clearance, impedes cell migration/angiogenesis. Increased plasmin, excessive ECM degradation.	Increased plasminogen activation in venous leg ulcers.	[153]
Fibrinogen	Converted by thrombin into fibrin. Essential for proper clot formation.	Improper processing into fibrin delaying clot formation. Increased fibrin generation.	Fibrin cuffs are a main feature of venous ulcers.	[154]
Vitronectin	Integrin binding, growth factor binding promoting keratinocyte migration and proliferation.	Disruption of RGD site, reduced integrin binding and impaired keratinocyte migration/proliferation. Disruption of growth factor binding (eg. IGF-1).	Fragmented in wound fluid from patients with chronic non-healing wounds. Fragments are not observed in acute wound fluid.	[134]

Table 2 (continued).

Protein	Role in wound healing	Potential consequence of cleavage by GzmB	Status in impaired wound healing and/or fibrotic diseases	References
Laminin	Expressed by keratinocytes near dermal-epidermal junction. Helps to facilitate cell migration.	Disruption of matrikine elements leading to impaired binding to EGF receptors, reduced keratinocytes migration/wound closure. Reduced fibroblast migration.	Reduced levels of laminin-332 detected in diabetic ulcers along the dermal epidermal junction compared to acute excisional wounds. Present in fibrin cuffs in venous ulcers.	[142]
Fibrillin-1	Supports a proper elastin framework within the healed tissue.	Effects on elastin distribution during wound healing, potentially impacting scarring/fibrosis.	Altered fibrillin-1 composition in normal, hypertrophic and keloid scars. Changes in distribution with age but mRNA remains unchanged.	[155-157]
IL-1α	Pro-inflammatory cytokine important for mediating inflammation.	Hyperactivation of IL-1 α encouraging persistent/chronic inflammation. Increased collagenase production by fibroblasts.	Elevated IL-1 α levels in chronic wound fluid compared to acute wound fluid.	[131]

1.13 Apolipoprotein E in aging and inflammation

Trafficking and metabolism of lipids requires the work of special proteins that bind to lipids and transport them throughout the body. These lipoproteins, as they are called, are critical for maintaining proper lipid homeostasis. Apolipoprotein E (ApoE) is a protein that binds to lipids and cholesterol and can be found as part of the chylomicron and intermediate-density lipoproteins. In humans, there are several different isoforms of ApoE but 3 of these isoforms are by far the most common: ApoE2, ApoE3 and ApoE4. Among these 3, most people possess the ApoE3 isoform, which is recognized as the most physiologically normal phenotype. ApoE polymorphisms have been associated with type III hyperlipidemia with the ApoE2 and ApoE4 isoforms linked to hypertriglyceridemia and hypercholesterolemia, respectively [158]. The ApoE4 isoform has also been associated with an increased risk of Alzheimer's disease [159].

Research on individuals with different isoforms of ApoE have suggested that ApoE is an important factor influencing healthy aging and longevity. Cardiovascular disease and Alzheimer's disease are 2 major age-related afflictions that affect millions of people worldwide and are heavily influenced by ApoE [reviewed in 160]. Interestingly, although ApoE2 is linked to type III hyperlipidemia, some studies have found that individuals who live beyond 100 years of age are more likely to carry the ApoE2 allele [161]. While the exact reasons for this are not completely known, these observations further implicate ApoE as a mediator of healthy aging and longevity.

Additional physiological roles for ApoE beyond lipid transport have also been identified, and have implications for healthy aging. Numerous studies have reported important immune-regulating activities of ApoE. ApoE was found to be the component responsible for inhibiting cell proliferation when lipoproteins were added activated T cells [162-166]. This effect was

found to be the result of reduced DNA synthesis and phospholipid production [167]. ApoE has also been shown to regulate multiple signaling pathways within T cells and suppress Th1-mediated immune responses [168-170]. Furthermore, ApoE has demonstrated an ability to regulate the production of pro-inflammatory cytokines such as TNF- α , IL-1 β and IL-6 in mice when responding to LPS injection [171].

Immune regulation by ApoE can also be extended to neutrophils. Terkeltaub *et al* showed that neutrophil stimulation by monosodium urate crystals can be inhibited by ApoE [172]. Macrophages can also express ApoE which may act by regulating their ability to activate T cells [173]. When isolated from ApoE knockout (ApoE-KO) mice, macrophages featured increased MHC class II and co-stimulatory molecules on their cell surface following stimulation [173]. When stimulated, macrophages also downregulate ApoE to facilitate a pro-inflammatory response [174, 175]. Additionally, macrophages treated with ApoE show reduced production of pro-inflammatory cytokines such as TNF- α and IL-1 β [176].

1.14 Apolipoprotein E knockout mice

ApoE-KO mice are hypercholesterolemic and spontaneously develop atherosclerosis and xanthomatosis [160]. ApoE-KO mice fed a high fat diet develop these pathologies more severely and earlier in life compared to their regular chow fed counterparts [177]. Recently, based on studies using ApoE-KO mice, it has been suggested that ApoE plays an important role in aging and longevity [160, 178]. In addition to atherosclerosis, ApoE-KO mice are used to study Alzheimer's disease due to defects in memory function and increased permeability of the blood brain barrier [179, 180]. ApoE-KO mice have also demonstrated a reduced lifespan, as well as atrophy of the seminiferous tubules along with decreased spermatogenesis [181]. Early

observations focusing on the skin of ApoE-KO mice have also noted the susceptibility to age-related phenotypes such as hair loss and hair greying in addition to the development of inflammatory skin disease. The susceptibility of ApoE-KO mouse skin to chronic inflammation associated with accelerated aging make the skin of ApoE-KO mice a potentially useful model to study the role of extracellular GzmB and its role in ECM remodelling during aging and disease.

2. Rationale, hypothesis and aims

As our understanding of granzymes continues to evolve, it is becoming clear that both the physiological and pathological roles of these enzymes are more complex than was once thought. GzmB is an enzyme with a diverse repertoire of biological activities, capable of influencing several aspects of inflammation and wound repair. Numerous lines of evidence support the notion that GzmB can impact not only susceptibility to injury, but contribute to delayed wound healing as well [reviewed in 182]. The lack of evidence for an extracellular regulator of GzmB activity suggests a detrimental role for excessive extracellular GzmB activity during chronic inflammation. GzmB inhibition may be a useful alternative to protease inhibitors targeting other enzymes such as MMPs, whereby non-specific inhibition of the wrong MMPs could interfere with healthy physiological healing processes. Future studies are likely to uncover additional roles for GzmB in the context of age-related skin injury and wound repair, warranting consideration for the use of such inhibitors to treat chronic, non-healing skin wounds.

Given what is now known about the diverse proteolytic activities of GzmB, particularly with respect to the ECM during chronic inflammation, considerable rationale exists for considering GzmB as a key enzyme in the context of skin aging and chronic wound pathogenesis. Unlike other proteases that are important for normal wound healing processes (eg. MMPs), GzmB not only retains its activity in bodily fluids such as plasma [183] and bronchoalveolar lavage [184] but also has no known inhibitors in the extracellular fluids, suggesting extracellular GzmB activity in the context of wound healing is not regulated. GzmB is also released constitutively and non-specifically by NK cells and lymphocytes into the extracellular spaces during chronic inflammation, even in the absence of target cell engagement

[185]. Excess GzmB activity therefore could have a dramatic effect in a chronic wound. These observations also implicate GzmB in inflammaging [186].

I hypothesize that GzmB plays a pivotal role in skin aging, injury and repair through the modification and degradation of ECM proteins.

Specific Aims:

1. *To phenotypically characterize the effects of ApoE deficiency and a high fat diet on aging of the skin in C57BL/6 mice.* Preliminary work done prior to my degree suggested that ApoE-KO mice age and become frail at an accelerated rate compared to WT mice. ApoE-KO mice showed evidence of hair graying, hair loss and inflammatory skin lesions that increased in severity as the mice aged. The preliminary observation was also made that these mice tended to display these age-related phenotypes even earlier in life when fed a high fat diet. I therefore began by further characterizing the ApoE-KO mouse as a model that mimics premature skin aging for the purposes of studying the role of GzmB in aging of the skin.
2. *To determine the role of GzmB in the accelerated aging phenotype observed in high fat diet-fed ApoE-KO mice.* Chronic, low-grade inflammation is thought to be a major factor contributing to tissue wear and tear over time. In addition, age-related changes to the immune system result in increased pro-inflammatory cytokines and activated immune cells. As ApoE-KO mice display a skin phenotype that is susceptible to chronic inflammation, I used the ApoE-KO mouse as a model to study the extracellular role that GzmB plays in ECM remodeling during aging. Because the skin provides a useful and

accessible model organ, abundant in ECM, the skin is an ideal model for studying GzmB-mediated ECM remodeling during chronic inflammation and aging.

3. *To investigate the role of GzmB in age-related skin injury and impaired wound healing.*

Age-related impaired wound healing is a common problem for elderly individuals. Chronic wounds feature inflammation that fails to resolve, resulting in increased proteolytic activity and excessive ECM degradation preventing timely wound closure. As wound healing in the skin involves many ECM proteins susceptible to GzmB-mediated degradation, GzmB may be a key protease contributing to excessive ECM degradation in the context of a chronic wound.

a. To explore the ApoE-KO mouse as a model of impaired wound healing. The skin of ApoE-KO mice has demonstrated susceptibility to chronic inflammation, frailty and excessive ECM degradation. I therefore examined the ApoE-KO mouse as a model of chronic wound healing. Increased or excessive inflammation in response to injury would potentially result in increased proteolytic activity and ECM degradation that could delay or prevent proper wound closure.

b. To determine the role of GzmB in impaired wound healing in ApoE-KO mice. Excessive inflammation in ApoE-KO mouse skin during wound repair could feature increased GzmB activity and GzmB-mediated ECM degradation, contributing to impaired healing. As ApoE is known to influence T cell proliferation and macrophage activation (both GzmB expressing cells), a deficiency in ApoE may result in excessive GzmB activity during wound healing.

3. Materials and methods

3.1 *Animals and diets*

All animal procedures were performed in accordance with the guidelines for animal experimentation approved by the Animal Care Committee of the University of British Columbia. Male WT C57BL/6, ApoE-KO and GzmB knockout mice were purchased from The Jackson Laboratory (Bar Harbor, ME). GzmB knockout mice were bred with ApoE-KO mice to generate ApoE/GzmB double knockout (DKO) mice. All knockout mice are derived from a C57BL/6 background. Mice were bred on site and housed at The Genetic Engineered Models (GEM) facility (James Hogg Research Centre, University of British Columbia/St. Paul's Hospital, Vancouver, BC). In all experiments, only male mice were used. Mice used in all experiments were fed ad libitum on either a high fat (21.2% fat, TD.88137, Harlan Teklad; Madison, WI) or regular chow (equal parts PicoLab Mouse Diet 20: 5058 (9% fat) and PicoLab Rodent Diet 20: 5053 (5% fat), LabDiet; Richmond, IN) diet beginning at 6–8 weeks of age for either 0, 5, 15 or 30 weeks. At their respective time points, mice were weighed, and euthanized by isofluorane and carbon dioxide inhalation as per University of British Columbia guidelines. Life span was measured using only mice designated for the 30 week time point. In all cases mortality was the result of euthanasia due to severe illness in the form of open skin lesions and xanthomatous lesions. The degree of disease severity requiring euthanasia was determined in a blinded manner by an independent animal care technician within the GEM facility. Briefly, animals were considered for euthanasia if they appeared to be in distress or pain that could not be alleviated. Because the animals cannot receive pain medication, mice deemed to be suffering because of open skin lesions or severe xanthomas required euthanasia.

3.2 Wound healing surgical procedure

At 7 (young) or 37 (old) weeks of age, mice were given a 1 cm full thickness skin wound on their mid backs. Because mice given a high fat diet began the diet at 6-8 weeks of age, mice wounded at 7 weeks of age were only ever fed a regular chow diet. Mice wounded at 37 weeks were either fed a high fat diet or maintained on a regular chow diet for 30 weeks starting at 6-8 weeks of age. During surgery, mice were kept at a constant body temperature using a heating pad. Mice were initially anesthetized using isoflurane/oxygen mixture in an induction chamber. Once sedated, the mice were transferred from the chamber to a heating pad while their nose was placed in a nose cone providing the isoflurane/oxygen mixture to maintain anesthesia. Eye lube was applied to the eyes to prevent drying and back hair was shaved using an electric razor. After shaving, mice were given a subcutaneous injection of buprenorphine (0.05 mg/kg) away from the wound site for analgesia. The skin surface to be wounded was then sterilized using ethanol. A 1 cm diameter punch biopsy was then used to outline the wound area and the skin was carefully excised using surgical scissors (including the underlying panniculus carnosus muscle layer). Immediately following wounding, pictures were taken of the wound in the presence of a ruler to capture wound size at day 0. Mice were then allowed to recover and placed into individual cages during the healing phase of the study to prevent damage to the wound from fighting. Mice were allowed to heal for either 2, 8 or 16 days. At the selected time point, mice were euthanized by isoflurane and carbon dioxide inhalation and wounded tissue was harvested.

3.3 Tissue collection and processing

For experiments described in chapters 4 and 5, once mice were sacrificed, back hair was shaved and dorsal skin was removed from the mid to lower back. Half of the skin sample was

fixed in 10% phosphate buffered formalin. Fixed skin sections were processed, embedded in paraffin and cut to 5 μm cross-sections for histology and immunohistochemistry. The other half of the dorsal skin sample was treated with a hair removing cream to completely remove all hair from the surface of the skin. These skin samples were then flash frozen in liquid N_2 and stored at -80°C until further use for multi-photon microscopy.

For wound healing experiments described in chapters 6 and 7, mice were sacrificed and the wound was first cut in half vertically down the centre. One half was then fixed in formalin for 24 h and embedded in paraffin for histological analysis and immunohistochemistry. The other half of the wound was flash frozen in liquid N_2 and stored at -80°C for analysis of ECM fragments by western blot.

3.4 Contraction measurements

Wound contraction was measured for all animals in chapters 6 and 7. During the healing phase, the rate of contraction was measured every second day by taking digital pictures of the wounded area in the presence of a ruler. Contraction was then measured from the pictures using the imaging software, Image Pro Plus® version 4.5.0.29 for Windows (Media Cybernetics Inc, Rockville, MD). First, the outside of the wound at Day 0 was traced and the original area of the wound was determined. The boundary of the wound used to measure contraction was seen as the border between the original, unwounded skin and the wounded area. Unwounded skin was evident by the presence of hair (shaved) while the newly formed tissue was smoother and without hair. All wound areas from subsequent days were normalized to the wound area from the corresponding animal at day 0 and expressed as a percent of the original wound size.

3.5 Histology and immunohistochemistry

Paraffin embedded skin cross-sections were stained with hematoxylin and eosin (H&E) for evaluation of morphology and with picrosirius red to examine collagen content [187]. Luna's elastin was used to examine elastic fibers [188]. Collagen was observed in picrosirius red stained sections using 100% polarized light and pictures were taken at a fixed exposure. GzmB immunohistochemistry was performed by first boiling deparaffinised slides in citrate buffer (pH 6.0) for 15 min. Background staining was blocked by incubating slides with 10% goat serum for 30 min. The primary antibody used was a rabbit anti-mouse GzmB antibody (Abcam, Cambridge, MA) at 1:100 dilutions. As a negative control, 10% goat serum with no primary antibody was used. Following the 30 min incubation with goat serum, the serum was aspirated, primary antibodies were applied and slides were incubated at 4°C overnight. Slides were then incubated with biotinylated goat anti-rabbit secondary antibody for 30 min at a 1:350 dilution (Vector Laboratories, Burlingame, CA), washed 3 times in tris buffered saline (TBS) followed by a 30 min incubation with ABC reagent (Vector Laboratories). Slides were washed again 3 times in TBS and staining was visualized by incubating with DAB peroxidase substrate (Vector Laboratories) for 5 min. All slides were then counterstained with hematoxylin. Decorin immunohistochemistry was performed by immersing deparaffinised slides in citrate buffer (pH 6.0) at 80°C for 10 min. Slides were blocked with 10% rabbit serum for 30 min. Blocking solution was then aspirated and a goat anti-mouse decorin antibody (1 µg/ml) (R&D Systems, Minneapolis, MN) was then added to the slides and incubated at 4°C overnight. Biotinylated rabbit anti-goat secondary antibody was used (1:350) (Vector Laboratories) along with VECTASTAIN Elite ABC reagent (Vector Laboratories) and DAB substrate (Vector Laboratories) as described above. The GzmB/mast cell dual stain was accomplished by first

performing immunohistochemistry for GzmB as described above, except VECTASTAIN ABC-AP and Vector Red (Vector Laboratories) were used instead of DAB substrate. Slides were then rinsed with water and incubated for 15 min in 0.7 N HCl followed by staining with alcian blue (1 g alcian blue powder in 100 ml of 0.7 N HCl) for 20 min, washed in 0.7N HCl for 5 min and rinsed with water before allowing to dry.

3.6 Histological analysis and measurements

Measurement of skin thickness was completed using H&E stained sections under a 40X objective lens and a calibrated ocular micrometer scale. Measurements were taken across the entire cross-sectional surface of the skin at multiple sites and averaged for each mouse. For the wounded skin, skin cross-sections from mice at 2, 8 and 16 days of healing were then stained using H&E and analyzed histologically for re-epithelialization using a 40X objective lens and a calibrated ocular micrometer scale. Re-epithelialization was measured beginning from the edge of the newly formed granulation tissue as the distance along the basal keratinocyte layer that had migrated toward the centre of the wound. For each section, two measurements were made, one on each end. For mice whose wounds were closed, the re-epithelialization distance was measured once and divided in half to represent the distance migrated from both ends of the wound.

3.7 Multi-photon microscopy

Frozen skin samples with the hair completely removed were thawed at room temperature and immobilized on a flat surface inside a small dish. Skin samples were washed several times and immersed in phosphate buffered saline. Second harmonic generation (SHG) signals were emitted by the collagen in the skin samples and quantified as a measure of collagen density.

Methods used were similar to those described previously [189]. Briefly, the laser used was a mode-locked femto-second Ti:Sapphire Tsunami (Spectra-Physics, Mountain View, CA) and was focused on the specimen through a 20X/0.5 NA HCX APO L water dipping objective. An excitation wavelength of 880 nm was used and backscattered SHG emissions from the sample were collected through the objective lens. Leica Confocal Software TCS SP2 was used for the image acquisition. Images (8 bit) acquired were frame-averaged 10 times to minimize the random noise. For each sample, about 200–250 Z-section images with a thickness of about 0.63 μm were acquired at decreasing tissue depths for a total thickness measurement of approximately 130–160 μm per sample. These measurements were taken completely within the dermis of each sample as the thinnest dermal layer observed was 250 μm , therefore any decrease in signal is due to a decrease in density rather than a lack of dermal collagen material. Z-section images were compiled and finally the 3D image restoration was performed using Volocity software (Improvisions, Inc., Waltham, MA). A noise-removal filter whose kernel size of 3×3 was applied to these 3D images and SHG signals that fell within a set threshold were quantified for the entire 3D image using Velocity software (Improvisions Inc.).

3.8 Histological quantification of collagen

Quantification of collagen was achieved by colour segmentation in 5 μm thick fixed skin sections stained with picosirius red. Images were taken at the wounded site under polarized light at 20X magnification. Using the imaging software, Image Pro Plus® version 4.5.0.29 for Windows (Media Cybernetics Inc), the number of pixels within the area of interest whose colour was above a set threshold was counted and expressed as the percent positive pixels.

3.9 Skin homogenization and analysis of fibronectin fragments

Frozen skin containing the wounded tissue was thawed and cut into identically sized 1 cm² pieces. Skin pieces were then placed into 1.5 ml tubes containing 350 µl CellLytic MT lysis buffer (Sigma-Aldrich), 4 µl protease inhibitor cocktail (Sigma-Aldrich) and a 7 mm stainless steel bead (Qiagen, Germantown, MD). Tubes were then placed in a TissueLyser LT (Qiagen) and homogenized at 50 Hz for 4 min, 3 times for a total of 12 min. Tubes were placed on ice for 30 s in between the 3 homogenization cycles to prevent excessive heating. Tissue homogenate was then centrifuged at maximum rpm at 4 °C and supernatant was collected. Total protein content was then measured in the supernatant solutions using a Nanodrop 8000 (Thermo Scientific, Waltham, MA) and samples were then normalized by total protein before being used for western blotting experiments. Laemmli buffer (12 ml 0.5 M Tris-HCl (pH 6.8), 8 ml glycerol, 2.4 g SDS, 1.86 g DTT and 50 mg Bromophenol Blue for a 20 ml 6X stock solution) was then added to the supernatant samples followed by heating at 95 °C for 5 min. Samples were then run on a 6 – 15% gradient polyacrylamide gel and transferred to a nitrocellulose membrane. Membranes were blocked for 1 h using 2.5% skim milk followed by overnight incubation with anti-fibronectin antibody (Abcam) at a 1:1500 dilution in 2.5% skim milk. Membranes were then washed 3 times in TBS and incubated for 1 h with IRDye® 800 conjugated goat anti-rabbit secondary antibody at 1:10,000 (Rockland Inc, Gilbertsville, PA). Following secondary antibody incubation, membranes were washed with TBS and detection/quantification of fibronectin fragment densitometry was achieved using the Odyssey Infrared Imaging System (LI-COR Biotechnology, Lincoln, NE).

3.10 Decorin cleavage assay

Recombinant decorin (0.4 µg, Abnova, Walnut, CA) was incubated with 100 nM purified human GzmB (Axxora, San Diego, CA), at room temperature for 24 h. Reactions were run in 50 mM Tris buffer, pH 7.4. For GzmB inhibition, 20 µM of the GzmB inhibitor, Compound 20 [190] (UBC Centre for Drug Research and Discovery, Vancouver, BC) was pre-incubated with GzmB for 30 min prior to addition of the decorin substrate. Samples were denatured, run on a 10% polyacrylamide gel and imaged with Bio-safe Coomassie Blue Stain (Biorad, Hercules CA).

3.11 Mouse fibronectin cleavage assay

Skin homogenate from a WT mouse wound harvested 8 days following wounding was generated using the procedure described above. For this experiment however, protease inhibitors were not included in the buffer in order to facilitate GzmB activity. A volume of 10 µl was then pipetted into microcentrifuge tubes. Mouse GzmB (Sigma-Aldrich) was added to a final concentration of either 0 nM, 100 nM or 200 nM. Tubes were then incubated at 37 °C for 24 h. Following the incubation, the reaction was stopped by adding Laemmli buffer (same recipe as above) and western blot analysis for fibronectin performed as described above.

3.12 Statistical analyses

Survival data were analyzed for significance using the Mantel-Cox test with $P < 0.05$ considered significant. One- or two-way ANOVA with Bonferroni post test was used for group comparison analyses and $P < 0.05$ was considered significant. Statistical calculations were computed using GraphPad Prism version 5.01 for Windows, GraphPad Software, San Diego California USA, www.graphpad.com.

4. Accelerated skin aging in high fat diet-fed apolipoprotein E knockout mice

4.1 Introduction

Healthy aging of the skin not only has an important social impact, but can be a useful indicator of an individual's overall health. Many different models of aging have been utilized in aging research to study the functional and structural changes that occur in our bodies over time [reviewed in 160]. Mouse models of aging offer a useful alternative to smaller, non-mammalian organisms such as worms or yeast. Mice provide a more relevant model of human aging and disease while still remaining a practical organism to study lifespan. A laboratory mouse can live for up to 2.5 years, which can make timely aging studies difficult yet still more practical than studies using higher, longer-lived mammals.

Different mouse models of aging have been utilized by a number of research groups, and are most useful for their ability to mimic many of the age-related diseases that often accompany aging in humans. Mouse models such as the *Wrn/Terc* double knockout mouse mimic human premature aging syndromes such as Werner syndrome [191]. Other models such as the *klotho* knockout mouse, feature several age-related phenotypes such as skin thinning, hair loss, infertility, kyphosis, atherosclerosis and osteoporosis [192]. Several other mouse models have also been used to study aging and age-related disease [reviewed in 160]. These models are useful in testing intervention strategies for combating the deleterious effects of human aging with the added benefit of only having to age the animal for months, rather than several years.

Several lines of evidence have implicated ApoE in aging and longevity. As mentioned above, different isoforms of ApoE carry different degrees of efficiency and are associated positively or negatively with diseases like atherosclerosis, hyperlipidemia, Alzheimer's disease

and even longevity. ApoE-KO mice are hypercholesterolemic and spontaneously develop atherosclerosis and xanthomatosis, a phenotype made more severe when fed a high fat diet [160]. Previous observations by our laboratory have identified ApoE-KO mice as displaying several additional phenotypes indicative of premature aging such as hair graying, hair loss and reduced longevity. In this chapter, we investigate the ApoE-KO mouse as a novel model of accelerated skin aging, featuring increased susceptibility to chronic inflammation and ECM remodeling.

4.2 Results

4.2.1 Morbidity and skin pathology

ApoE-KO mice have been shown to spontaneously develop cutaneous xanthomatosis on their backs and shoulders. To assess the effects of age and diet on the occurrence and severity of these lesions, we monitored animal morbidity for 30 weeks while mice were fed either a regular chow, or high fat diet. All instances where an animal required euthanasia prior to 30 weeks was attributed to severe open or xanthomatotic skin lesions that required the animal to be euthanized for humane reasons. Consistent with previous reports, ApoE-KO mice in this study exhibited a marked decline in health compared to WT controls resulting in increased morbidity and frequency of required euthanasia over a 30 week span (Figure 7). While placing WT mice on a high fat diet did not alter survival over the 30 week span, the necessity for euthanasia was significantly increased when the ApoE-KO mice were fed a high fat diet with only about 69% surviving to the 30 week time point (Figure 7). As shown in Figure 8, ApoE-KO mice exhibited signs of frailty, hair loss, hair graying and the formation of subcutaneous lesions or xanthomas on their backs and shoulders at 30 weeks. These phenotypes were more severe and occurred much earlier in life when ApoE-KO mice were fed a high fat diet (Figure 8). When examined histologically, ApoE-KO mouse skin was heterogeneous, with some sections appearing normal, or non-diseased, and other sections showing obvious signs of xanthomatosis (Figure 9A). These lesions featured noticeable immune cell infiltrate including lymphocytes and macrophage foam cells (Figure 9B). Of all ApoE-KO mice on a regular chow diet, 9/31 (29%) exhibited xanthoma/skin pathologies with the earliest case at 18 weeks and the majority of the cases (7/9) appearing when examined at 30 weeks. When fed a high fat diet however, 13/32 (41%) ApoE-KO mice showed evidence of xanthomas/skin pathology with 10/13 occurring prior to the 30

week time point. These data suggest that a high fat diet accelerates the frequency and onset of these inflammatory skin lesions in ApoE-KO mice.

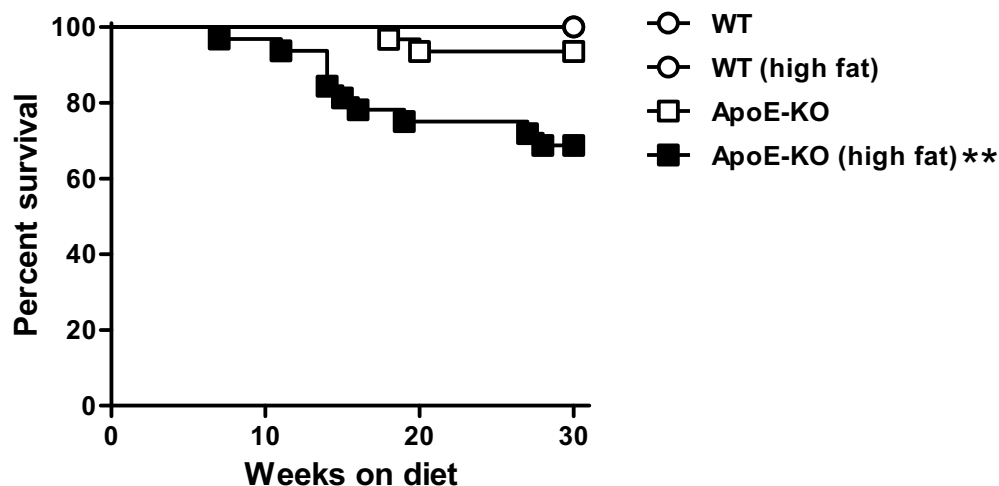


Figure 7. Increased morbidity in apolipoprotein E knockout mice fed a high fat diet. All wild type (WT) mice survived to the 30 week time point on either a high fat (n=18) or regular chow (n=19) diet while 94% of chow-fed apolipoprotein E knockout (ApoE-KO) mice (n=31) were kept alive for 30 weeks. A high fat diet significantly reduced survival in ApoE-KO mice (n=32) compared to the WT group with only 69% remaining healthy enough to survive for the entire 30 week span. ** $P < 0.01$ vs WT (Mantel-Cox test).

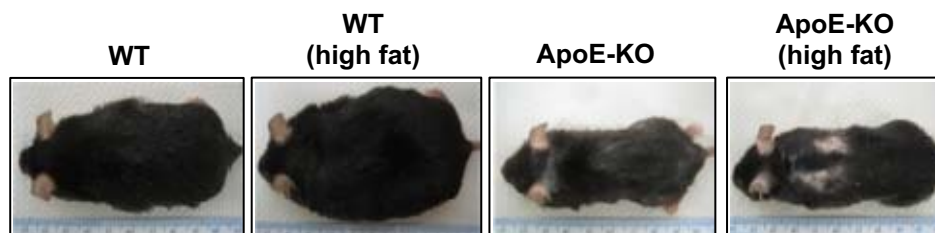


Figure 8. Representative images of wild type and apolipoprotein E knockout mice at the 30 week time point. Wild type (WT) mice fed a chow diet for 30 weeks appeared healthy and strong. A high fat diet resulted in considerable weight gain in WT mice while apolipoprotein E knockout mice appear frail and have diseased skin, which increases in severity when fed a high fat diet.

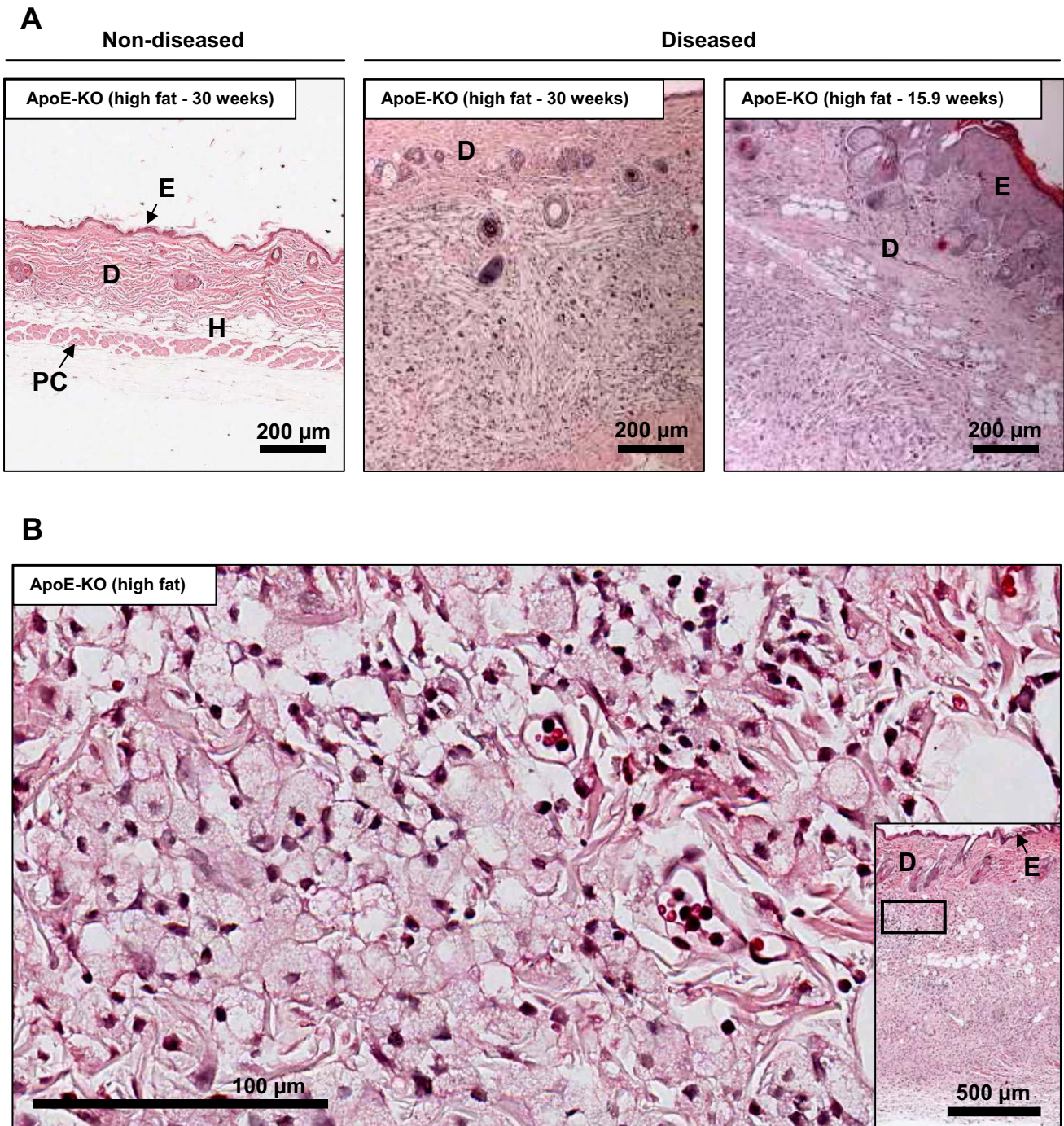


Figure 9. Normal and diseased skin in apolipoprotein E knockout mice. (A) Examples of diseased and non-diseased skin sections from apolipoprotein E knockout (ApoE-KO) mice fed a high fat diet for 30 weeks and 15.9 weeks. The ApoE-KO mouse aged 15.9 weeks required early euthanasia due to the severity of the skin lesion. E = epidermis, D = dermis, H = hypodermis, PC = panniculus carnosus. (B) Immune infiltrate in the skin of a high fat diet-fed ApoE-KO mouse containing xanthoma featuring lymphocytes and macrophage foam cells.

4.2.2 *Weight gain*

To further examine changes occurring in ApoE-KO mice over time, both WT and ApoE-KO mice were grown (starting at 7 weeks of age) for either 0, 5, 15 or 30 weeks on a high fat or regular chow diet. Mice were weighed at each of these end points to examine weight gain/loss with age. When weight gain was examined at the 0, 5, 15 and 30 week time points, WT mice on a high fat diet showed a significant increase in weight as early as 5 weeks on the diet compared to the chow fed controls and remained higher throughout the course of the study (Figure 10A). ApoE deficiency alone resulted in no difference in weight gain compared to the chow-fed WT controls until 30 weeks when the chow-fed ApoE-KO group stopped gaining weight (Figure 10B) and adopted a frail phenotype (Figure 8). At this point chow fed ApoE-KO mice weighed significantly less than chow fed WT mice (Figure 10B). When ApoE-KO mice were fed a high fat diet, they appeared to gain weight at a similar rate to the WT control group and possibly to a greater extent at 15 weeks (Figure 10C). However by 30 weeks they exhibited weight loss and displayed frail and diseased skin weighing significantly less than the chow fed WT mice (Figure 10C). These results suggest that ApoE-KO mice fed a high fat diet for 30 weeks are prone to premature weight loss and frailty.

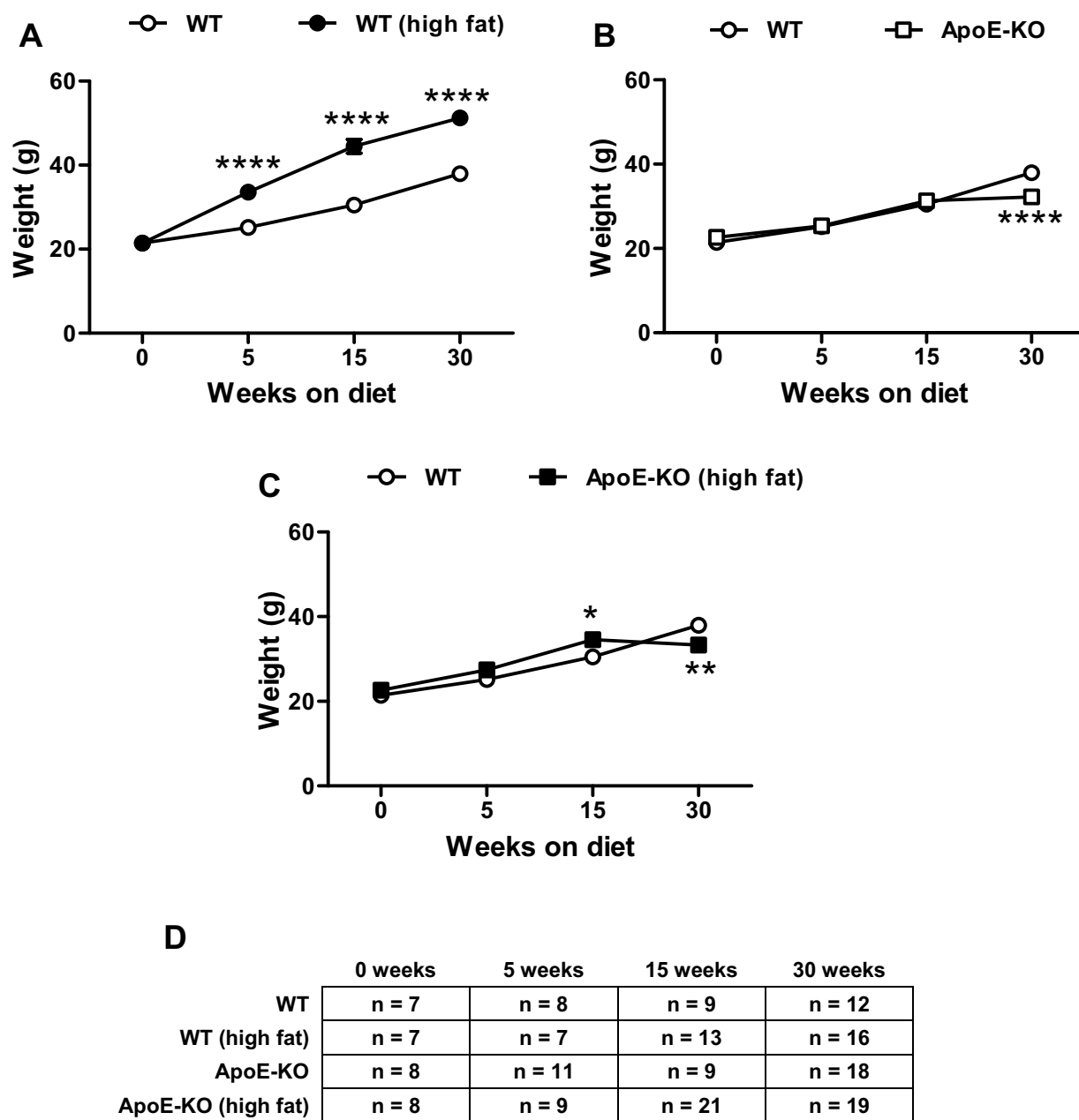


Figure 10. Age-related weight gain in wild type versus apolipoprotein E knockout mice. Weight was measured at 0, 5, 15 and 30 weeks for the wild type (WT) mice compared to (A) WT (high fat), (B) apolipoprotein E knockout (ApoE-KO) and (C) ApoE-KO (high fat) groups compared to WT. (D) Summary of the number of mice used for each time point for each group. (Error bars represent the mean \pm SEM, some error bars are within the symbol). * $P < 0.05$, ** $P < 0.01$, **** $P < 0.0001$ (2-way ANOVA with bonferroni post test).

4.2.3 Skin thickness

Skin thinning and atrophy is a characteristic feature that occurs with age both in humans and mice [193, 194]. To determine whether ApoE-KO mice exhibit this trait, we analyzed formalin fixed skin sections from the mid to lower back of the WT and ApoE-KO mice on a chow or high fat diet using H&E staining at 0, 5, 15 and 30 weeks and measured total skin thickness. Due to the heterogeneous nature of the skin in ApoE-KO mice and the fact that xanthoma development has a dramatic effect on skin thickness (Figure 9), skin samples from ApoE-KO mice were separated into two groups depending on the histological presence of xanthoma: “non-diseased” and “diseased” skin. As the diseased skin phenotype is primarily a consequence of apoE deficiency, rather than age alone, only non-diseased skin was used to measure age-specific changes such as skin thinning (Figure 11). When fed a high fat diet, WT mice had significantly thicker skin than the control group at the 5, 15 and 30 week time points (Figure 12A). ApoE deficiency alone resulted in no significant difference over time compared to WT controls as shown in Figure 12B. Interestingly, skin from the high fat diet-fed ApoE-KO group, was significantly thinner than the WT control group at 30 weeks, despite being slightly thicker than the control group at 15 weeks when thickness was measured over time (Figure 12C). This suggests that these changes are not simply a result of developmental differences but rather a change that occurs at an accelerated rate over time compared to the WT controls. Skin thinning in ApoE-KO mice appeared most apparent in the subcutaneous fat layer, which was noticeably thinner than the WT controls on a chow and especially on a high fat diet (Figure 11). These results suggest that ApoE-KO mice fed a high fat diet display premature skin atrophy and a loss of subcutaneous fat.

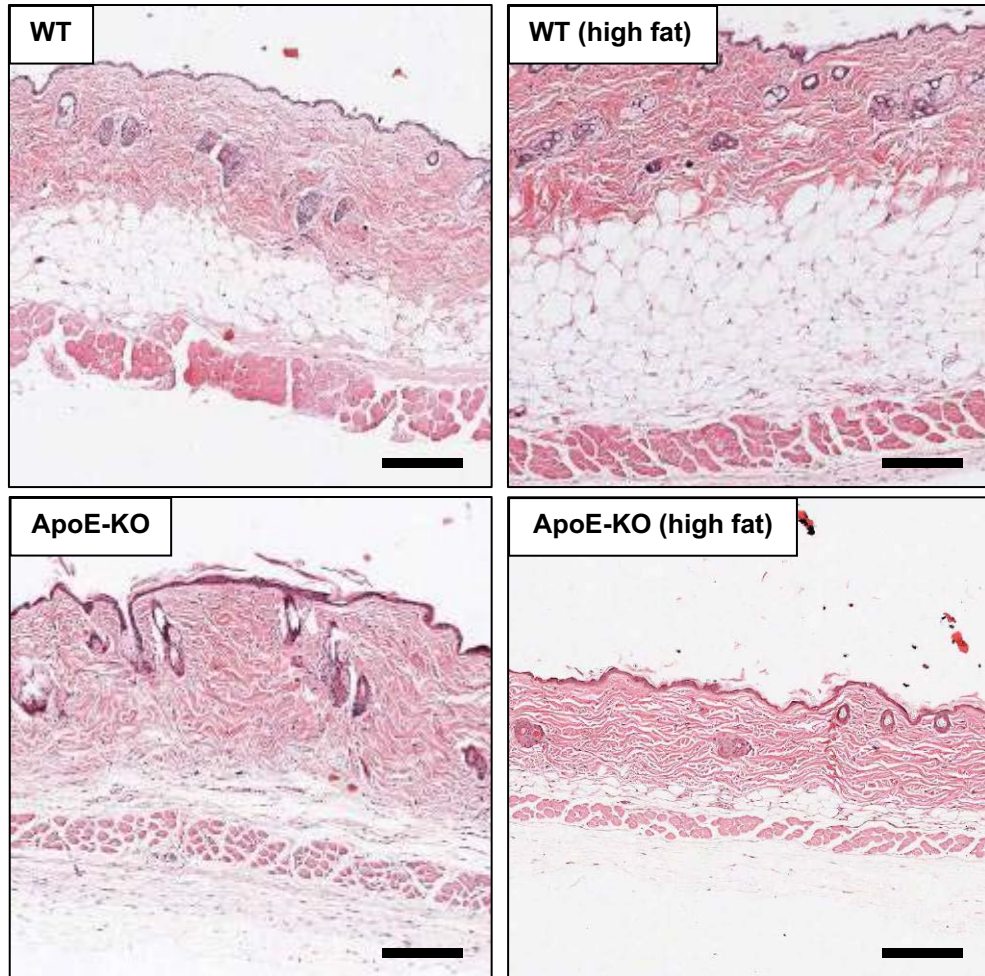


Figure 11. Skin histology of wild type versus apolipoprotein E knockout mice at 30 weeks. Representative hematoxylin and eosin stained skin cross-sections from wild type and apolipoprotein E knockout mice fed a regular chow or high fat diet for 30 weeks. Scale bars = 200 μ m.

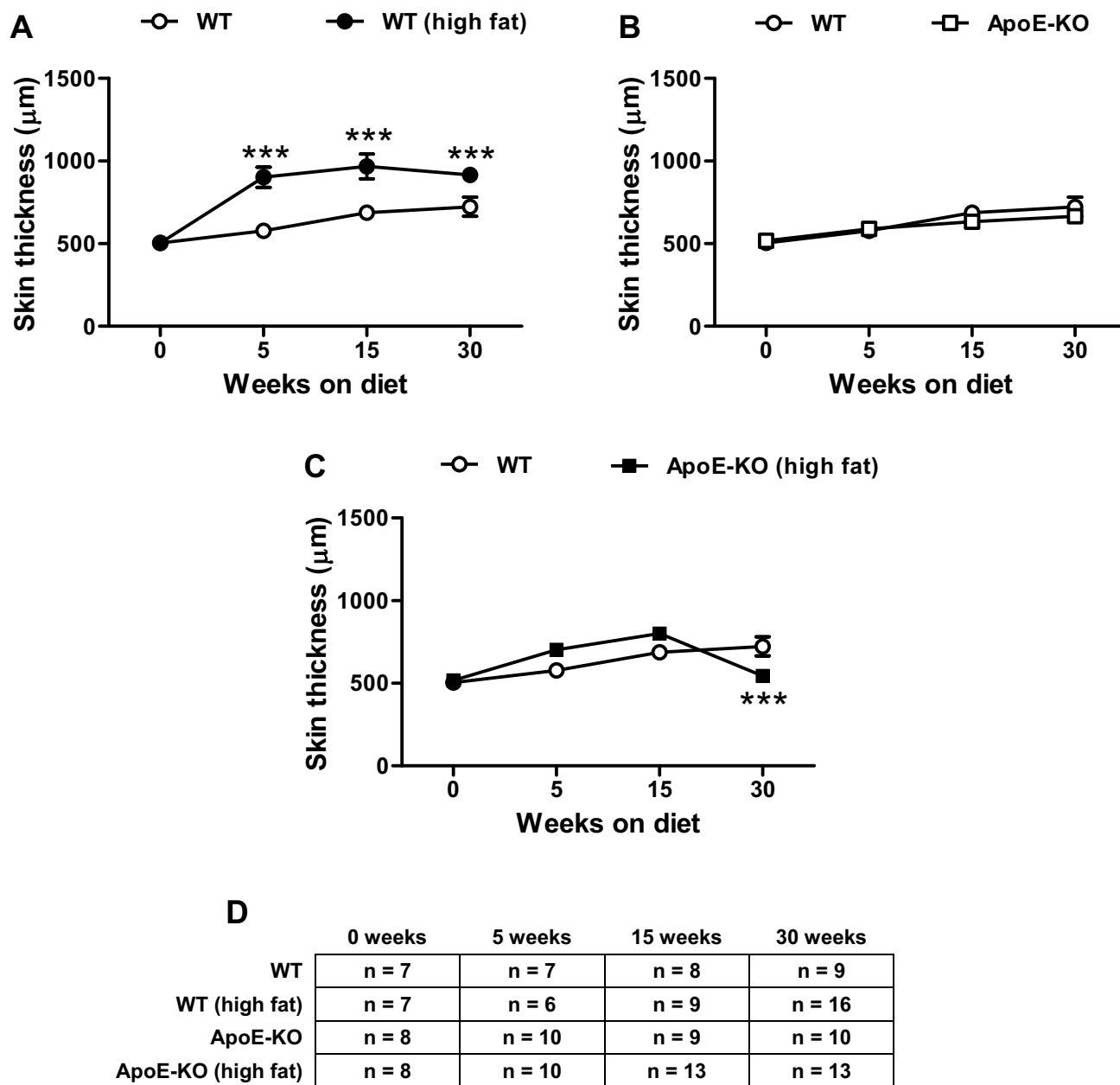


Figure 12. Age-related change in skin thickness of wild type versus apolipoprotein E knockout mice. Skin thickness of wild type (WT) mice compared to (A) WT (high fat), (B) apolipoprotein E knockout (ApoE-KO) and (C) ApoE-KO (high fat) groups was measured at 0, 5, 15 and 30 weeks using non-diseased skin sections. (D) Summary of the numbers of mice used for each time point in each group. (Error bars represent the mean \pm SEM, some error bars are within the symbol). *** $P < 0.005$ (2-way ANOVA with bonferroni post test).

4.2.4 Collagen disorganization

Intrinsic aging of the skin is typically associated with a decrease in dermal collagen organization and density [195, 196]. To determine if ApoE-KO mice exhibit differences in collagen content in the non-diseased skin, picrosirius red staining was used on formalin fixed skin sections and analyzed for changes in collagen content and structure. Dermal collagen from the chow-fed WT control group exhibited typical red/orange staining of thick, dense collagen fibres at the 30 week time point (Figure 13). In contrast, the non-diseased skin from high fat diet-fed ApoE-KO mice often displayed dermal collagen that was loosely packed, and less structured than the control group (Figure 13).

These observations were expanded upon using multi-photon microscopy. Although analysis of fixed, thin sliced sections can provide useful information regarding collagen content and structure, important three dimensional and organizational properties may be missed or altered during processing. We took advantage of the birefringent properties of collagen to visualize collagen structure and organization in unfixed, unstained thick skin samples in three dimensional space using multi-photon microscopy. Highly ordered fibril-forming collagens (Type I, II, III, etc.) produce second harmonic generation (SHG) signals without the need for any exogenous label [197, 198]. These SHG signals correlate with the density and organization of the collagen matrix rather than total collagen content. Only non-diseased skin was used for these experiments to ensure any ECM changes observed were not the result of xanthoma formation but rather the result of a more intrinsic aging process. When collagen density was monitored over time, the 0 week time point appeared similar for the WT and ApoE-KO groups (Figure 14). The chow-fed WT group appeared to show a slight decrease in collagen density over time while the ApoE-KO mice fed a high fat diet exhibited a reduced SHG signal as a function of age beginning at 5

weeks and at a greater rate than the WT controls demonstrating an increased rate of collagen modification and disorganization resulting in a significant loss of collagen density by 30 weeks (Figure 14). To confirm that the skin used in these experiments was regular, non-diseased skin, samples were fixed in 10% buffered formalin following these experiments and examined histologically using H&E staining. Upon histological examination, the high fat diet-fed ApoE-KO skin chosen for these experiments did not show evidence of xanthomatosis, confirming the observed changes in collagen density are an intrinsic property, rather than brought on by xanthoma formation (data not shown). These results suggest that age-related ECM changes are occurring in the skin of high fat diet-fed ApoE-KO mice even in skin sections without xanthoma formation at an increased rate compared to WT mice leading to premature skin aging.

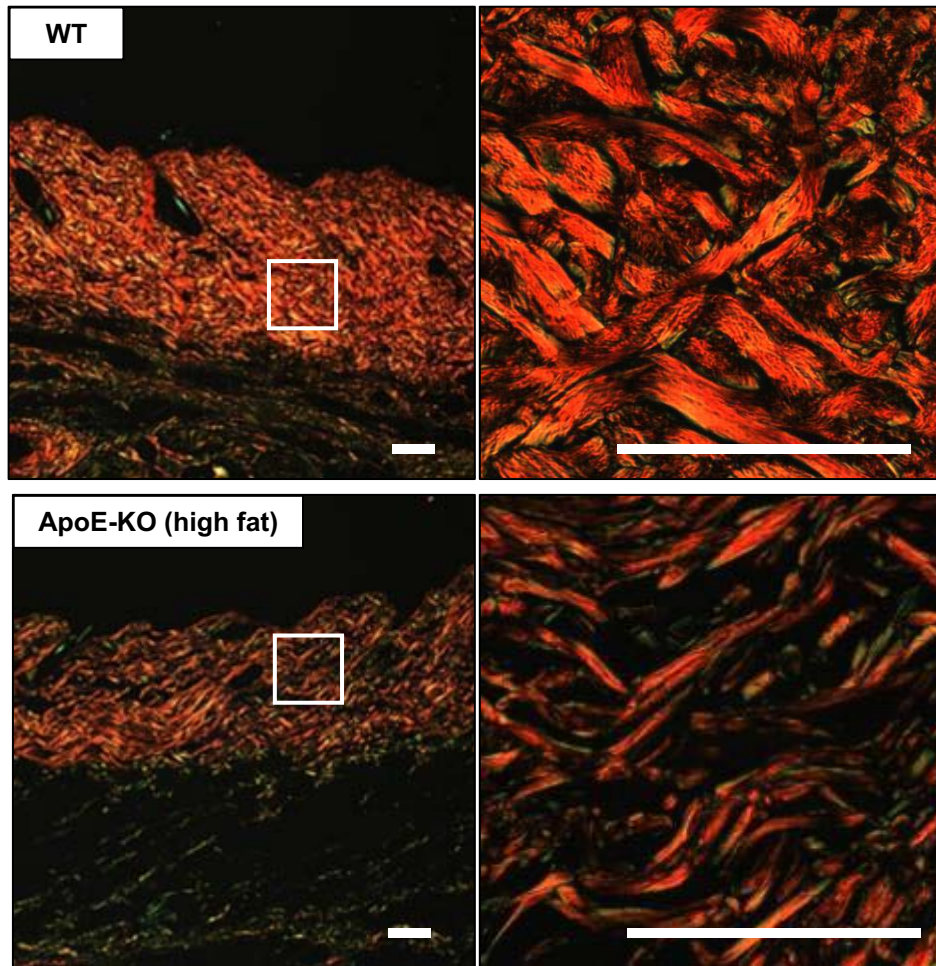


Figure 13. Reduced dermal collagen in apolipoprotein E knockout mice fed a high fat diet. Non-diseased skin sections from wild type and apolipoprotein E knockout mice fed a high fat diet stained for collagen using picrosirius red. Mice are at the 30 week time point. Scale bars = 100 μ m.

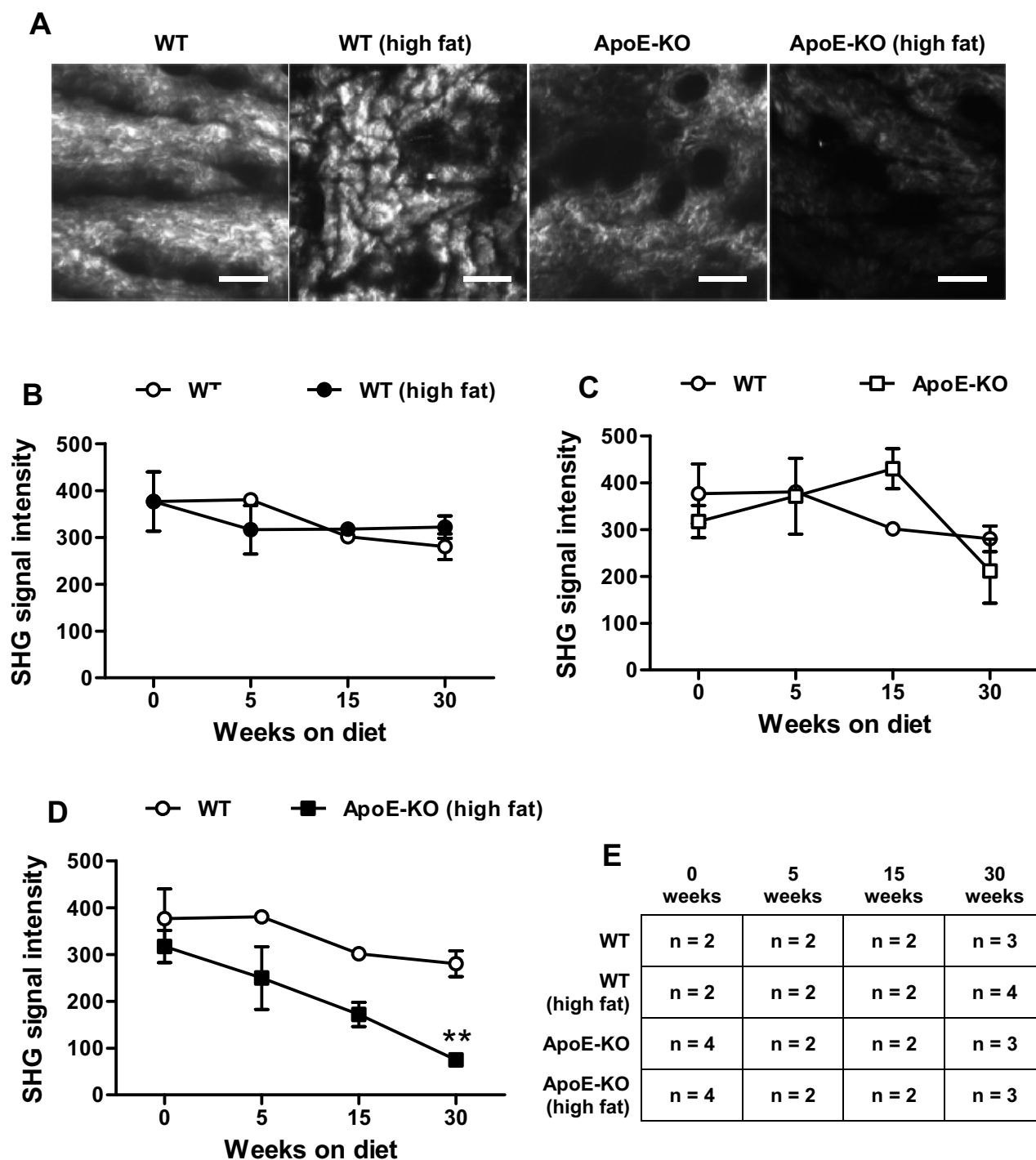


Figure 14. Accelerated loss of dermal collagen density in apolipoprotein E knockout mice fed a high fat diet. (A) Representative pictures of flattened three dimensional second harmonic generation (SHG) images taken from wild type (WT) or apolipoprotein E knockout (ApoE-KO) mice fed a regular chow or high fat diet for 30 weeks. (B-D) Collagen density as a function of time expressed as the intensity of the SHG signal for WT mice compared to WT (high fat), ApoE-KO and ApoE-KO (high fat) groups. (E) Summary of the numbers of mice used for each time point in each group. (Error bars represent the mean \pm SEM, some error bars are within the symbol). Scale bars = 80 μ m. ** $P < 0.01$ (2-way ANOVA with bonferroni post test).

4.2.5 Collagen and elastin abnormalities in diseased skin

Following investigation of the non-diseased skin for age-specific changes, diseased skin sections were further examined to assess the nature of skin disease in this model. Diseased skin sections were stained with picrosirius red and visualized using polarized light. As shown in Figure 15, the diseased skin lesions display clear alterations in collagen organization and structure compared to non-diseased skin from WT control mice (Figure 15). Collagen fibres were often arranged in a more parallel orientation with thinner collagen bundles in the diseased skin (Figure 15), which would help to explain the increased stiffness and skin frailty that was observed in these lesions.

To examine elastin content in the diseased skin, Luna's elastin stain was used. While the WT control mice at 30 weeks demonstrated diffuse elastin distribution with thin elastic fibres and minimal large elastin bundles (Figure 16), the diseased skin of ApoE-KO mice displayed increased elastin deposition in the papillary dermis as well as abnormal elastin bundle deposits in the dermis (Figure 16). These elastin abnormalities are similar to that which is observed during solar elastosis in photodamaged human and mouse skin [196, 199], suggesting similar mechanisms may be involved in the onset of these elastin abnormalities.

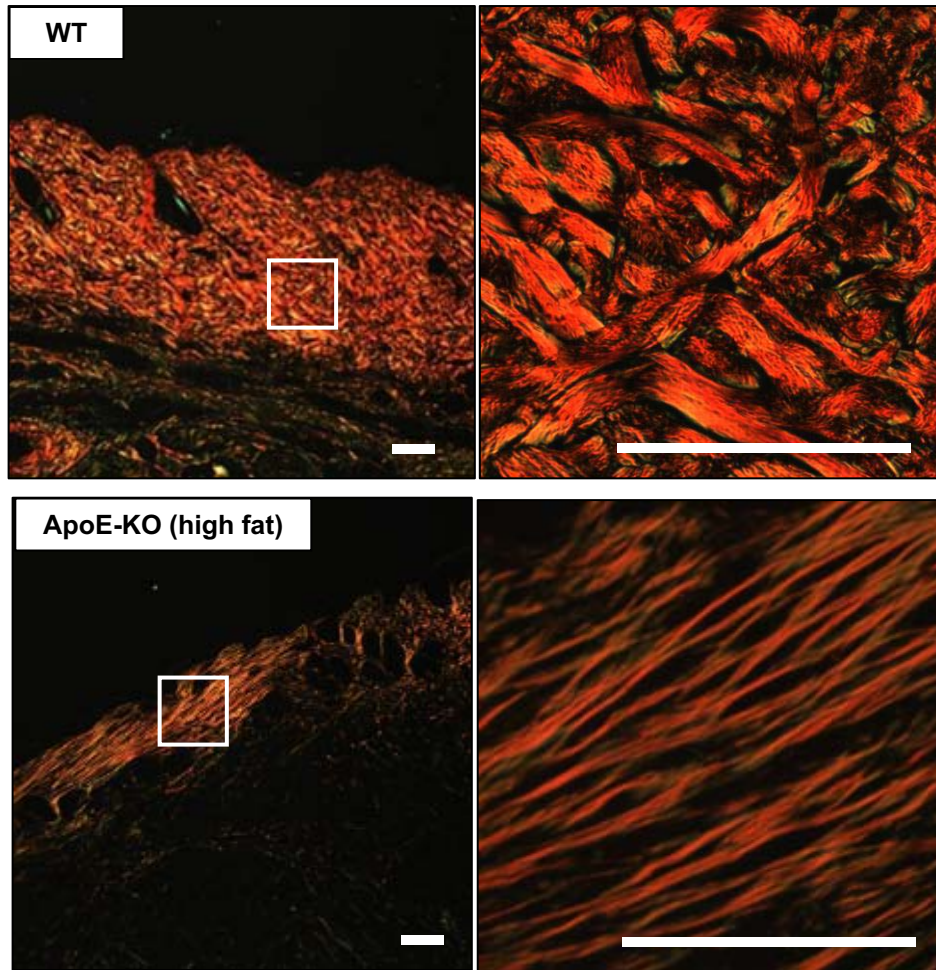


Figure 15. Collagen remodelling in diseased skin from apolipoprotein E knockout mice. Diseased skin cross-sections sections from a wild type control mouse and an apolipoprotein E knockout mouse fed a high fat diet containing xanthoma. Sections are stained for collagen using picrosirius red. Both mice are at 30 weeks. Scale bars = 100 μ m.

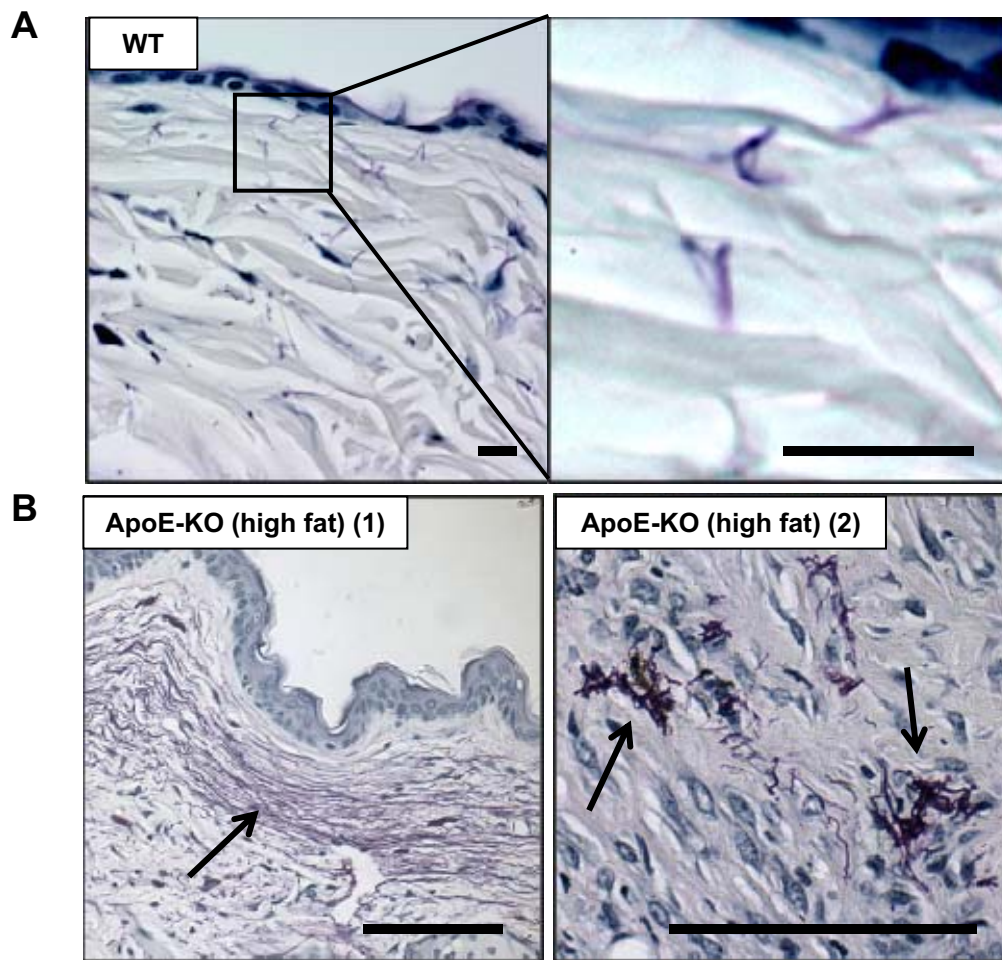


Figure 16. Abnormal elastin deposits in diseased skin from apolipoprotein E knockout mice. (A) Non-diseased skin from a wild type mouse stained with Luna's elastin (elastin stains dark purple - arrows) (scale bars = 10 μm). (B) Diseased skin from an apolipoprotein E knockout mouse fed a high fat diet stained with Luna's elastin showing abnormal elastin deposits (arrows) (scale bars = 100 μm). All mice are at 30 weeks.

4.3 Discussion

ApoE is linked to longevity and a number of age-related diseases in addition to the well described atherosclerosis phenotype [160, 178, 181]. In the present chapter, we demonstrate that a high fat diet has a profound effect on healthy aging of the skin in ApoE-KO mice. Previous studies have also demonstrated that a high fat diet increases the severity of xanthomatous lesions in the skin of ApoE-KO mice and feature noticeable immune infiltrate including lymphocytes, macrophages, foam cells [177]. In this study, not only does a high fat diet affect the frequency and severity of these inflammatory lesions as the mice age, but also results in a frail, thinned skin state along with considerable age-related alterations in the structural organization of collagen in the absence of xanthoma. When ApoE-KO mice were fed a high fat diet for 30 weeks, they demonstrated frailty and increased morbidity compared to the WT controls. This was also observed histologically in the form of increased skin lesions and skin thinning along with a loss of subcutaneous adipose tissue. Although xanthoma development occurred regardless of diet in ApoE-KO mice, only the high fat diet-fed ApoE-KO mice displayed intrinsic aging characteristics in the non-diseased skin such as skin thinning and loss of dermal collagen density at 30 weeks. Analysis of collagen and elastin in the diseased skin samples demonstrated considerable remodelling of collagen along with abnormal elastin deposits. The presence of age-related changes in the non-diseased skin of ApoE-KO mice, together with the thickened, remodelled, pro-inflammatory state of the xanthoma skin suggest that ApoE-KO mice demonstrate features of both intrinsic/chronological skin aging and extrinsic aging similar to photoaging with both resulting in ECM changes that mimic these forms of skin aging in humans. In humans, skin thinning is a hallmark of aging skin in the absence of disease [86]. In the present study, we observed significant thinning of the non-diseased skin in the high fat diet-fed ApoE-

KO mice compared to WT controls over time, which appeared to be largely due to a loss of subcutaneous fat. In addition to thinning, skin aging also involves changes in ECM content, including the loss and disorganization of collagen fibres [195, 196]. Non-diseased skin in high fat diet-fed ApoE-KO mice also demonstrated decreased collagen density in skin sections stained with picrosirius red. A significant loss in collagen density in the dermis of high fat diet-fed ApoE-KO mice was also shown by SHG and multi-photon microscopy. Subsequent fixation and histological analysis of these skin tissues confirmed that the decrease in collagen density occurred in non-diseased skin and that the decreased SHG signal was not simply due to the presence of xanthoma. Previous studies in ApoE-KO mice have documented increased pro-inflammatory cytokines such as IL-6 in multiple organs compared to WT mice that increase further with age [178]. This pro-inflammatory state may be related to the anti-inflammatory and anti-oxidative properties of ApoE [200]. ApoE is also expressed and secreted by adipocytes in the skin and is involved in fat and cholesterol intake and storage by adipocytes [201, 202]. Not surprisingly, decreased adipocyte content was obvious in the skin of ApoE-KO mice at 30 weeks while noticeable immune infiltrate was present, particularly in areas containing xanthomas. Macrophage-derived ApoE also facilitates cholesterol efflux from macrophages, resulting in the formation of lipid-loaded foam cells seen in the skin of ApoE-KO mice [177, 203-205]. Macrophage foam cells are also a known source of pro-inflammatory mediators and have been considered as an important player in inflammatory diseases such as atherosclerosis [reviewed in 80]. Future work investigating a potential role of skin-derived ApoE in regulating inflammation in the skin will improve our understanding of the mechanisms involved in skin aging and disease observed in high fat diet-fed ApoE-KO mice.

Current theories of aging suggest that oxidative stress and inflammation are major contributors to the aging process. The free radical theory of aging was proposed over 50 years ago and states that oxidative stress due to reactive oxygen species causes damage to cellular and molecular components which leads to an overall decline in function [77]. More recently the “inflammation hypothesis of aging” was proposed suggesting that inflammation resulting from reactive oxygen and/or reactive nitrogen species is involved in tissue damage, deterioration and pathogenesis that occurs with increasing age [79]. Our current findings suggest that ApoE deficiency combined with a high fat diet results in an increased susceptibility to inflammatory skin conditions along with other age-related changes such as skin thinning and collagen disorganization. In summary, ApoE-KO mice fed a high fat diet can be used to model hallmark changes in normal aging skin such as skin thinning and a loss of dermal collagen density.

5. Granzyme B contributes to skin aging and extracellular matrix remodeling in apolipoprotein E knockout mouse skin

5.1 Introduction

GzmB was once thought to function exclusively as a cytotoxic lymphocyte-secreted, proapoptotic protease in immune-mediated killing of target cells [9, 206]. However, recent evidence is challenging this paradigm as a pathogenic role for GzmB in ECM cleavage and loss of tissue integrity is emerging [207, 208]. ApoE-KO mice fed a high fat diet exhibit an increased susceptibility to chronic inflammatory skin disease, featuring the presence of several immune cell types known to express GzmB during chronic inflammation. Additionally, substantial remodelling of the ECM also occurs in the diseased skin of these animals. ApoE-KO mice fed a high fat diet often developed inflammatory skin lesions early in life (in as little as 7 weeks on a high fat diet) that became severe enough to warrant early euthanasia for humane reasons. In addition, remodeling and thinning of the dermis was also observed featuring a significant loss of collagen density and organization.

ECM remodeling by GzmB in the skin during chronic inflammation could potentially occur through the degradation of a number of different ECM substrates. Importantly however, *in vitro* experiments performed by our laboratory and by others have confirmed that collagen is not cleaved by GzmB [63 and unpublished observations]. It is therefore unlikely that the collagen disorganization observed in ApoE-KO mouse skin is due to a direct interaction of GzmB with collagen. Despite this, several other components of the ECM are able to interact with collagen, and can have a dramatic effect on the organization and spacing of collagen fibres. Decorin is a small leucine-rich proteoglycan that has been shown to be essential for proper collagen organization and spacing in the skin [94, 95]. Mice deficient in decorin have highly disorganized collagen as well as thin and fragile skin that is prone to tearing [95]. An increasing number of

GzmB substrates, including decorin, have been identified in recent years however the impact of GzmB-mediated cleavage of these substrates *in vivo* is still in its infancy [64, 66].

Given what was observed in the skin of ApoE-KO mice fed a high fat diet, the susceptibility to chronic inflammation and remodeling of the ECM, we investigated the role of GzmB in this process using GzmB/ApoE double knockout (DKO) mice to determine if GzmB-mediated degradation of ECM contributes to accelerated skin aging in ApoE-KO mice.

5.2 Results

5.2.1 Granzyme B deficiency reduces morbidity and weight loss

To determine the effect of GzmB on age-related morbidity and weight loss in ApoE-KO mice, DKO mice were given either a regular chow or high fat diet for 30 weeks. Interestingly, the appearance of severe xanthomas was delayed in the high fat diet-fed DKO mice compared to the ApoE-KO mouse group with the first case requiring euthanasia appearing at 19.9 weeks (Figure 17 and Table 3). By comparison, at 19.9 weeks, 8 mice from the high fat diet-fed ApoE-KO group (25%) already required euthanasia, with the first occurring as early as 7 weeks (Figure 17 and Table 3). DKO mice fed a regular chow diet appeared to develop xanthomas in some cases (2/11 or 18%) but were never severe enough to require euthanasia prior to 30 weeks unlike the chow fed ApoE-KO mice, of which 2/31 (6%) required premature euthanasia (Figure 17). These results suggest that GzmB contributes to lesion severity and that reduced GzmB delays the onset of these skin pathologies. Table 3 summarizes the incidence and severity of the skin lesions in all groups.

To examine the role of GzmB in the weight loss that occurred in ApoE-KO mice at 30 weeks, DKO mice were also weighed after being fed a regular chow or high fat diet for 30 weeks. While the high fat diet ApoE-KO mice weighed significantly less than the WT control mice DKO mice fared much better, with the high fat diet-fed DKO mice weighing significantly more than ApoE-KO mice fed a high fat diet for 30 weeks (Figure 18). No major differences in weight were observed between genotypes when fed a regular chow diet for 30 weeks. These results suggest that GzmB contributes to frailty and weight loss in ApoE-KO mice and that DKO mice exhibit better health overall when fed a high fat diet for 30 weeks.

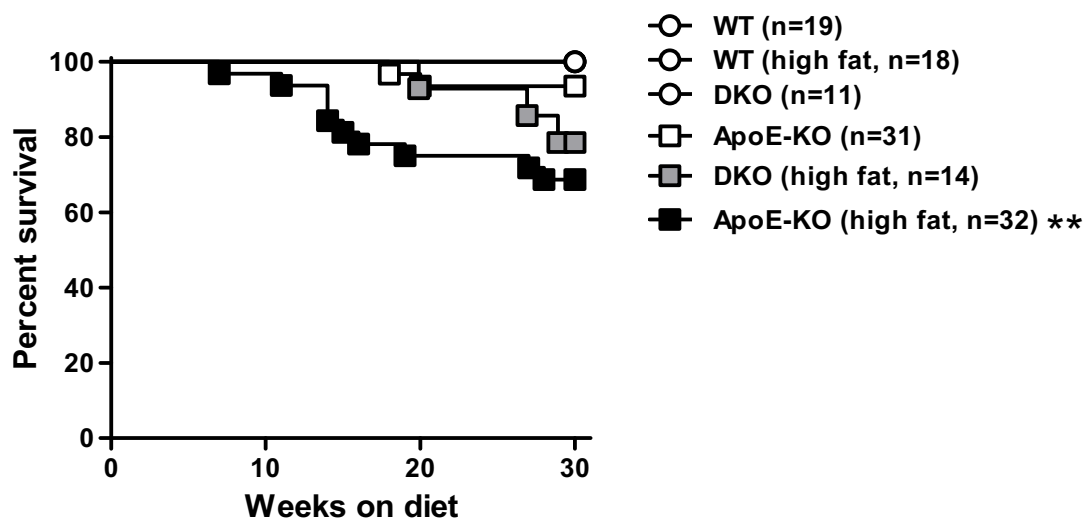


Figure 17. Delayed morbidity in granzyme B deficient apolipoprotein E knockout mice fed a high fat diet. Survival curve for wild type (WT), apolipoprotein E knockout (ApoE-KO) and double knockout (DKO) mice fed a chow or high fat diet for 30 weeks. While ApoE-KO (high fat) mice require euthanasia as early as 7 weeks, DKO (high fat) mice all survived until nearly 20 weeks. Fewer DKO mice overall required euthanasia compared to ApoE-KO mice when fed a high fat diet. $**P < 0.01$ compared to WT (Mantel-Cox test).

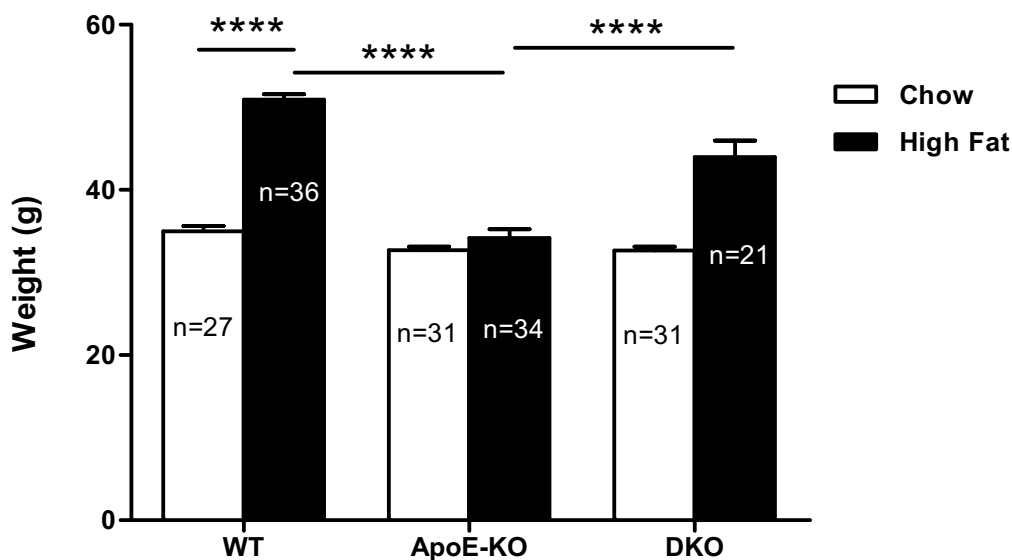


Figure 18. Weights of wild type, apolipoprotein E knockout and double knockout mice at 30 weeks. Weights of all groups of mice at the 30 week time point (error bars represent the mean \pm SEM). $****P < 0.001$ (One-way ANOVA with bonferroni post test).

Table 3. Summary of xanthoma/skin pathology incidence.

	WT	WT (high fat)	ApoE-KO	ApoE-KO (high fat)	DKO	DKO (high fat)
Total incidence of xanthoma/skin pathology	0/19 (0%)	0/18 (0%)	9/31 (29%)	13/32 (41%)	2/11 (18%)	3/14 (21%)
Skin pathologies resulting in premature euthanasia	0/19 (0%)	0/18 (0%)	2/31 (6%)	10/32 (31%)	0/11 (0%)	3/14 (21%)
Skin pathology identified at 30 weeks	0/19 (0%)	0/18 (0%)	7/31 (23%)	3/32 (9%)	2/11 (18%)	0/14 (0%)

5.2.2 *Granzyme B* deficiency protects against skin thinning in apolipoprotein E knockout mice

To determine whether GzmB deficiency protects against skin thinning and frailty in ApoE-KO mice, skin from DKO mice on a regular chow or high fat diet was also examined at 30 weeks. As mentioned above, the high fat diet for 30 weeks caused a significant decrease in thickness in ApoE-KO mice compared to the WT controls (Figure 19). High fat diet-fed DKO mice however were protected from skin thinning and displayed a significant increase in total skin thickness compared to the high fat diet-fed ApoE-KO group at 30 weeks (Figure 19), suggesting that GzmB contributes to age-related skin thinning and frailty in ApoE-KO mice.

Closer analysis of the individual layers of the skin at 30 weeks revealed that changes in total skin thickness in the non-diseased skin samples in ApoE-KO mice were due primarily to changes in the dermal and/or adipose tissue layers (Figure 20). While no significant differences were observed in epidermal thickness at the 30 week time point for any of the groups, dermal thickness was significantly thicker in both the chow-fed and high fat diet-fed DKO groups compared to the dermis of the high fat diet-fed ApoE-KO mice (Figure 20). Changes in the thickness of the adipose tissue layer varied the most, with the high fat diet-fed WT group demonstrating a significant increase and both ApoE-KO groups along with the chow-fed DKO group having significantly thinner adipose tissue layer than the chow-fed WT controls (Figure 20C). High fat diet-fed DKO mice showed no significant difference in adipose tissue thickness compared to either the chow-fed controls or the ApoE-KO groups (Figure 20C). These results confirm our previous observation and suggest that ApoE deficiency results in a decrease in total skin thickness due in large part to a decrease in adipose tissue while GzmB deficiency protects against skin thinning due in part to an increase in dermal thickness.

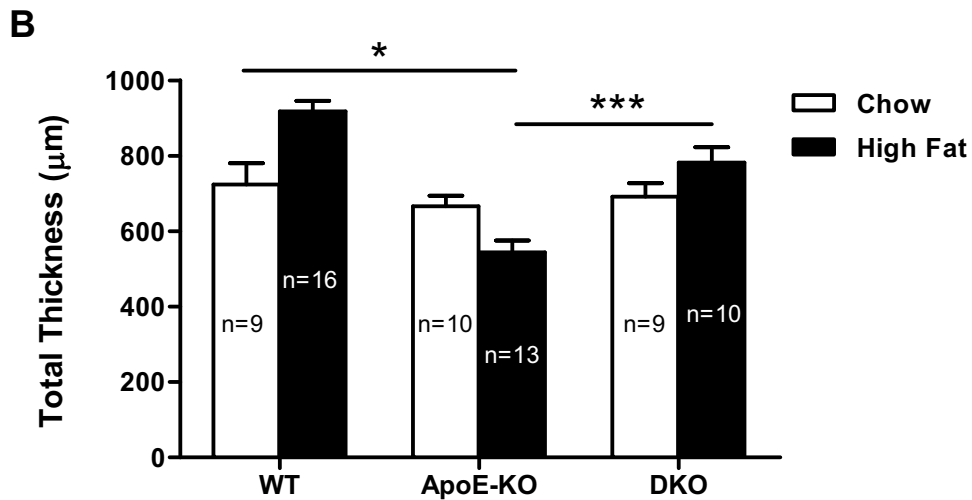
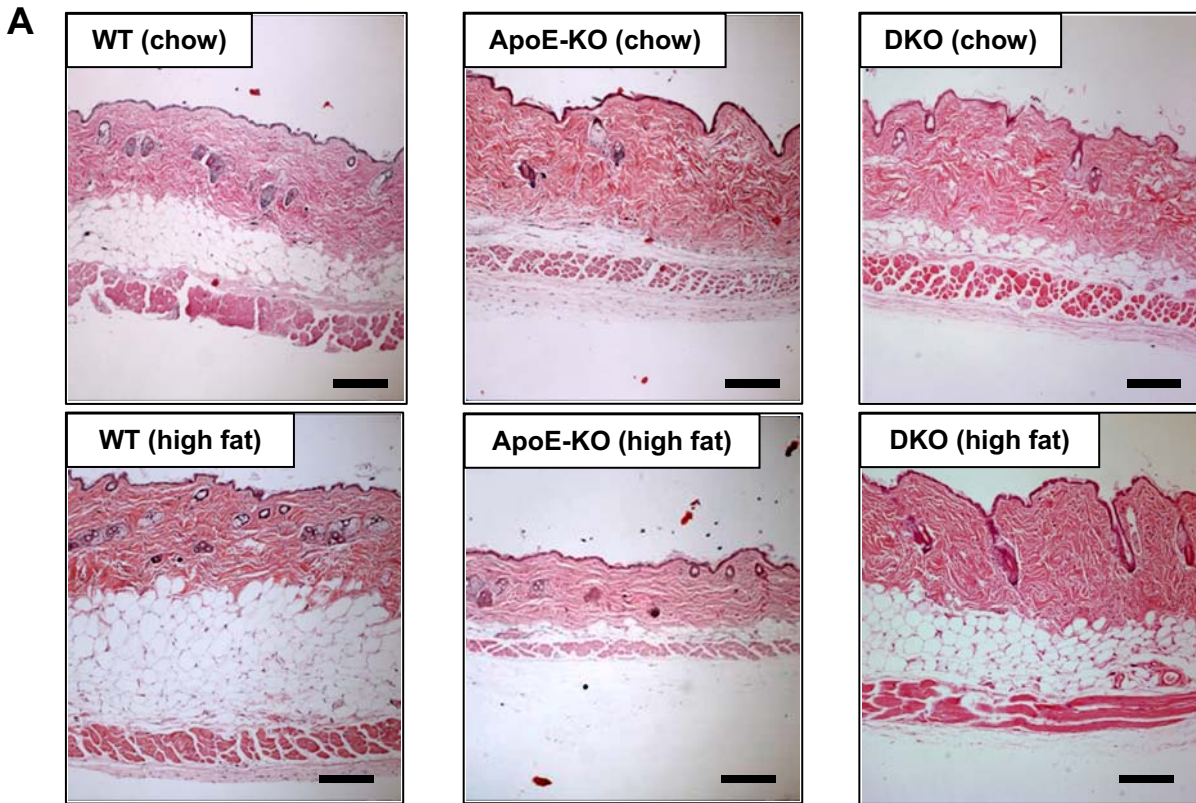


Figure 19. Granzyme B contributes to skin thinning in apolipoprotein E knockout mice. (A) Representative images of H&E stained skin cross sections from wild type (WT), apolipoprotein E knockout (ApoE-KO) and double knockout (DKO) mice. Scale bars = 200 µm. (B) ApoE-KO (high fat) mice had significantly thinner skin compared to WT controls while DKO (high fat) mice showed protection against skin thinning. Skin thickness from regular diet-fed mice remained relatively constant. All mice are at 30 weeks. Error bars represent the mean \pm SEM. * $P < 0.05$, *** $P < 0.005$ (One-way ANOVA with bonferroni post test).

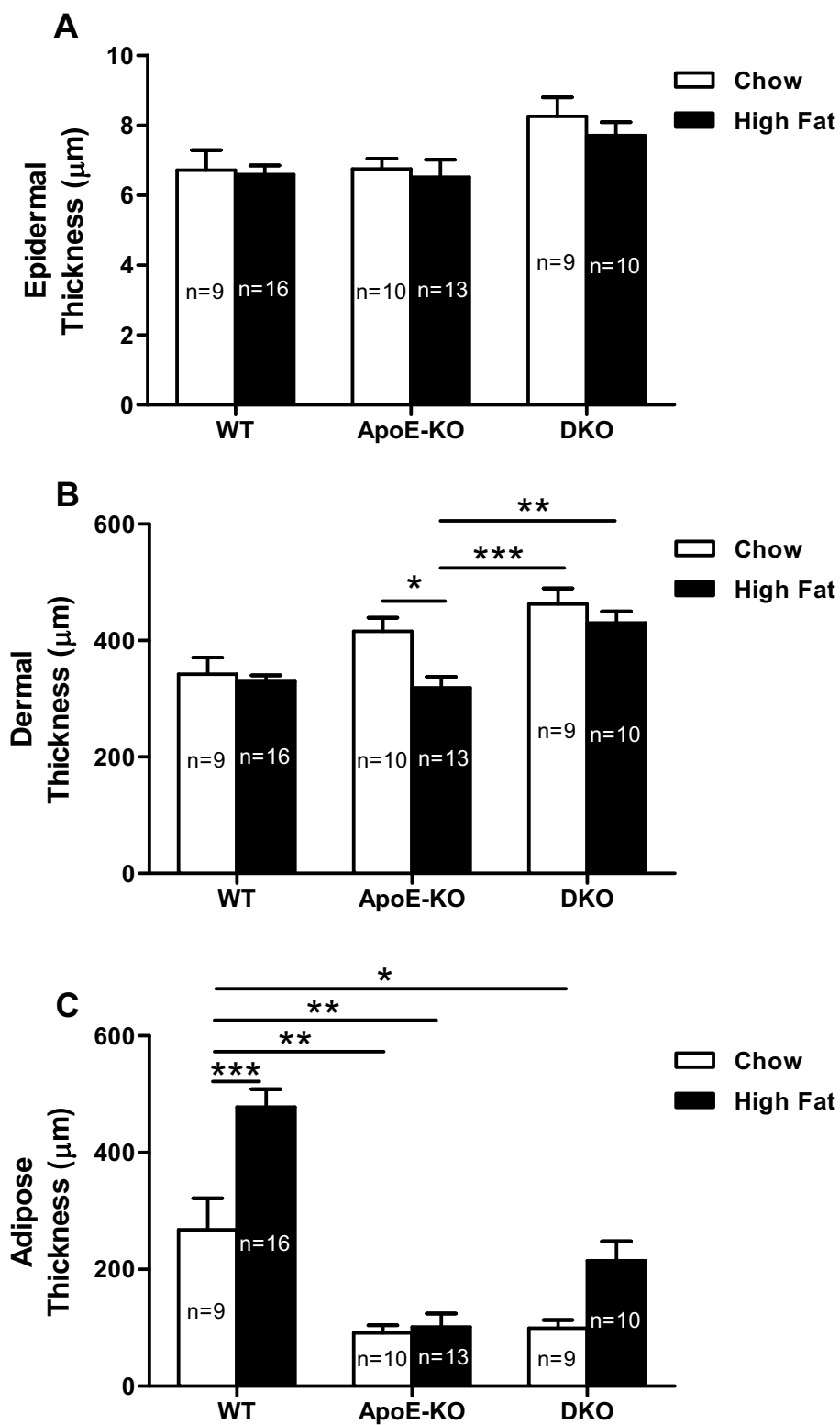


Figure 20. Analysis of skin layer thickness. Thickness of (A) epidermal, (B) dermal and (C) adipose tissue layers at 30 weeks for the wild type (WT), WT-high fat, apolipoprotein E knockout (ApoE-KO), ApoE-KO-high fat, double knockout (DKO) and DKO-high fat groups. Error bars represent the mean \pm SEM. * $P < 0.05$, ** $P < 0.01$, *** $P < 0.005$ (One-way ANOVA with bonferroni post test).

5.2.3 *Granzyme B* deficiency increases skin collagen density in apolipoprotein E knockout mice

To further examine the role of GzmB in the observed loss of collagen density in ApoE-KO mouse skin, DKO mouse skin was also examined using SHG after being fed a chow or high fat diet for 30 weeks as this was the time point where the most extreme differences were observed. Representative flattened three dimensional SHG images originating from the collagen matrix (grey) are shown in Figure 21A for all groups at the 30 week time point. As mentioned above, at the 30 week time point only the high fat diet-fed ApoE-KO mice exhibited significantly decreased collagen density in the skin compared to the chow-fed WT group as shown by the decreased SHG signal (Figure 21B) suggesting ApoE deficiency combined with a high fat diet result in a loss of skin collagen density. Both groups of DKO mice on either diet demonstrated a significant increase in skin collagen density when compared to the high fat diet-fed ApoE-KO group, suggesting that GzmB plays a role in the intrinsic aging process in the skin by facilitating the age-dependant disorganization of dermal collagen.

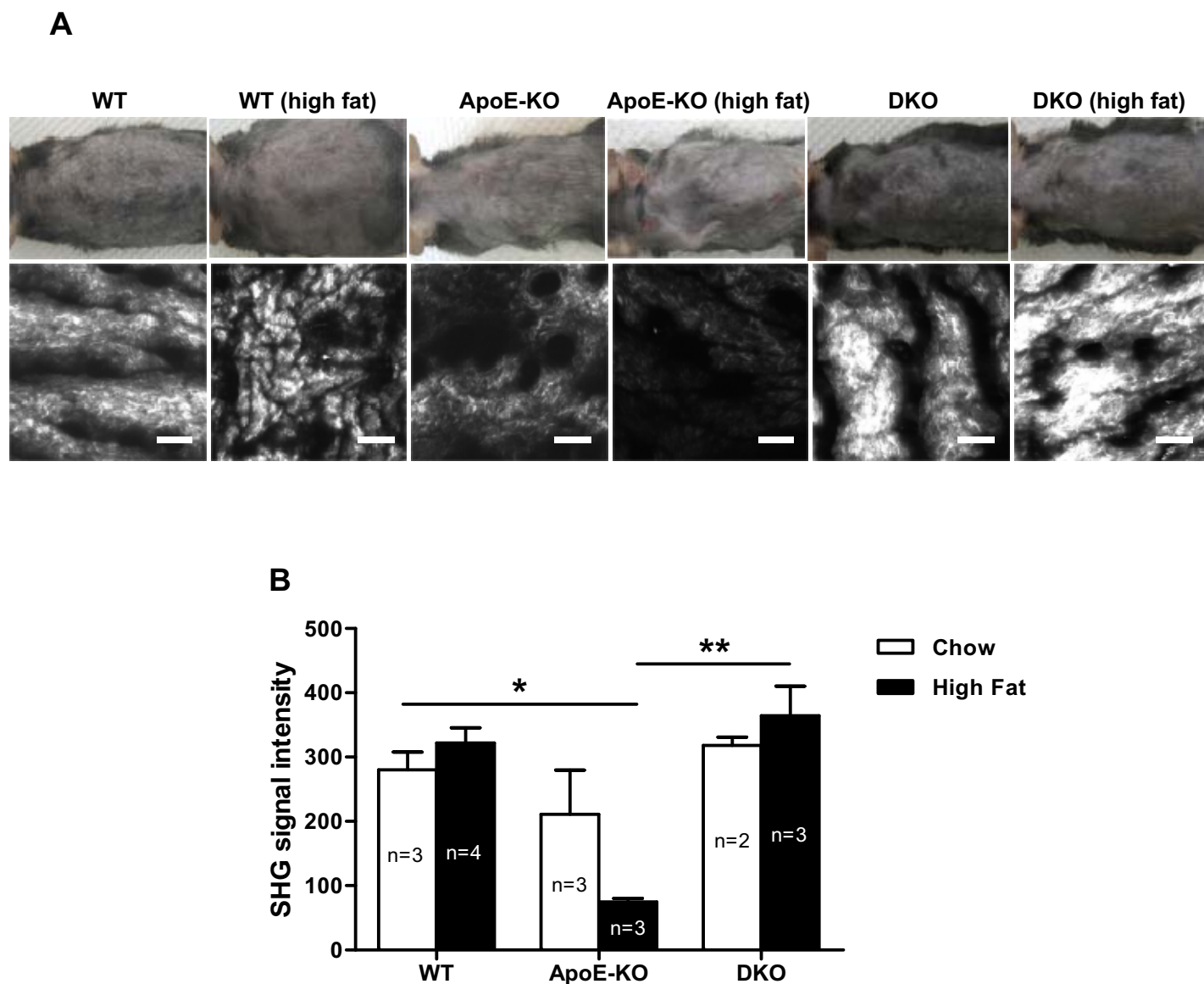


Figure 21. Loss of dermal collagen density in apolipoprotein E knockout mice rescued by knocking out granzyme B. (A) Representative three dimensional merged plane images of fresh ex-vivo unfixed, unstained non-diseased skin tissues obtained from wild type (WT), apolipoprotein E knockout (ApoE-KO) and double knockout (DKO) mice at 30 weeks fed either a regular chow or high fat diet. Gray colors are the second harmonic generation signal and represent the collagen matrix (scale bars = 80 μ m). (B) Quantification of collagen density at the 30 week time point for all groups. Error bars represent the mean \pm SEM. * $P < 0.05$, ** $P < 0.01$ (One-way ANOVA with bonferroni post test).

5.2.4 Decorin remodeling and granzyme B expression in the skin of apolipoprotein E knockout mice

Decorin is a proteoglycan that is critical in the regulation of collagen spacing and organization. We first demonstrated that GzmB is capable of cleaving decorin *in vitro* by incubating decorin with GzmB and analysing decorin by western blot (Figure 22). When 100 nM of GzmB was added to decorin and incubated for 24 h at room temperature, a complete loss of the full length decorin fragment was observed. This GzmB-mediated decorin degradation was prevented by the potent GzmB inhibitor, Compound 20 (Figure 22). When skin samples from non-diseased skin were stained with anti-decorin antibody, WT skin showed decorin staining throughout the dermis with an increasing intensity near the dermal epidermal junction (Figure 23A). The ApoE-KO mice on a high fat diet showed similar but more diffuse decorin staining (Figure 23A). Interestingly, DKO mice fed a high fat diet appeared to exhibit even more intense decorin staining than the WT control group in the non-diseased skin, particularly around the dermal-epidermal junction (Figure 23A). In the diseased skin sections of high fat diet-fed ApoE-KO mice, a marked loss of decorin was observed (Figure 23B). This loss of decorin was not observed to the same extent in the DKO mice when fed a high fat diet (Figure 23B). These results suggest that GzmB is capable of degrading the proteoglycan, decorin, and that GzmB-mediated decorin degradation may occur in the skin of high fat diet-fed ApoE-KO mice, potentially contributing to a loss of collagen density and organization.

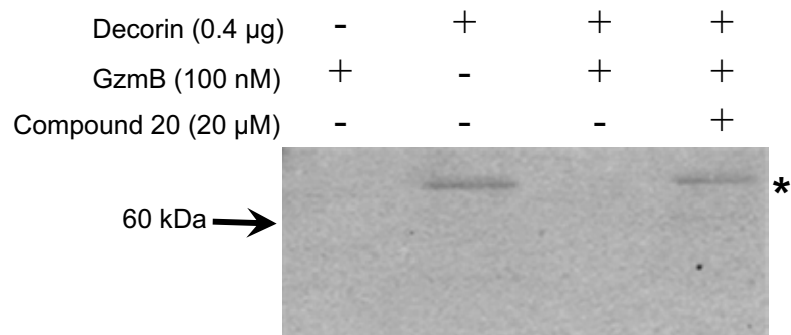


Figure 22. Granzyme B cleaves decorin *in vitro*. The addition of granzyme B (GzmB) to purified decorin results in degradation and apparent loss of full length glycosylated protein by 24 h. This is prevented when the potent GzmB inhibitor, Compound 20, is included. Asterisk = full length protein.

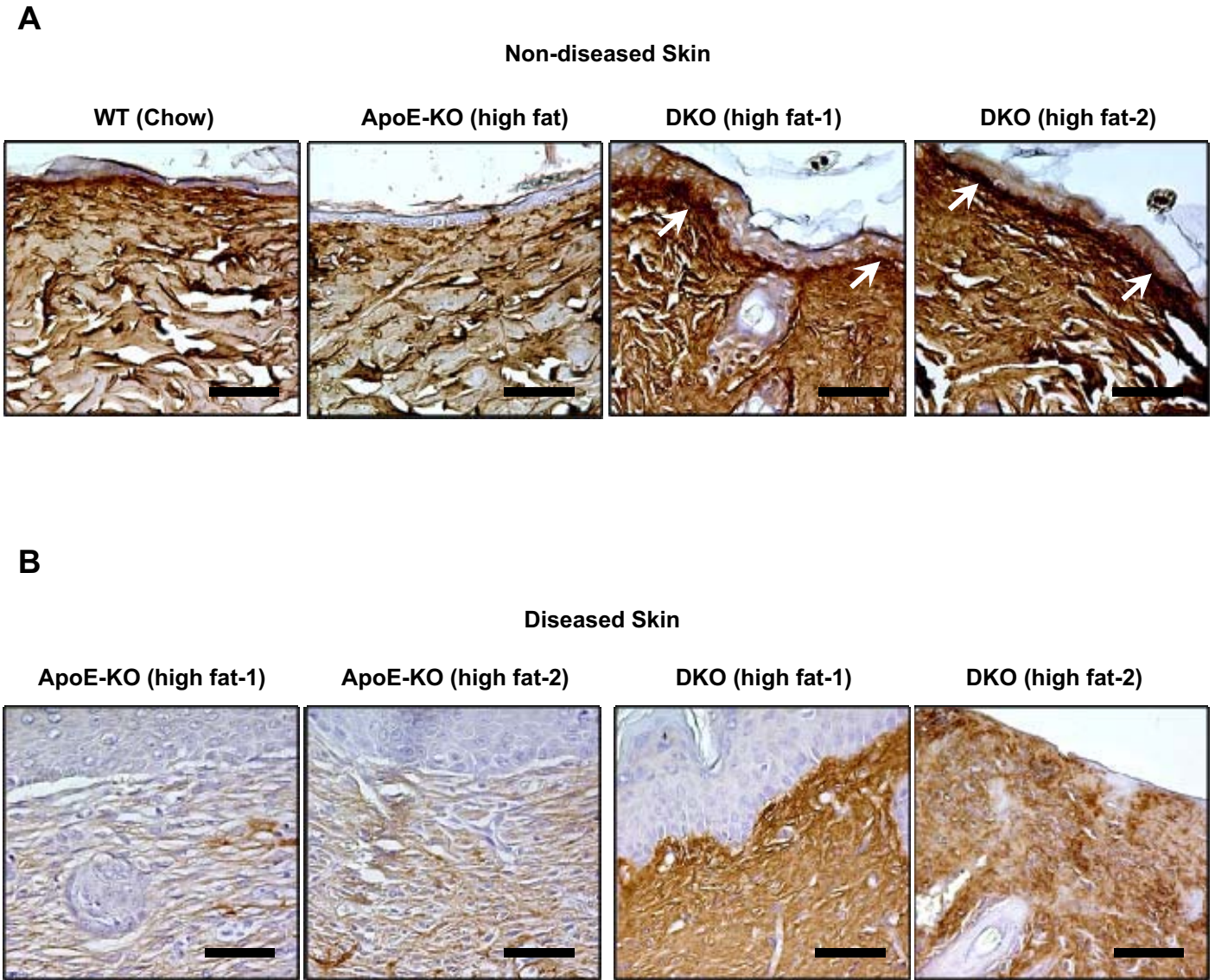


Figure 23. Granzyme B deficiency protects against loss of decorin in apolipoprotein E knockout mouse skin. (A) Decorin immunohistochemistry (brown) in the non-diseased skin from wild type (WT) mice, high fat diet-fed apolipoprotein E knockout mice (ApoE-KO) and high fat diet-fed double knockout mice (DKO). White arrows point to increased decorin near the dermal-epidermal junction (scale bars = 50 μ m). (B) Decorin immunohistochemistry (brown) in diseased skin from ApoE-KO (high fat) and DKO (high fat) mice (scale bars = 50 μ m).

5.2.5 Granzyme B localization and expression by mast cells

To look closer into the cell types that could be responsible for extracellular GzmB in the skin of ApoE-KO mice, dual staining for GzmB and mast cells was performed. Mast cells represent a potentially important source of extracellular GzmB in the skin as they are known to express GzmB but not perforin. Little to no GzmB positivity was observed in non-diseased skin sections, however when diseased skin sections from high fat diet-fed ApoE-KO mice were stained with anti-GzmB antibody, GzmB was readily observed in the lesions and was particularly prominent in proximity to the papillary dermis near the dermal-epidermal junction (Figure 24A). GzmB was also regularly observed in other areas of the injured skin. In particular, GzmB was abundant in proximity to microvessels (Figure 24A). The presence of GzmB in the injured skin corresponding to reduced decorin suggests that GzmB is capable of disrupting collagen spacing and organization in the skin through the cleavage of decorin. While the exact identity of the all GzmB-positive cells in the skin lesions is not known, dual staining for GzmB and mast cells revealed the presence of several GzmB-positive mast cells in the diseased skin. Because mast cells can express GzmB in the absence of perforin [26], mast cells may be an important source of extracellular GzmB in the skin of ApoE-KO mice although more work is needed to determine the exact percentage of mast cells that express GzmB and the exact role mast cell-derived GzmB plays in this model.

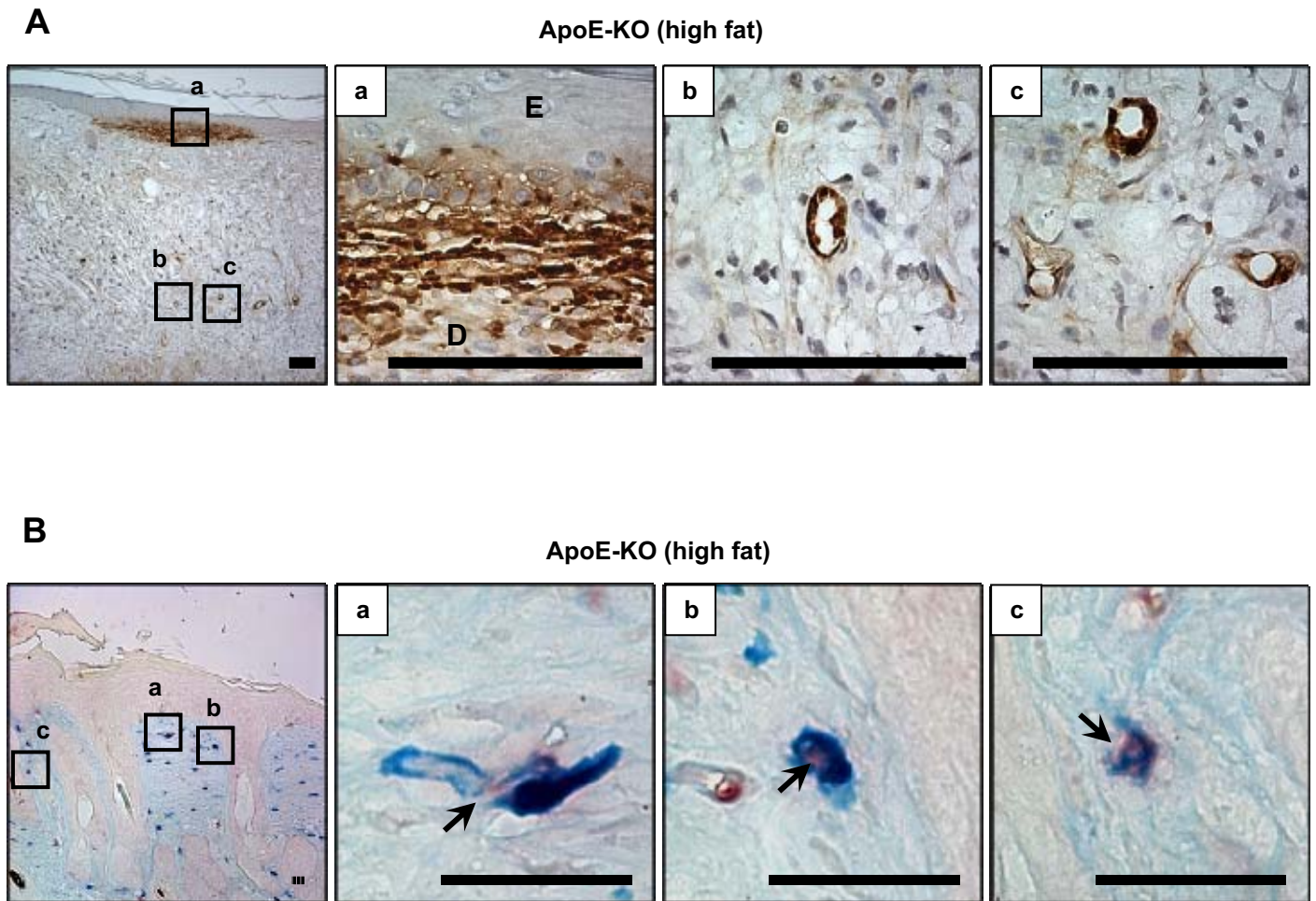


Figure 24. Mast cells express granzyme B in apolipoprotein E knockout mouse skin. (A) Granzyme B (GzmB) immunohistochemistry (brown) in diseased skin from a high fat diet-fed apolipoprotein E knockout (ApoE-KO) mouse. E denotes “epidermis” and D denotes “dermis”. (scale bars = 100 μ m). (B) Diseased skin from an ApoE-KO (high fat) mouse dual stained for mast cells and GzmB. Black arrows point to GzmB (red) inside mast cells (blue) (scale bars = 25 μ m).

5.3 Discussion

In this chapter, we provide evidence that the serine protease, GzmB, may play an important role in aging and disease of the skin through remodelling of key ECM proteoglycans such as decorin. Skin thinning in ApoE-KO mice was rescued by knocking out GzmB, as shown by analysing skin from high fat diet-fed DKO mice at 30 weeks, when the thinning observed in the high fat diet-fed ApoE-KO group was the most extreme. This is likely due to the increased dermal thickness observed in mice deficient in GzmB. The exact reason for this is unknown, however it is possible that the absence of GzmB in the DKO mice prevents certain GzmB-susceptible matrix components from being degraded, helping to maintain a thickened more dense dermal layer. We also show using the DKO mice, that the decrease in collagen density and organization observed in ApoE-KO mice may be rescued by blocking GzmB activity. This would support previous findings in which reduced ECM cleavage in DKO mice compared to ApoE-KO mice was observed in the context of angiotensin II-induced abdominal aortic aneurysm [13].

GzmB has been studied extensively for its ability to induce apoptosis in tumour and virally infected cells via its intracellular activity [9, 206]. GzmB is now known to cleave several important components of the ECM including fibronectin, vitronectin, laminin and fibrillin-1, whose cleavage could indirectly have profound effects on the major ECM constituents like collagen and elastin [12, 13, 63]. Decorin is another vital component of the ECM functioning to maintain proper collagen structure and organization [209]. Mice with a targeted disruption of decorin have fragile skin and abnormal collagen structure [95]. In this study we provide both *in vitro* and *in vivo* evidence that GzmB is capable of cleaving decorin. The presence of GzmB around the dermal-epidermal junction raises the possibility that GzmB is disrupting ECM

components such as decorin at this site. Indeed, DKO mice demonstrated an apparent increase in decorin staining in the skin near the dermal-epidermal junction. The presence of GzmB proximal to the epidermis of the skin raises the possibility of a non-immune cell source of GzmB in the lesion such as keratinocytes that are experiencing stress [210]. The presence of GzmB-expressing mast cells in the skin also provides a possible explanation for how GzmB gains access to the extracellular environment. Unlike other GzmB-expressing immune cells such as T cells and natural killer cells, mast cells express GzmB in the absence of perforin [26] suggesting that mast cell-derived GzmB is involved primarily in extracellular proteolysis in this model. Although little work has been devoted to precise actions of GzmB in skin pathologies, our work suggests that GzmB is an important player in ECM remodelling that takes place during intrinsic aging as well as the age-related inflammatory skin conditions observed in ApoE-KO mice.

Our current findings therefore suggest that ApoE deficiency results in an increased pro-inflammatory state in the skin, contributing to ECM remodelling and other age-related changes seen and that a high fat diet exacerbates these changes through a GzmB-mediated mechanism. These findings also suggest a novel role for GzmB in the skin involving the cleavage of decorin and the indirect remodelling of dermal collagen, a process that has major implications in ECM structure and skin fragility in aging and disease. The proposed mechanism is summarized in Figure 25.

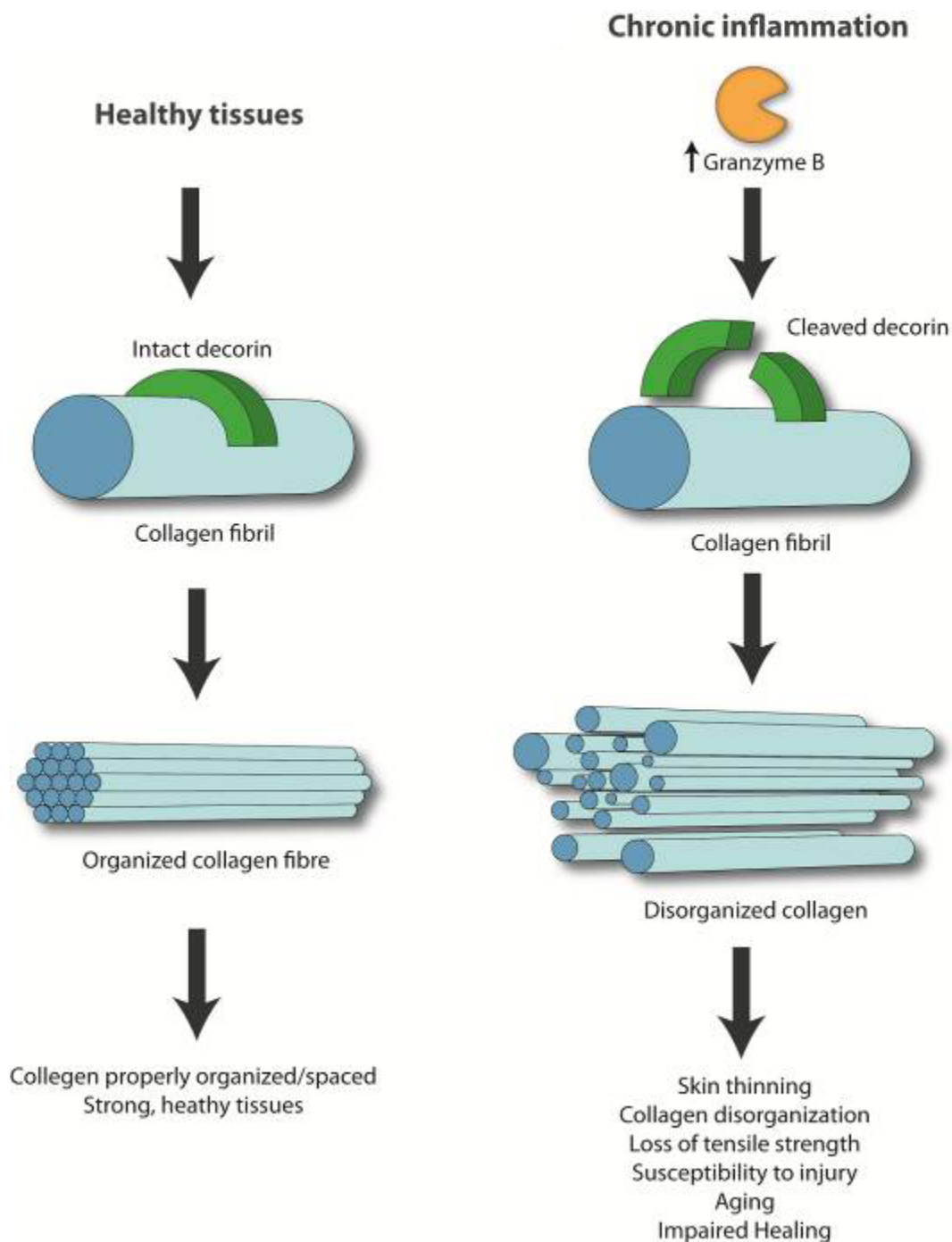


Figure 25. Potential consequences of granzyme B-mediated decorin degradation. Intact decorin binds strongly to collagen and assists in proper organization and spacing of collagen fibers. Degradation of decorin by granzyme B during aging and/or chronic inflammation could prevent proper interactions between collagen and decorin. This could lead to reduced collagen organization and improper spacing, contributing to skin aging and an increased susceptibility to injury.

6. Impaired wound healing in apolipoprotein E knockout mice

6.1 Introduction

ApoE-KO mice exhibit increased susceptibility to inflammation and inflammatory skin lesions that become more severe when fed a high fat diet [64, 177]. Several reports have documented the importance of ApoE in the skin, particularly with respect to adipose tissue [201, 202]. We have shown that ApoE-KO mice develop xanthomatous lesions that increase in severity with age and fail to heal/resolve requiring premature euthanasia for humane reasons.

Inflammation during wound repair plays a vital role in proper healing. A healthy immune response during wound healing helps to fight off infection, clear dead cells and other debris as well as matrix remodeling en route to a fully mature/healed wound. As important as inflammation is to acute wound healing, it is just as important that inflammation resolves when its role is finished. It is therefore critical that the immune response be very tightly regulated in order to function properly while at the same time, not causing excess damage. Chronic wounds exhibit chronic inflammation that fails to resolve. This can result in excessive matrix remodeling and tissue damage, causing the wound to remain open and delay healing. Several reports have documented a role for ApoE in regulating inflammation through the suppression of cytokines as well as lymphocyte, macrophage and neutrophil activation [162-176]. As mentioned above, ApoE-KO mice exhibit increased susceptibility to chronic inflammation in their skin and several other reports have documented altered immune responses in a variety of tissues.

These observations provide rationale for investigating the ApoE-KO mouse as a model that responds abnormally to cutaneous injury. As inflammation appears to be altered in the skin of these animals, we set out to determine if the ApoE-KO mouse experiences increased/chronic inflammation in response to injury resulting in delayed wound healing. As we have found that

age and diet have a profound impact on skin aging in ApoE-KO mice, we examined young and old mice on a regular chow or high fat diet for their ability to undergo normal wound healing.

6.2 Results

6.2.1 Impaired wound closure in apolipoprotein E knockout mice fed a high fat diet

WT and ApoE-KO mice were given a 1 cm diameter full thickness skin excision by punch biopsy at 7 (young) or 37 (old) weeks of age on their mid dorsum (Figure 26). All mice were fed a regular chow diet up until 7 weeks of age. Young mice were then wounded at 7 weeks while old mice were either maintained on a regular chow diet, or switched to a high fat diet for 30 weeks. At the end of the 30 weeks (37 weeks of age), old mice were wounded as described in Materials and Methods. Digital photographs were taken throughout the 16 day healing time and are summarized in Figure 26. For the young mice, both the WT and ApoE-KO groups showed complete wound closure after 16 days of healing. Likewise, wounds in the old WT and ApoE-KO mice all appeared to close fully by 16 days. However when old mice were fed a high fat diet for 30 weeks, only 40% of ApoE-KO mice showed complete wound closure compared to 100% in the high fat diet fed WT group. Histological analysis of the wounds at day 16 demonstrates a clear lack of wound closure in the ApoE-KO mice with clearly visible epithelial edges (Figure 27). All other groups show complete closure as seen by the closed keratinocyte layer. These results suggest that ApoE-KO mice fed a high fat diet are undergoing a malfunctioning wound healing response, resulting in delayed or impaired wound closure.

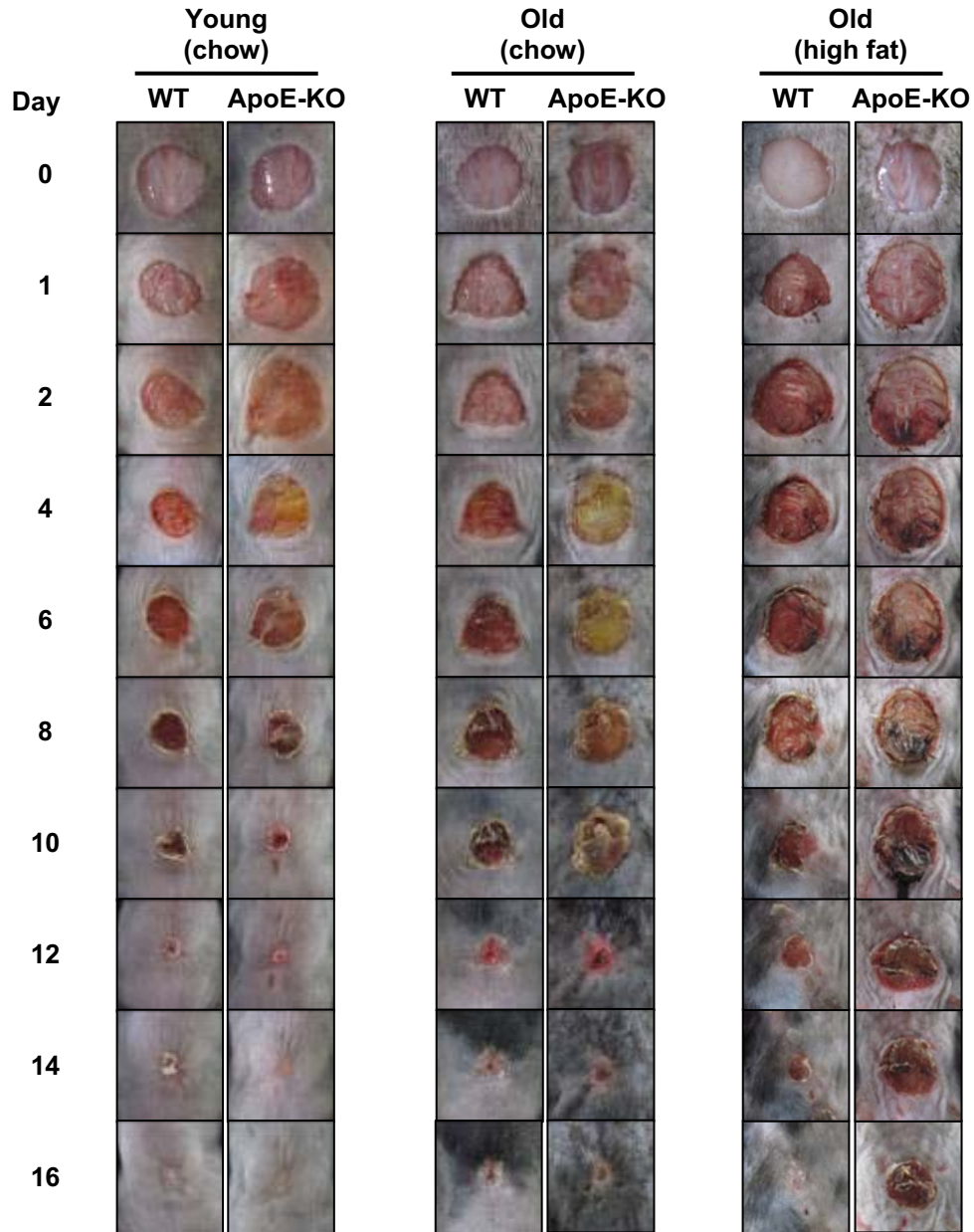


Figure 26. Delayed wound closure in high fat diet-fed apolipoprotein E knockout mice. Representative digital photographs of wild type (WT) and apolipoprotein E knockout (ApoE-KO) mice taken over the 16 day healing period. Old mice (37 weeks of age) were fed either a regular chow or high fat diet starting at 6-8 weeks of age while young mice (7 weeks) were fed only a regular chow diet.

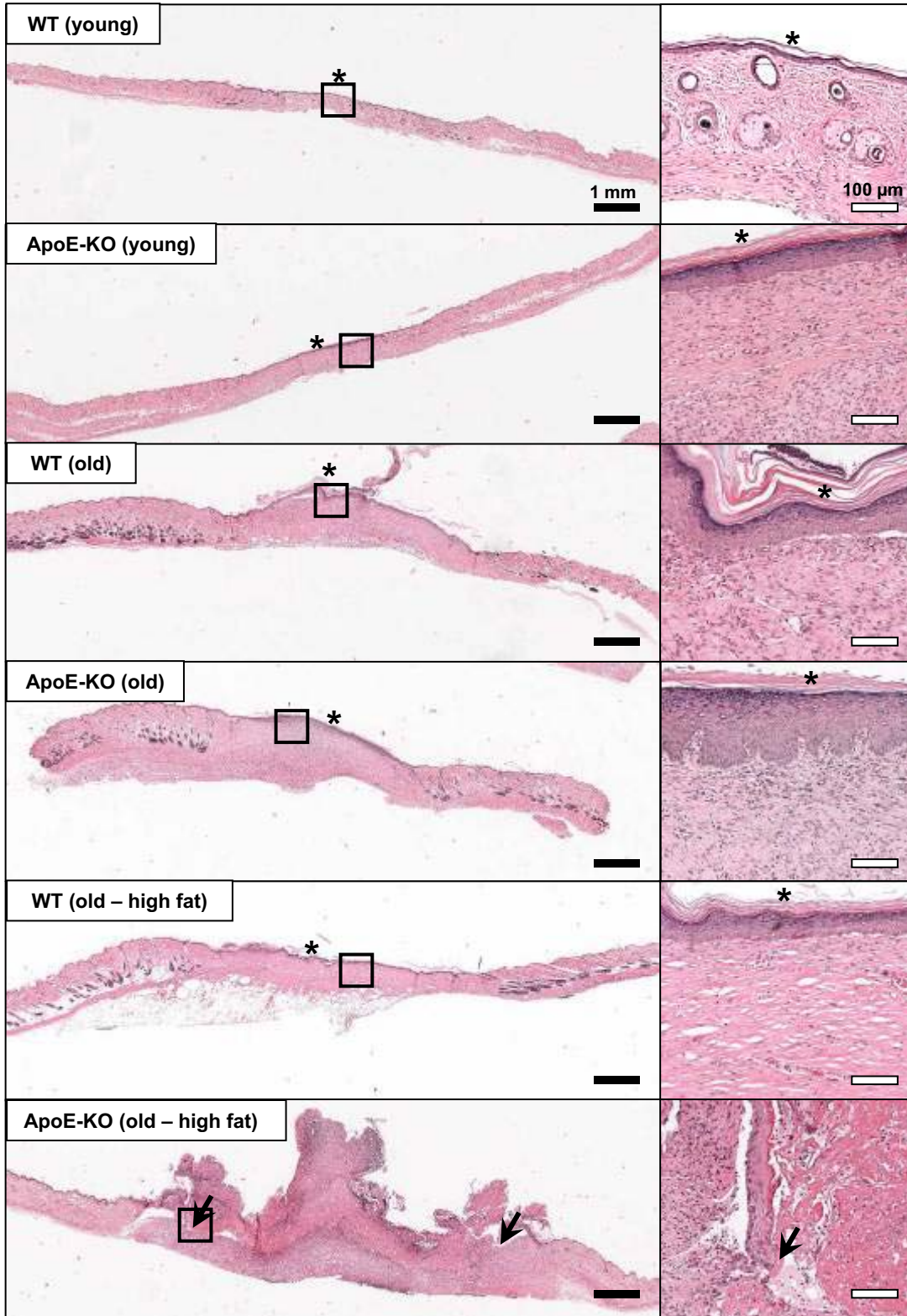


Figure 27. Wounded skin histology 16 days post-wounding. Representative hematoxylin and eosin stained cross-sections of wounded skin after healing for 16 days in young (7 weeks) and old (37 weeks) wild type (WT) and apolipoprotein E knockout (ApoE-KO) mice fed either a regular chow or high fat diet. Arrows represent keratinocytes edges. * represents a closed wound.

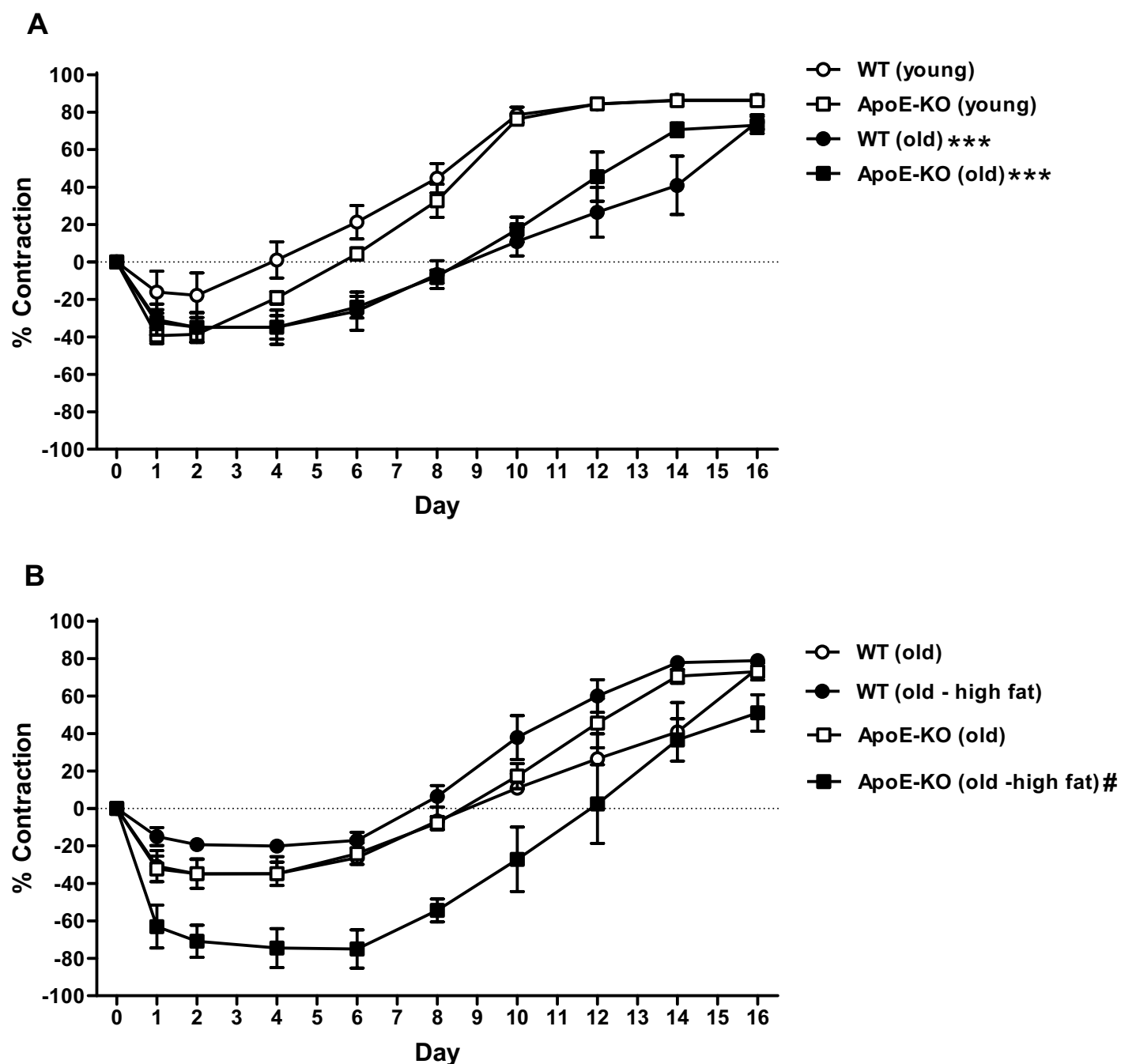
6.2.2 Age and a high fat diet delay contraction in apolipoprotein E knockout mice

At 7 weeks of age (young), both WT and ApoE-KO mice showed full wound closure by 16 days. Wounds healed mainly by contraction, accounting for approximately 85% of wound closure in both the WT and ApoE-KO mice (Figure 28A). In all cases, wound sizes initially expanded and then contracted to fully close the wound. Following the initial expansion period, WT mouse wounds contracted back to zero percent by day 4 while ApoE-KO mice took closer to 6 days to contract back to zero percent (Figure 28A). Overall, however, contraction rates were similar for both young WT and young ApoE-KO mice.

When WT and ApoE-KO mice were grown to 37 weeks of age (old), contraction rates again were similar between genotypes (Figure 28A). However, when compared to the young mice, the old mice showed a significantly slower contraction rate (Figure 28A), suggesting that age delays wound contraction and closure in both WT and ApoE-KO mice. While the initial rate of expansion immediately following wounding was similar between age groups, it took longer for the wounds to contract back to zero percent (about 9 days) compared to the young mice who contracted back to zero by 4 (WT) and 6 (ApoE-KO) days. At day 16, the final percent of wound closure achieved by contraction was less in the old mice (75%) compared to the young mice who healed about 85% by contraction (Figure 28A).

When old WT mice were fed a high fat diet for 30 weeks, wound closure rates appeared similar to old chow fed WT mice (Figure 28B). ApoE-KO mice however, when fed a high fat diet for 30 weeks, demonstrated a significant delay in contraction compared to both the chow and high fat diet-fed WT mice as well as chow fed ApoE-KO mice (Figure 28B). The initial expansion of wound size in high fat diet-fed ApoE-KO mice did not contract back to zero percent until day 12, compared to 7-9 days for the other old groups. These results suggest that

delayed contraction is a main contributor to impaired healing observed in high fat diet-fed ApoE-KO mice.



6.2.3 *Re-epithelialization*

Re-epithelialization plays an important role in wound healing during the proliferative phase and is essential for proper wound closure. Re-epithelialization is difficult to measure using digital pictures and planimetric methods due to the formation of a scab. Therefore, to determine if re-epithelialization was also affected in high fat diet-fed ApoE-KO mice, histological cross-sections were examined at 2, 8 and 16 days post-wounding and re-epithelialization distance was measured (Figure 29).

Re-epithelialization was evident as early as 2 days and became more advanced by day 8 (Figure 29). At 2 and 8 days, the amount of re-epithelialization was similar in all groups regardless of age, diet or genotype, suggesting that the delayed wound closure in high fat diet-fed ApoE-KO mice is primarily due to slower contraction rather than re-epithelialization (Figure 30A and B). The closed wounds of the young mice for both genotypes showed less newly formed epithelium at day 16 compared to the old groups (both chow and high fat diet) (Figure 30C). This is not surprising given the above mentioned observation that wounds in young mice contract faster than in the old mice (Figure 28A). Although not significant, re-epithelialization at day 8 was slightly greater in the young mice versus the old mice, suggesting that re-epithelialization takes place just as fast or possibly faster in young mice, but plays a lesser role in wound closure due to the even greater increase in the rate of contraction.

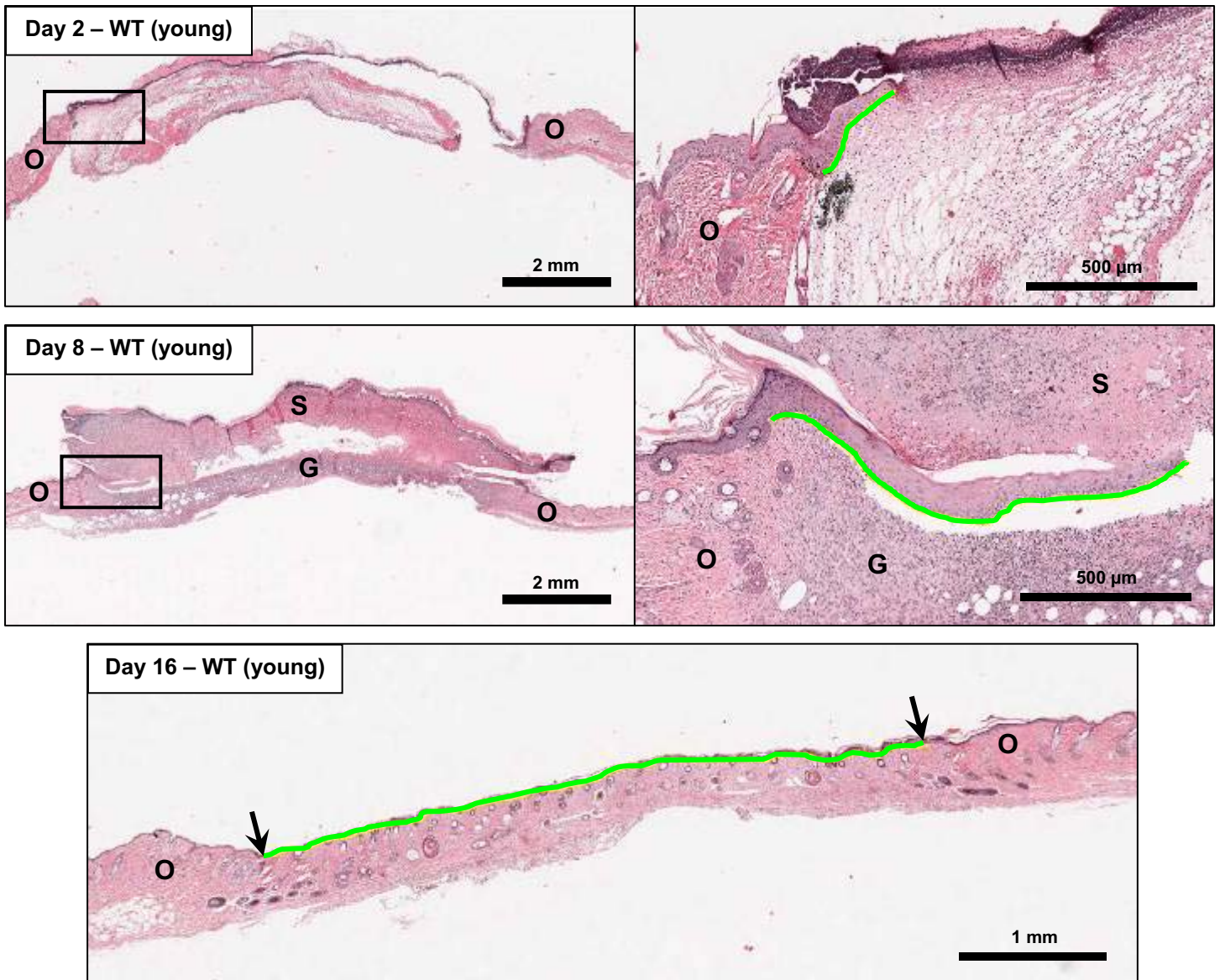


Figure 29. Histological representations of re-epithelialization at 2, 8 and 16 days. Representative hematoxylin and eosin stained cross-sections of wounded skin in a 7 week old WT mouse are shown at days 2, 8 and 16 post-wounding. Re-epithelialization can be seen as early as Day 2 and to a greater degree at Day 8. At Day 16, re-epithelialization has fully closed the wound. Green tracing represents re-epithelialization distance. O = original skin tissue, G = newly formed granulation tissue, S = scab.

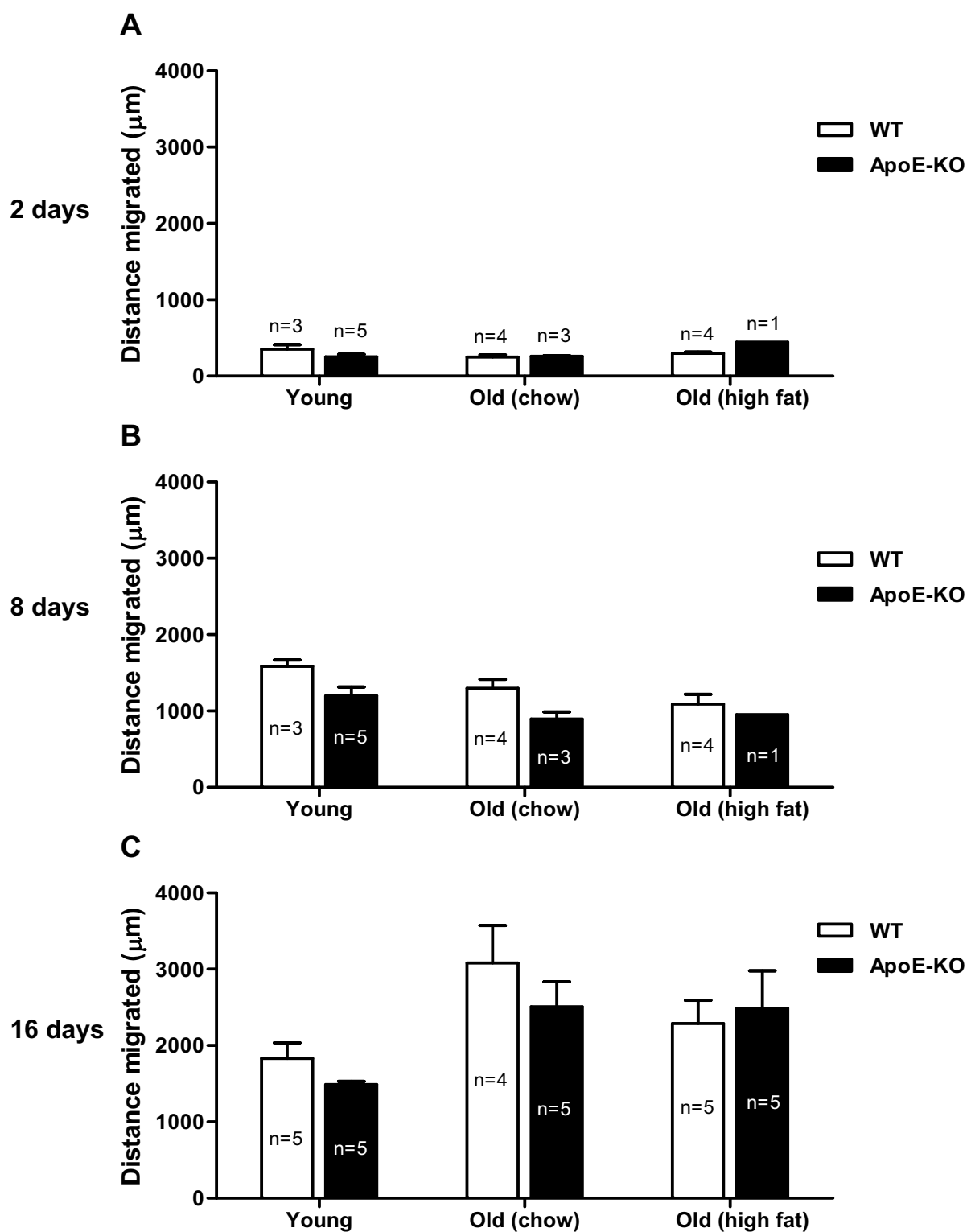


Figure 30. Re-epithelialization distance at 2, 8 and 16 days. Re-epithelialization distance was measured at 2, 8 and 16 days for the young (7 weeks) and old (37 weeks) wild type (WT) and apolipoprotein E knockout (ApoE-KO) mice fed either a regular chow or high fat diet. Re-epithelialization distances for all groups were similar at days 2 and 8. Young mice demonstrated reduced re-epithelialization at 16 days due to a higher rate of contraction resulting in faster wound closure.

6.2.4 Inflammation following wounding in apolipoprotein E knockout mice

Several reports have documented the immunosuppressive effects of ApoE [reviewed in 211]. In chapter 4, ApoE-KO mice fed a high fat diet exhibited increased susceptibility to inflammatory skin lesions. We therefore examined wounded skin tissue from ApoE-KO mice fed a high fat diet, to determine if inflammation was altered compared to WT mice. Wound cross-sections in young WT mice were examined first at days 2, 8 and 16 for immune cell content to investigate inflammation during healthy wound healing. An influx of inflammatory cells were seen at day 2 in the young WT mice featuring polymorphonuclear neutrophils (Figure 31). At day 8, macrophages were seen in abundance at the wound site within the newly formed provisional matrix and granulation tissue (Figure 31). Lymphocytes and some remaining neutrophils were also seen. By day 16, the number of inflammatory cells was greatly reduced, signifying an end to the inflammatory phase and progression through the proliferation and remodeling phases towards a fully healed wound (Figure 31). The effect of age on inflammation during wound healing was observed by examining wounded cross-sections from old mice at days 2, 8 and 16. WT mice at day 2 again showed mostly neutrophils while macrophages were more numerous at day 8. At day 16, more inflammatory cells were observed in the healed wound compared to young mice however there was still evidence of resolution of inflammatory cells as the wound healing progressed and closed the wound.

Of all groups wounded, only the old ApoE-KO mice fed a high fat diet demonstrated an inability to fully heal over 16 days. To determine if this chronic wound healing was associated with chronic persistent inflammation, high fat diet-fed WT and ApoE-KO mice were also examined at days 2, 8 and 16. WT mice showed a similar pattern as described above with neutrophils and macrophages being the primary cell type at days 2 and 8 respectively. Day 16

again saw a reduction of inflammatory cells in the closed wounds compared to day 8 as wound healing progressed (Figure 32). In contrast, ApoE-KO mice showed a greater degree of inflammatory cells when compared to the WT controls at day 16. Analysis at the wounded site revealed the remaining presence of macrophages, macrophage foam cells, neutrophils and lymphocytes. Macrophage and lymphocyte content was further confirmed by staining for F4/80 and CD3 respectively (Figure 32). Neutrophils and foam cells were detected by their polymorphonuclear and “foamy” appearance respectively in H&E stained sections (Figure 32). These cells were particularly noticeable in ApoE-KO mouse wounds that had not yet closed (Figure 32). The exact contribution of each of these cell types to chronic wound healing ApoE-KO mice is not yet known, however these results suggest that non-healing wounds in ApoE-KO mice are associated with increased persistent inflammation, typical of a chronic wound.

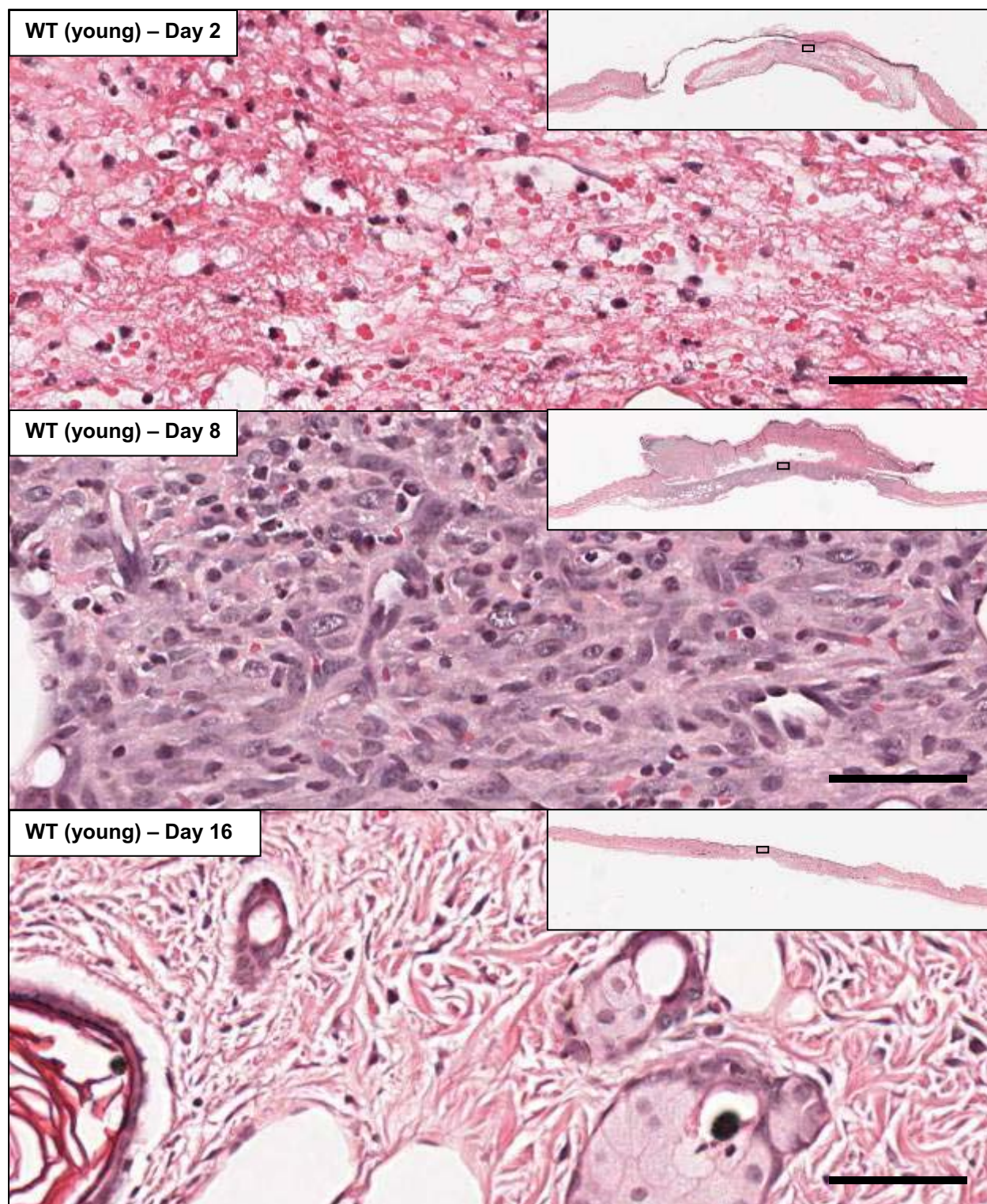


Figure 31. Inflammation in young wild type mouse skin at 2, 8 and 16 days post-wounding. Representative hematoxylin and eosin stained cross-sections of wounded skin from young (7 weeks) wild type (WT) mice at 2, 8 and 16 days post-wounding. Inflammation inside the wounded area revealed several infiltrating neutrophils at Day 2, followed by an influx of macrophages at Day 8 and general resolution of inflammation by Day 16. Scale bars = 50 μ m.

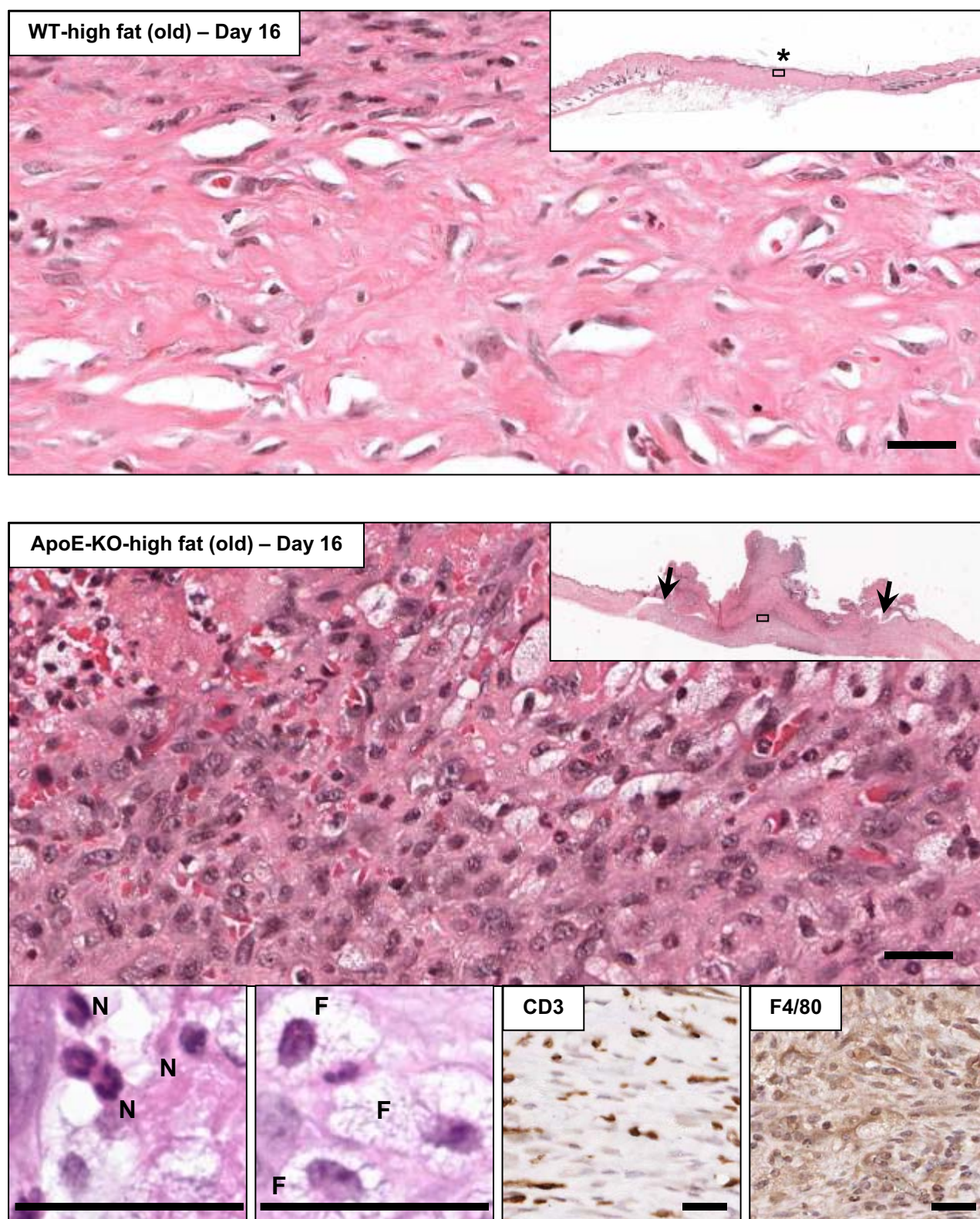


Figure 32. Inflammation at Day 16 in wild type versus apolipoprotein E knockout mice. Representative hematoxylin and eosin stained cross-sections of wounded skin from wild type (WT) and apolipoprotein E knockout (ApoE-KO) mice. High fat diet-fed WT mouse skin shows relatively few inflammatory cells at the wounded site at Day 16. In contrast, ApoE-KO mice fed a high fat diet demonstrate numerous inflammatory cells including macrophages (F4/80), lymphocytes (CD3), foam cells (F) and neutrophils (N). Chronic inflammation was greatest in wound sections that were not yet healed. Arrows indicate keratinocytes edges, * indicates a closed wound. Scale bars = 25 μ m.

6.2.5 Collagen

The final stages of wound healing involve a replacement of the temporary provisional matrix with newly formed, mature collagen. As all of the wounds (with the exception of the high fat diet-fed ApoE-KO mice) were fully closed by Day 16, we investigated the collagen content of the healed tissue as a further indicator of healing. All groups of mice were stained with picrosirius red and collagen was visualized under polarized light. Young WT and ApoE-KO mice had noticeably more collagen in the newly formed tissue compared to the older groups (Figure 33). When young WT mice were compared to the young ApoE-KO mice, there was significantly more collagen at the wounded site in the WT mice, suggesting that even young ApoE-KO mice have slower wound remodeling after the wound has been closed. Differences between the old groups of mice, regardless of diet, failed to reach significance at Day 16 (Figure 33).

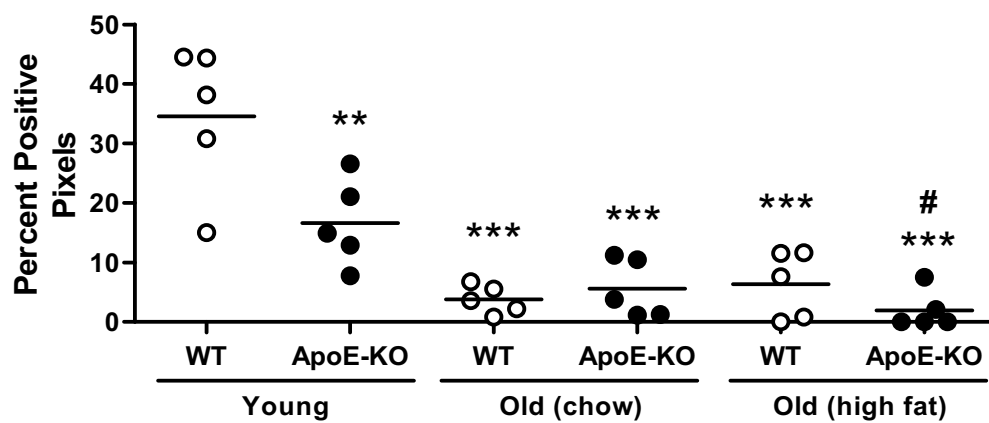
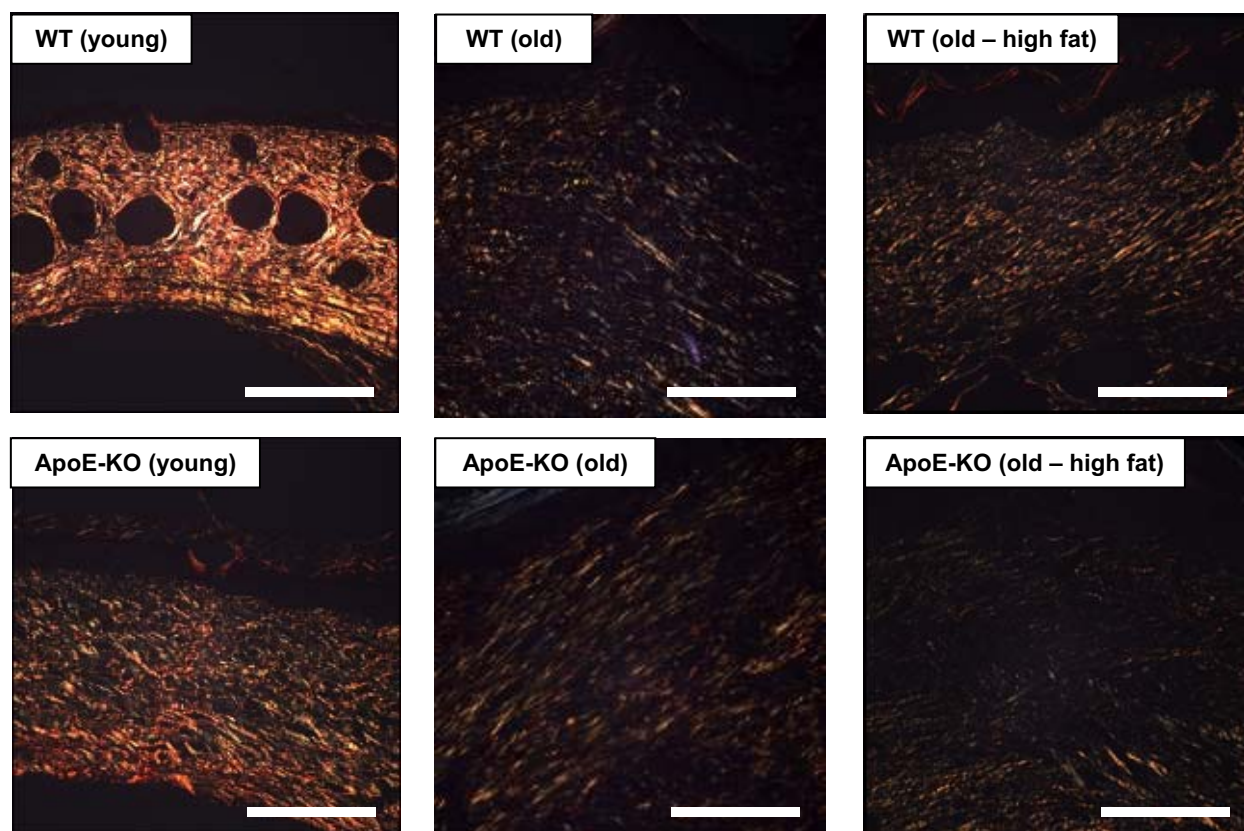


Figure 33. Collagen content at Day 16. Wounded skin cross-sections were stained with picosirius red and photographed under polarized light. Colour segmentation was used to quantify collagen and was expressed as the percent pixels that were above a set threshold. Scale bars = 200 μ m. ** $P < 0.01$ versus WT-young, *** $P < 0.005$ versus WT-young, # $P < 0.05$ versus ApoE-KO-young (One-way ANOVA with bonferroni post test).

6.3 Discussion

In this chapter, we describe a novel mouse model of impaired wound healing. ApoE-KO mice fed a high fat diet for 30 weeks demonstrated reduced contraction, impaired wound closure and increased, persistent inflammation featuring macrophages, neutrophils and lymphocytes. Age was shown to have a considerable effect on wound healing in both WT and ApoE-KO mice as seen by delayed contraction and less mature collagen fibres at 16 days post-wounding. Diet was also shown to influence wound healing in ApoE-KO mice with a high fat diet resulting in poorer wound healing compared to chow fed mice.

Wound healing in this study was found to occur mainly by contraction, with about 85% of wound closure the result of contraction as seen in the young groups. This was also reflected in the amount of re-epithelialization observed at day 16 with the young groups showing less than the old groups, suggesting contraction played a greater role in the healing process in young mice compared to old mice. Re-epithelialization was also found to occur and play an important role in the healing process. Nevertheless, re-epithelialization played a relatively minor role compared to contraction and was not found to be significantly different between the groups examined.

Wound contraction, while an important process in human wound healing, does not typically represent the major mechanism of wound healing in humans, who tend to heal primarily by re-epithelialization although this can depend on the size and location of the wound [212]. While the degree of re-epithelialization was measured in this model, the large amount of contraction prevented the effect of ApoE deficiency on re-epithelialization to be properly examined. Healed wounds on day 16 feature a completely closed epidermal layer, eliminating the need for further keratinocyte migration and re-epithelialization. It is therefore not possible to compare the re-epithelialization distances properly at day 16 between groups that have healed

and those that have not healed. Future studies using additional time points between 8 and 16 days, before full wound closure is achieved, are needed to properly identify any differences in re-epithelialization in this model.

ApoE is known to function in a number of roles in the body besides lipid transport. Among those are its ability to influence inflammation. ApoE-KO mice fed a high fat diet for 30 weeks demonstrated increased macrophages, neutrophils and lymphocytes compared to the WT mice, suggesting inflammation in these mice is persistent and slower to resolve. Specifically, ApoE has been shown to suppress neutrophil and macrophage activation as well as lymphocyte proliferation. Additionally, macrophage foam cells were observed in the wounded tissue of ApoE-KO mice on day 16, reflecting the high lipid content and are typical cell types present in diseased ApoE-KO mouse skin.

As shown in chapter 4, ApoE-KO mice required a high fat diet to exhibit age-related skin changes such as skin thinning and collagen disorganization. Similarly, a high fat diet was required for impaired wound healing to be observed in the skin of ApoE-KO mice. The requirement of a high fat diet in ApoE-KO mice suggests these phenotypes occur through mechanisms dependant not just on ApoE deficiency, but on a more severe dyslipidemia. Inflammatory processes could provide a link between worsened hyperlipidemia and these age-related phenotypes. For example, cholesterol is capable of stimulating endothelial cells to up-regulate expression of adhesion molecules such as VCAM-1 used to bind to and recruit circulating immune cells such as lymphocytes and monocytes/macrophages into the blood vessel intima during atherosclerotic plaque development [213, 214]. Additionally, the accumulation of lipid by macrophages (made worse through the impairment of cholesterol efflux in the absence of ApoE) causes the formation of foam cells, which can release cytokines that further encourage

an inflammatory phenotype [80, 177]. Previous reports have also confirmed that a high fat diet increases the number of these foam cells present in the skin of ApoE-KO mice compared to ApoE-KO mice fed a regular chow diet [177]. As mentioned above, inflammation, when present in excess, can damage tissue integrity through multiple mechanisms contributing to an increased susceptibility to aging and age-related diseases [78, 215]. Although not investigated in this study, these potential pro-inflammatory consequences of worsened hyperlipidemia could help explain why a high fat diet is required for this phenotype to occur in ApoE-KO mice as compared to regular diet-fed ApoE-KO mice, especially when combined with the lack of immunosuppressive activities of ApoE. As both lymphocytes and macrophages are known to express GzmB, this worsened inflammation could provide a link between worsened hyperlipidemia and increased GzmB activity although this remains to be shown. Further work is needed to confirm the precise mechanism in which worsened hyperlipidemia causes the phenotypes observed in ApoE-KO mouse skin.

Analysis of skin tissue prior to wounding revealed that some, but not all differences observed in the high fat diet-fed ApoE-KO groups occur in response to injury. One high fat diet-fed ApoE-KO mouse exhibited evidence of xanthoma prior to wounding, a situation in which chronic inflammation is already present. Interestingly, this ApoE-KO mouse with xanthoma showed more advanced wound closure compared to other ApoE-KO mice without xanthoma in terms of its ability to re-epithelialize and close. Although healing in this mouse was still abnormal, featuring disorganized collagen and poor morphology, these results suggest that the delayed wound healing in ApoE-KO mice observed is at least partially due to altered responses to injury, and not purely the result of already diseased skin.

When collagen was investigated in the wounded skin of young mice at Day 16, WT mice showed significantly more collagen compared to ApoE-KO mice. Although both of these groups of mice showed similar rates of contraction and wound closure, these results suggest that other aspects of wound healing and remodeling may be affected in ApoE-KO mice, even at 7 weeks of age. The overall strength of healed wounds and the degree of scarring are both affected by ECM remodeling events that take place in the final stages of wound healing. These results also demonstrate the dramatic effect of age on wound healing speed. Old mice not only showed slower wound contraction but also exhibited significantly delayed ECM remodeling and collagen formation at the site of wounding. Although no significant differences were observed among the old groups, it is possible that any existing differences between groups would require examination at a time point longer than 16 days. These results raise the possibility that ApoE-KO mice, even at 7 weeks of age, might be worth investigating in the context of scar formation and skin strength following wound healing. Future work examining old mice at time points beyond 16 days would also be warranted in this regard.

7. Granzyme B contributes to impaired wound healing in apolipoprotein E knockout mice

7.1 Introduction

GzmB is expressed in higher amounts during several chronic inflammatory diseases [reviewed in 9]. Additionally, many different cell types that normally do not express GzmB begin to produce GzmB in chronic inflammatory conditions. Chronic wounds feature persistent, chronic inflammation, warranting investigation into the presence and role of GzmB in maintaining the pathology of chronic wound healing. Mast cells, macrophages, T cells and neutrophils are all possible sources of GzmB in a chronic wound. The ability of GzmB to degrade several key ECM components that are critical for proper wound healing implicate GzmB in this process. Should GzmB activity be present in excess in a chronic wound, this excess degradation of the ECM could serve to impede the healing process.

As mentioned above, ApoE-KO mice not only develop inflammatory skin disease and accelerated skin aging, but also show impaired healing when fed a high fat diet for 30 weeks. This impaired healing was associated with increased inflammation featuring macrophages, neutrophils, lymphocytes and mast cells.

In chapter 5, evidence was presented to suggest that GzmB contributes to skin aging in ApoE-KO mice fed a high fat diet through the degradation of ECM proteins such as decorin. GzmB was identified as present in the skin of ApoE-KO mice and mast cells were shown to be a potentially important source of extracellular GzmB in the diseased skin of these mice. We therefore utilized DKO mice to determine if GzmB influences chronic wound healing in high fat diet-fed ApoE-KO mice.

7.2 Results

7.2.1 Granzyme B deficiency improves wound closure in apolipoprotein E knockout mice

To determine the role that GzmB plays in the delayed healing of high fat diet-fed ApoE-KO mice, DKO mice were also fed a high fat diet for 30 weeks, wounded and allowed to heal for 16 days. DKO mice demonstrated improved wound closure compared to ApoE-KO mice (Figure 34) with 80% of the animals achieving full wound closure at day 16, compared to only 40% of ApoE-KO mice (Figure 35). As shown in Figure 35, the majority of healed wounds in the high fat diet-fed DKO group demonstrate a joined/closed keratinocyte layer, in contrast to the majority of ApoE-KO mice, that exhibited incomplete closure and clearly visible keratinocyte edges. These results provide the first evidence that GzmB is involved in the delayed/impaired wound healing observed in high fat diet-fed ApoE-KO mice.

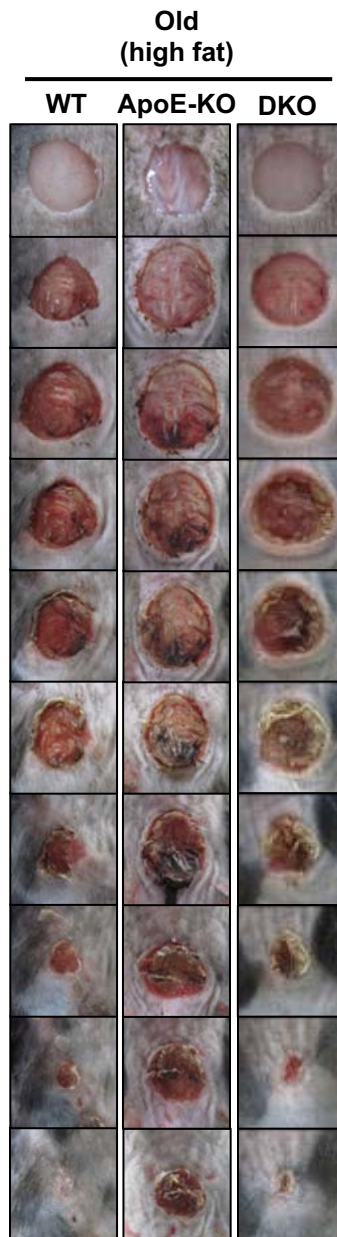


Figure 34. Granzyme B deficiency improves wound healing in apolipoprotein E knockout mice. Representative digital pictures of wounds from old (37 weeks) wild type (WT), apolipoprotein E knockout (ApoE-KO) and double knockout (DKO) mice fed a high fat diet. Wounds are shown at different time points from 0 to 16 days post-wounding.

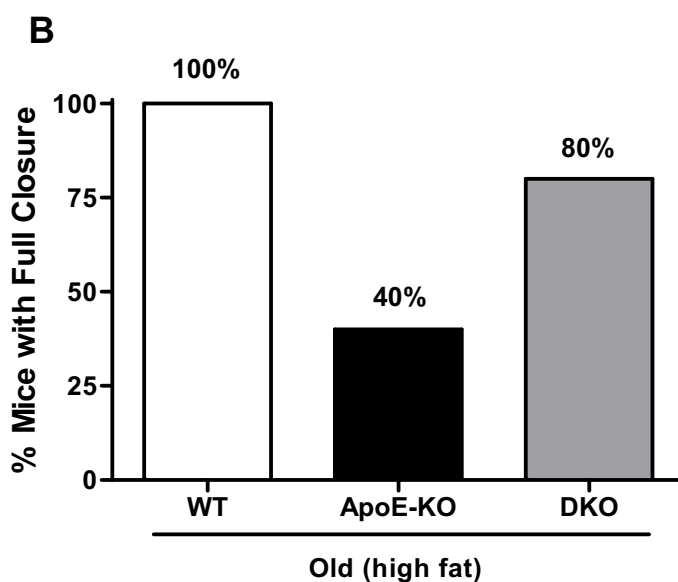
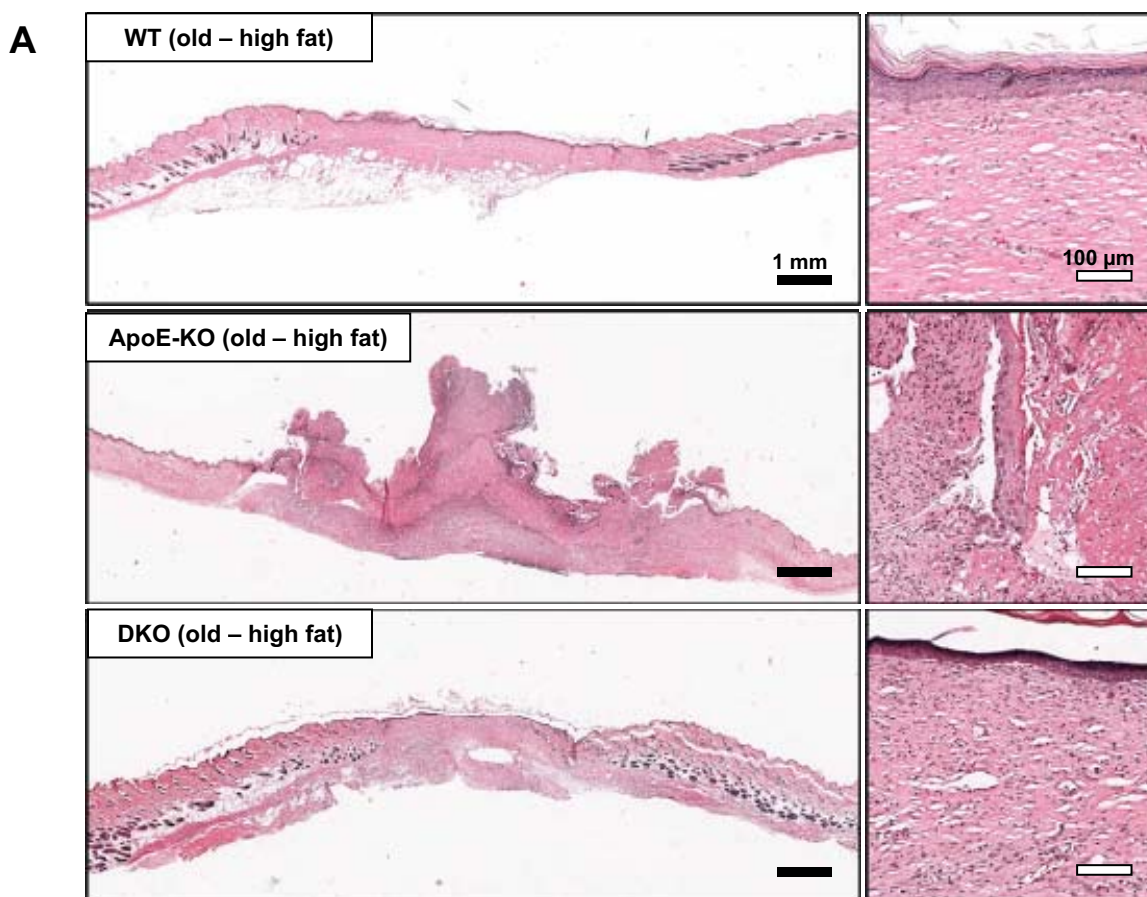


Figure 35. Granzyme B deficiency improves wound closure in apolipoprotein E knockout mice. (A) Wound closure was assessed histologically using H&E stained cross-sections of wounded skin from wild type (WT), apolipoprotein E knockout (ApoE-KO) and double knockout (DKO) mice. A fully closed wound featured a completely closed keratinocyte layer that had finished migrating. (B) One hundred percent of the WT mice showed complete wound closure at Day 16, compared to only 40% (2/5) of the ApoE-KO mice. Granzyme B deficiency improved this outcome with 80% (4/5) of DKO mice achieving full wound closure by Day 16. All mice were fed a high fat diet for 30 weeks.

7.2.2 Contraction and re-epithelialization

To determine how GzmB affects wound healing kinetics, we examined the rate of contraction as well as re-epithelialization at 2, 8 and 16 days post-wounding. Contraction was measured using digital photographs of the wound site in the presence of a ruler. Wound size was normalized to the initial wound area and expressed as a percentage of the original wound size. As shown in Figure 36, there was a significant difference in the contraction curve of the DKO mice compared to the ApoE-KO mice, with the DKO group demonstrating a consistent increase in the percent of contraction throughout the 16 day period. This included reduced expansion of the wound immediately following wounding, and faster contraction back to 0% and ultimately wound closure.

Skin sections were also analyzed histologically at days 2, 8 and 16 to determine the degree of re-epithelialization at each of these time points. Similar to results described above, re-epithelialization showed very little difference between the genotypes (Figure 37). It is likely that wound closure in this model does not occur enough by re-epithelialization to observe any potential differences between the groups. These data suggest that differences in the rate of wound closure between high fat diet-fed ApoE-KO and DKO mice in these experiments is due primarily to contraction, rather than re-epithelialization.

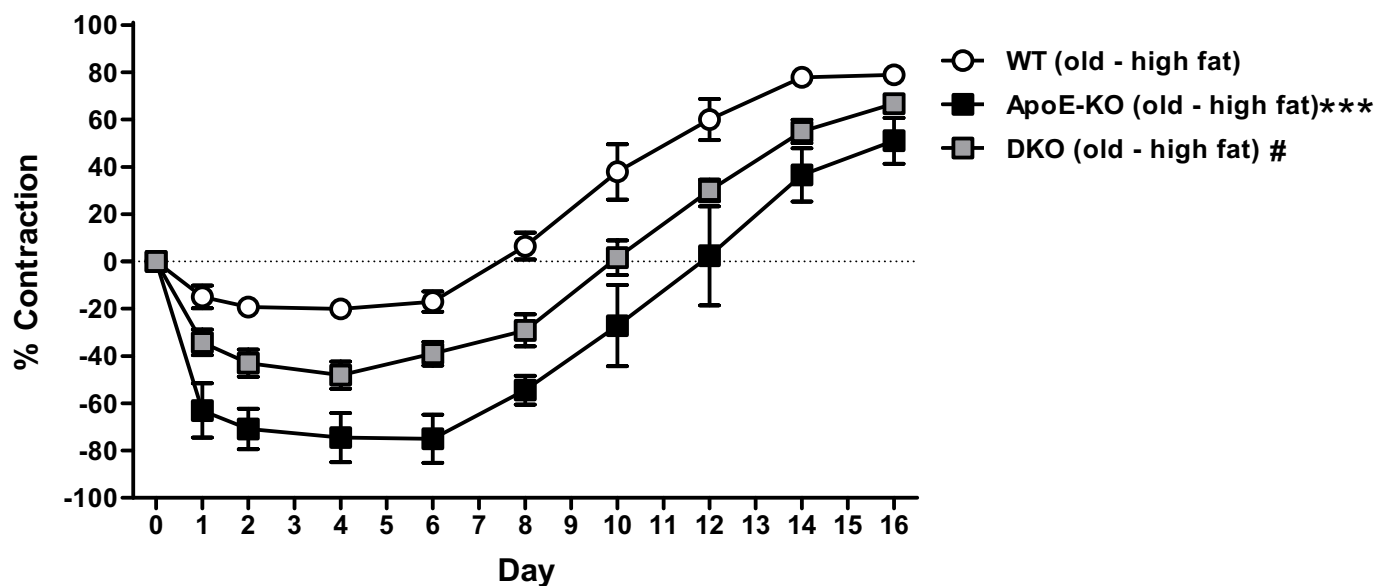


Figure 36. Improved contraction in granzyme B deficient apolipoprotein E knockout mice. Wild type (WT) mice fed a high fat diet showed normal wound contraction that was significantly faster than apolipoprotein E knockout (ApoE-KO) mice fed a high fat diet. Double knockout (DKO) mice fed a high fat diet also showed increased contraction and faster wound closure compared to high fat diet-fed ApoE-KO mice. Contraction was higher in the DKO mice throughout the 16 day healing period (n = 5 for all groups). ***P < 0.001 vs WT-high fat, #P < 0.001 vs. ApoE-KO-high fat (2-way ANOVA).

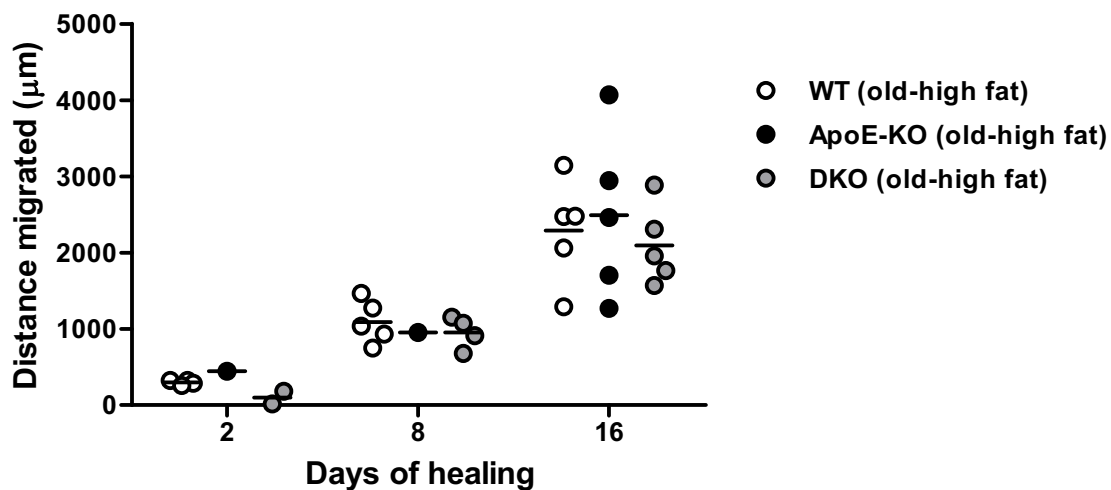


Figure 37. Re-epithelialization over 16 days in old mice fed a high fat diet. Re-epithelialization distance was measured using hematoxylin and eosin stained cross-sections at 2, 8 and 16 days post-wounding. The amount of migration increased over time however no significant difference was observed between the old (37 weeks) wild type (WT), apolipoprotein E knockout (ApoE-KO) or double knockout (DKO) mice. All mice were fed a high fat diet.

7.2.3 Extracellular matrix remodeling

GzmB is capable of degrading several components of the ECM important in wound healing. Excessive degradation of these components could result in improper remodeling, delayed provisional matrix formation and impaired wound healing. In Chapter 5, GzmB-mediated decorin degradation was found to be a potential mechanism behind collagen disorganization and skin aging in ApoE-KO mice.

To examine the possible role of GzmB-mediated decorin degradation in a chronic wound model, we performed immunohistochemistry analysis for decorin content at Day 16. At 16 days post-wounding, WT mice show decorin staining throughout the newly formed dermis (Figure 38). ApoE-KO mice, however, showed a reduction in positively stained tissue in the wounded area with less intense staining, suggesting less decorin is present. DKO mice however show increased decorin staining at 16 days post-wounding, suggesting a more advanced healing stage compared to ApoE-KO mice. Collagen content in the wounded skin tissue at Day 16 was also examined using picrosirius red (Figure 38). Similar to what was observed with decorin, more collagen was observed at the wounded site in the WT mice compared to ApoE-KO mice. Again, DKO mice demonstrated increased collagen content at the wounded site compared to ApoE-KO mice, suggesting wounds in DKO mice are at a more advanced stage of healing. The degree to which GzmB-mediated decorin degradation is directly responsible for this difference is unknown, however these data suggest that GzmB deficiency results in greater decorin and collagen levels in wounded tissue, contributing to improved healing.

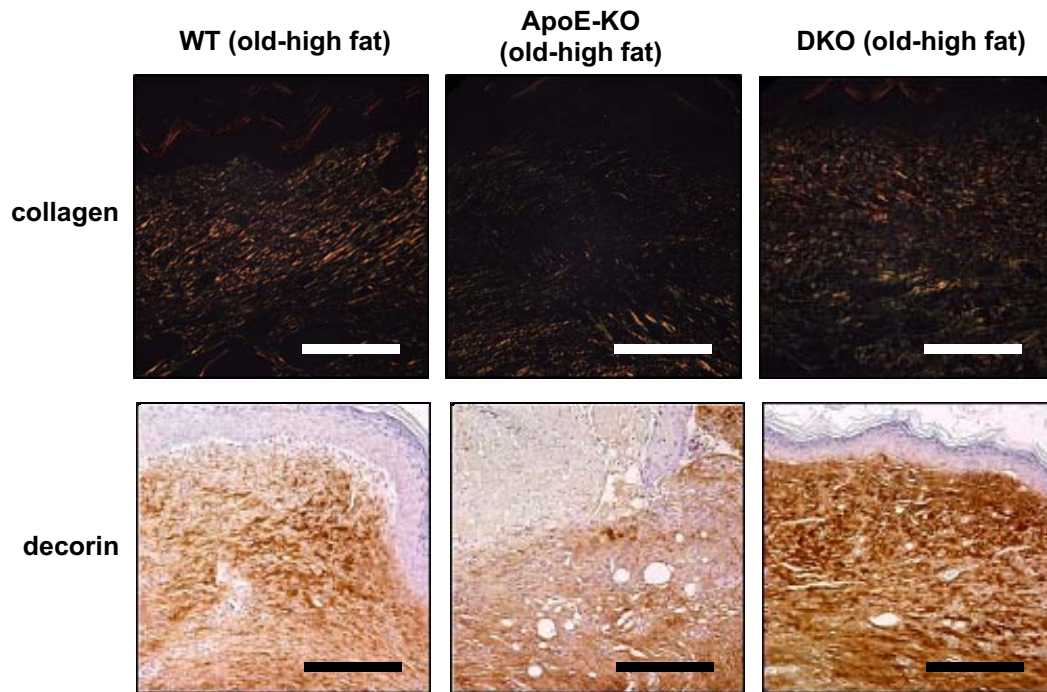


Figure 38. Collagen and decorin content at Day 16. Representative skin cross-sections of wounded tissue at Day 16 stained for collagen and decorin. Decorin staining was more intense in the DKO mice compared to ApoE-KO mice, particularly in wounds that were not healed. Scale bars = 200 μm.

7.2.4 Granzyme B-mediated fibronectin degradation in non-healing wounds

Fibronectin plays a major role in proper wound healing. The provisional matrix is composed of ECM proteins including fibronectin, which serves to mediate cell migration through its interaction with different integrins and growth factors. Fibronectin also helps to provide an important physical scaffold to facilitate proliferation and migration. To determine the status of fibronectin in our wound healing model, *ex vivo* skin sections were harvested at the wounded site, homogenized and analyzed for fibronectin by western blotting. Fibronectin levels in wounded skin increased at days 2 and 8 post-wounding when compared to the original, unwounded skin (Figure 39). When normalized to GAPDH, fibronectin levels were greatest at day 8. By day 16, fibronectin levels again resembled the original, unwounded skin, signifying tissue remodeling and replacement of the fibronectin-rich provisional matrix with new, mature collagen fibres.

To determine the effect of GzmB on the proper functioning and remodeling of fibronectin in our chronic wound model, skin from old high fat diet-fed WT, ApoE-KO and DKO mice was analyzed for fibronectin by western blot analysis (Figure 41A). All WT mice examined at day 16 showed relatively little fibronectin levels, similar to the young WT control at the same time point. In contrast, ApoE-KO mice showed increased fibronectin content including significantly more fibronectin fragments. DKO mice on the other hand, all showed fibronectin levels similar to the WT group, suggesting appropriate and physiological ECM remodeling took place during wound healing. When GzmB was probed for using immunohistochemistry, GzmB positive staining was observed in the non-healed skin of ApoE-KO mice (Figure 42). Although the exact cell types expressing GzmB in ApoE-KO mice are unknown, several GzmB positive cells are morphometrically representative of macrophages.

To further examine the role of GzmB in this process, we examined the ability of mouse GzmB to degrade fibronectin within skin homogenate derived from WT mice. Although fibronectin is an established substrate for GzmB [12, 63], studies to date have focused primarily of human proteins. Several differences in substrate specificities have been reported between mouse and human GzmB [216] and the effectiveness of mouse GzmB in degrading mouse fibronectin is not as established in mice compared to humans. Mouse GzmB was therefore added to skin homogenate from WT mice and incubated at 37 °C for 24 h. After 24 h, complete degradation of the full length fibronectin fragment was observed when mouse GzmB was added at concentrations as low as 100 nM (Figure 40). Incubation with GzmB resulted in the generation of a lower molecular weight fragment at approximately 220 kDa. This fragment corresponded to a similar sized fragment observed in the skin homogenate of ApoE-KO mice at Day 16, whose wounds had failed to heal (Figure 41A). Although traces of this fragment were seen in both the WT and DKO mice, this fragment was present in significantly greater amounts in the ApoE-KO mice compared to both WT and DKO groups (Figure 41B). These results provide evidence that GzmB contributes to the degradation of fibronectin in C57BL/6 mice during wound healing. Excessive GzmB activity may be at least a partial explanation for the increased presence of this fragment in the non-healed ApoE-KO mouse skin, and the inability of these mice to properly heal.

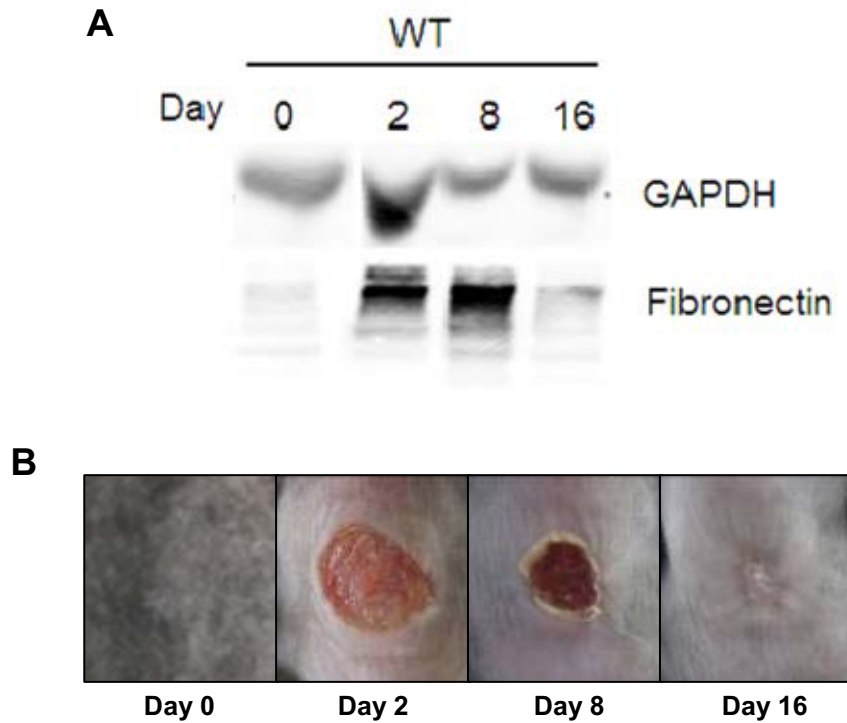


Figure 39. Fibronectin content during wound healing. (A) Wounded skin from a wild type (WT) mouse was analyzed at Day 0, 2, 8 and 16 for fibronectin by western blot. GAPDH was used as loading control. Prior to wounding (Day 0), fibronectin content is relatively low. Beginning at Day 2 to Day 8, the granulation tissue forms, featuring increased fibronectin levels. Fibronectin levels return to normal by Day 16 once the wound has been properly remodeled and healed. (B) Representative images of wounded sites prior to wounding (Day 0), and at Day 2, 8 and 16 post wounding.

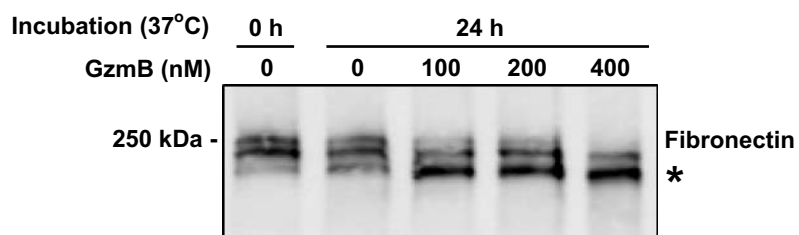


Figure 40. Mouse granzyme B cleaves mouse fibronectin. Mouse granzyme B (GzmB) was added to the skin homogenate from a wild type mouse harvested at Day 8 post wounding. As little as 100 nM of GzmB was sufficient to degrade the full length fibronectin protein when incubated for 24 h at 37 °C. *depicts a ~220 kDa GzmB-generated fragment.

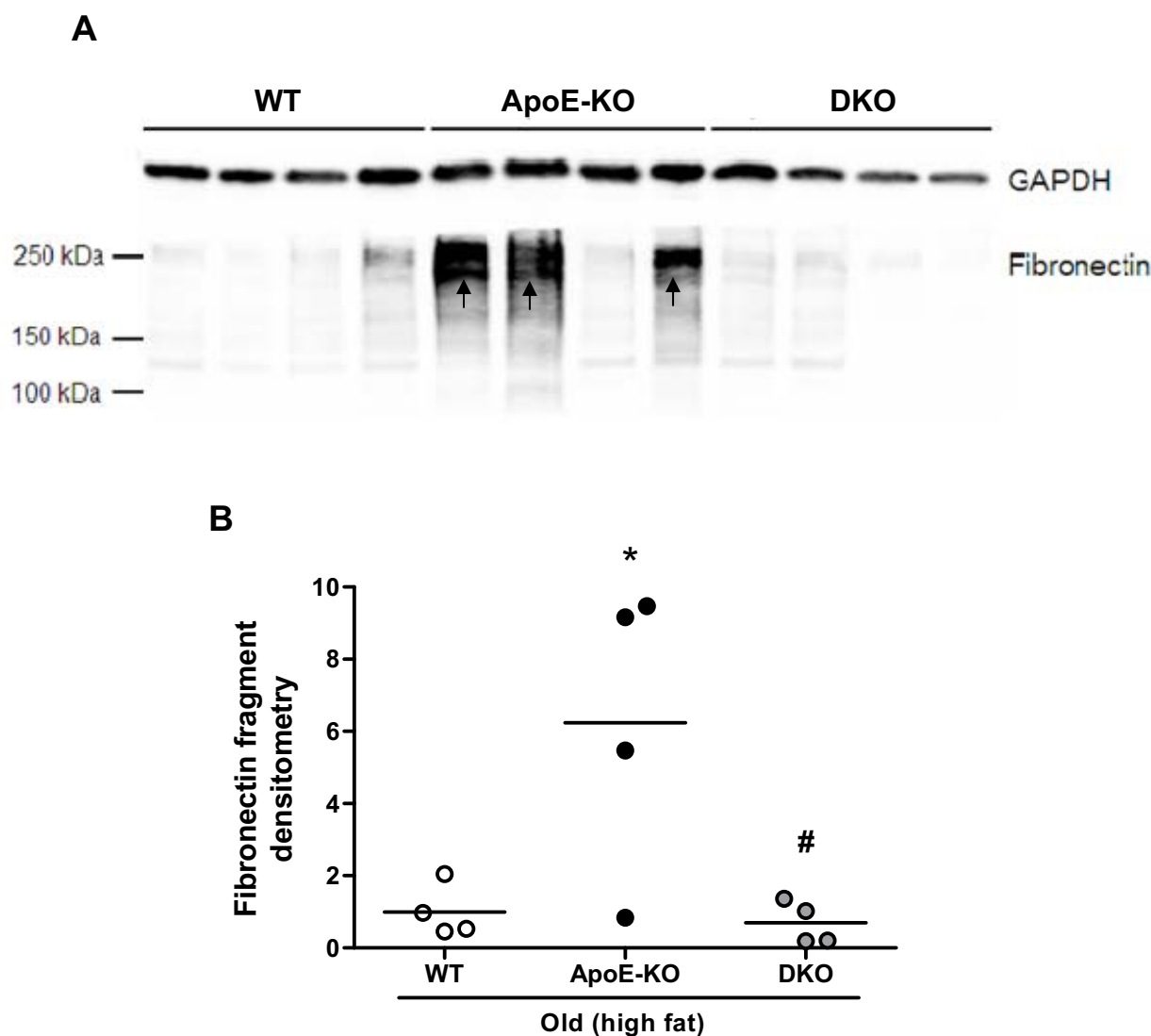


Figure 41. Fibronectin content at Day 16. (A) Healed skin from old (37 weeks), high fat diet-fed mice was analyzed at Day 16 for fibronectin by western blot. GAPDH was used as loading control. Wild type (WT) mice exhibited relatively little fibronectin content at Day 16. Apolipoprotein E knockout (ApoE-KO) mice exhibited increased fibronectin content including fragments which appeared to be reduced by knocking out GzmB. Arrows represent a fibronectin fragment at approximately 200 kDa. (B) Fragments below the 250 kDa full length protein were quantified by densitometry. A significant increase in fibronectin fragments were observed in ApoE-KO mice compared to WT mice, and this was prevented in the double knockout mice * $P < 0.05$ versus WT, # $P < 0.05$ versus ApoE-KO (One-way ANOVA with bonferroni post test).

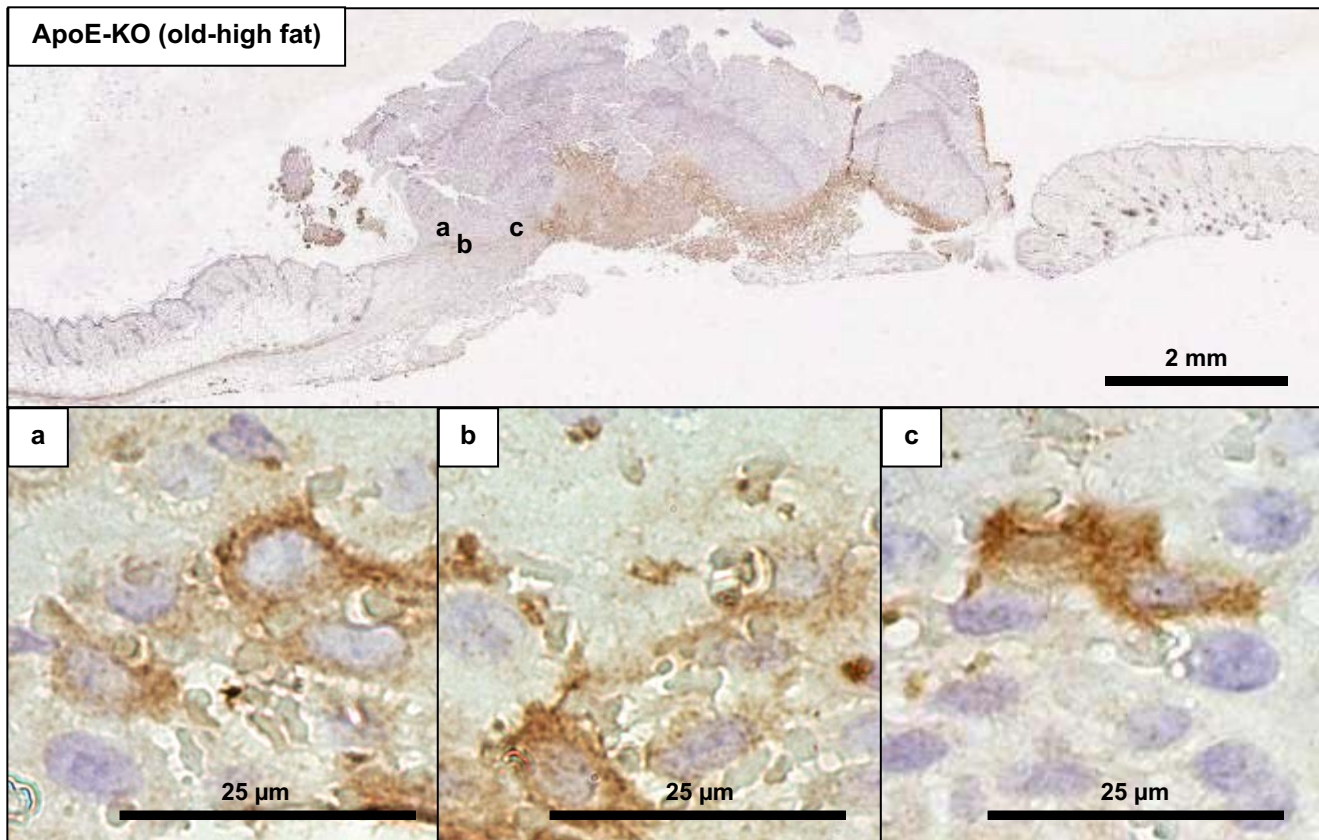


Figure 42. Granzyme B expressing cells in a non-healed wound from an apolipoprotein E knockout mouse. Multiple granzyme B (GzmB)-expressing cells were detected in the non-healed wounded skin of high fat diet-fed apolipoprotein E knockout (ApoE-KO) mice at Day 16. GzmB was detected in several cell types including macrophages, the dominant immune cell type identified in non-healing ApoE-KO mouse wounds.

7.3 Discussion

In this chapter, we provide evidence of improved wound healing in GzmB-deficient ApoE-KO mice fed a high fat diet. GzmB deficiency resulted in a greater percentage of wounds achieving full closure by 16 days (from 40% to 80%). This is likely due to increased contraction in DKO mice compared to ApoE-KO mice. Although the possibility of altered re-epithelialization in GzmB deficient ApoE-KO mice remains, this was difficult to assess in this study and no conclusions could be made regarding the beneficial or detrimental role of GzmB in re-epithelialization. In addition, GzmB deficiency in our chronic wound model resulted in a quicker replacement of fibronectin-rich provisional matrix with collagen and decorin at day 16, suggesting improved, healthier ECM remodeling and advanced healing.

Proper wound healing requires considerable remodeling and eventually replacement of the provisional matrix with new collagen fibres. Although proteases and remodeling events are crucial for proper healing, too much proteolysis can result in excessive degradation of key ECM proteins which can delay, rather than promote wound healing. Chronic wounds have been shown to exhibit increased fibronectin fragmentation while at the same time, increased fibronectin expression suggesting excessive proteolysis [134-137]. In this chapter, we observed increased fibronectin levels in wounded tissue of ApoE-KO mice at day 16 compared to WT mice with significantly more fragments, including a fragment shown to be produced by GzmB. This could be due to excessive proteolysis, contributing to impaired healing and resulting in an increase of fibronectin expression to compensate. DKO mice on the other hand, showed significantly less fibronectin fragments than the ApoE-KO group, including the 220 kDa fragment, suggesting that GzmB contributes to improper matrix remodeling and degradation in high fat diet-fed ApoE-KO mice.

The exact role of GzmB in this process remains to be fully elucidated. GzmB may contribute to this process through its ability to degrade ECM, such as decorin and fibronectin, however additional roles for GzmB in chronic wound healing are also possible. The high fat diet-fed ApoE-KO model of impaired wound healing features an altered inflammatory profile as seen by the number of remaining macrophages and foam cells in the wounded tissue at day 16 compared to the WT mice. GzmB activity also has the potential to influence inflammation, which could contribute to an increased pro-inflammatory environment. GzmB-mediated enhancement of IL-1 α and IL-18 activity are both potentially reduced in GzmB deficient animals [70, 71] and this reduction could compensate for the exaggerated immune response often seen in ApoE-KO mice fed a high fat diet.

In the non-healed wounds, GzmB positive staining was observed primarily in cell types resembling macrophages. Macrophages play a central role in wound healing and were observed in large amounts in the non-healed ApoE-KO mouse skin. ApoE is known to influence macrophage activation and although a direct link between ApoE deficiency and upregulation of GzmB by macrophages is not shown, future work investigating the activation status of macrophages in this model could shed light on a possible mechanism of increased GzmB expression during ApoE-KO mouse wound healing.

In this chapter, evidence was also provided to suggest that, similar to the human forms, mouse GzmB can cleave mouse fibronectin. The generation of a 220 kDa fragment was seen following incubation with GzmB at as low as 100 nM. Although no one knows the actual concentration of GzmB released into local extracellular spaces within tissues, recent work has suggested that lower nanomolar concentrations are more physiologically relevant when studying granzyme activity *in vitro* [10, 217] as opposed to micromolar concentrations that have

previously been used by some groups [218]. Other fibronectin fragments in the skin homogenate, including the full length fragment, showed near complete degradation following GzmB treatment. The ability of GzmB to degrade ECM proteins has been greatly expanded upon in recent years with the continued discovery of extracellular substrates. Elevated extracellular GzmB has also been detected in several bodily fluids in disease prompting the investigation of GzmB-mediated ECM remodeling as important disease causing events. Research using animal models have provided additional evidence that GzmB can act in an extracellular, perforin-independent manner to cause disease by degrading ECM components [13, 64, 72]. Mouse and human GzmB can have different specificities for some intracellular substrates [219], however these results provide evidence that the extracellular GzmB substrate fibronectin is susceptible to cleavage not only in humans [12], but in mice as well.

8. Major findings, study limitations and future directions

8.1 Major findings

The serine protease GzmB was investigated in this study for its role in skin aging and impaired wound healing. As inflammation represents a key mechanism behind tissue damage associated with aging and age-related diseases, we used a mouse model susceptible to chronic inflammation to mimic age-related alterations in structure and function of the skin. The skin offers a useful model organ to study age-related changes in ECM structure and function. ApoE-KO mice provided a model that exhibited an inflamed skin phenotype and served to model the potential effect of GzmB-mediated ECM remodeling during aging and disease.

ApoE-KO mice fed a high fat diet were found to exhibit accelerated skin aging and impaired wound healing. It was found that both age and diet were critical factors in this model as ApoE-KO mice required a high fat diet for 30 weeks to fully develop these characteristics. High fat diet-fed ApoE-KO mice were found to have skin that was significantly thinner than WT controls, and featured a significant loss of dermal collagen density and organization. These mice also demonstrated an increased susceptibility to inflammatory skin diseases and persistent, chronic inflammation during wound healing. This altered skin phenotype resulted in impaired wound healing including delayed contraction and slower wound closure.

The mechanism behind accelerated skin aging and impaired wound healing in ApoE-KO mice was also investigated. GzmB is known to be expressed by a number of different immune cells during chronic inflammation and its ability to exhibit cytotoxicity, degrade the ECM and activate cytokines provided a number of possible roles for GzmB in accelerated skin aging and impaired wound healing in ApoE-KO mice. It was found that in high fat diet-fed ApoE-KO mice

deficient in GzmB, accelerated skin aging and impaired wound healing was attenuated. First, DKO mice showed significantly thicker skin and increased collagen density and organization compared to ApoE-KO mice when fed a high fat diet. GzmB deficiency was also found to improve wound contraction and closure in ApoE-KO mice, suggesting that GzmB contributes to impaired healing in high fat diet-fed ApoE-KO mice.

As mentioned above, GzmB activity could contribute to these phenotypes in a number of different ways. In this study, we focused on the ability of GzmB to degrade and remodel the ECM. It was found that GzmB is capable of cleaving the proteoglycan decorin. Decorin interacts with collagen and is critical for collagen organization and proper spacing. GzmB deficiency increased the amount of decorin observed in the skin of ApoE-KO mice both in aged skin and wounded skin. Increased decorin in DKO mouse skin was also associated with increased collagen density and organization, which was significantly greater compared to the ApoE-KO mice when fed a high fat diet. Fibronectin fragments in wounded ApoE-KO mouse skin were also decreased in DKO mice raising the possibility that excessive fibronectin degradation by GzmB is a contributing factor to delayed healing in this model. *In vitro* cleavage assays using mouse GzmB confirmed the ability of the mouse enzyme to degrade mouse fibronectin from skin and generated fragments similar to those observed in the non-healed skin of ApoE-KO mice. GzmB was also found to be present in mast cells in ApoE-KO mouse skin, representing a potentially important source of extracellular GzmB in the skin of ApoE-KO mice.

Overall, these results suggest that GzmB contributes to accelerated skin aging and impaired wound healing in high fat diet-fed ApoE-KO mice. These results are summarized in Table 4. While work remains to be done to decipher additional, complimentary roles of GzmB in

this process, our results suggest that GzmB-mediated decorin and fibronectin degradation play an important role in the aging phenotypes observed in high fat diet-fed ApoE-KO mice.

Table 4. Summary of age-related phenotypes displayed by all groups of mice at 30 weeks.

Age-related phenotype	WT	WT (high fat)	ApoE-KO	ApoE-KO (high fat)	DKO	DKO (high fat)
frailty and weight loss	n	--	+	+++	n	-
chronic inflammation	n	n	+	++	+	+
susceptibility to injury and disease	n	n	+	+++	+	+
skin thinning	n	--	n	++	n	n
collagen disorganization	n	n	n	++	-	-
reduced decorin levels	n	n	n	+	-	-
delayed wound closure	n	n	n	++	n	+

n = normal

+ = more than normal

- = less than normal

8.2 Study limitations

Animal models provide useful tools for studying mechanisms of aging and disease, however it is of course important to note the limitations of these models when interpreting results with the intention of finding solutions for human pathologies. In this dissertation, the ApoE-KO mouse was used as a model that mimics aspects of human skin aging and chronic wound healing. ApoE-KO mice are deficient in ApoE, resulting in hyperlipidemia and increased susceptibility to inflammation and disease. Mechanisms of similar disease pathogenesis in humans however do not typically result from a lack of ApoE protein, as this is not a relevant or occurring human condition. Although humans can express different ApoE isoforms, with varying degrees of functionality, ApoE deficient individuals do not represent a significant portion of the population.

Important differences between biological mechanisms also exist between mice and humans. Mouse skin differs from human skin in that it contains a much thinner epidermis, greater hair density and the presence of an underlying skeletal muscle layer called the panniculus carnosus. These structural differences are important to note when interpreting age-related changes and mechanisms, particularly with respect to contraction during wound healing.

Wound healing in mice does not occur by identical mechanisms as in humans. The main difference is that mice heal mainly by contraction, as opposed to re-epithelialization. In this study, we found that nearly 90% of the wound was closed through contraction in some animals. Although contraction is still an important component of wound healing in humans, the difference in mechanisms and kinetics of healing are such that further experiments using more human-like models (such as pigs) are required to confirm the results obtained in mice are of relevance to human conditions.

We found that for ApoE-KO mice to be a suitable model of skin aging and chronic wound healing, a high fat diet employed for 30 weeks was necessary. At this time point, ApoE-KO mice developed several phenotypes that resembled premature aging and chronic wound healing in humans. One caveat to this model however is the fact that ApoE-KO mice often do not survive to 30 weeks when fed a high fat diet. This is due to the susceptibility of ApoE-KO mice to develop severe inflammatory skin lesions on their backs and shoulders requiring euthanasia for humane reasons. The consequence of this is that only the healthiest (longest lived) ApoE-KO mice are left at the end of the 30 week time point. Whether the results would be different if it were not for this selection effect is unknown, and the possibility exists that a slightly earlier time point, when more ApoE-KO mice are able to survive, would be a more ideal model and give an improved phenotype.

An important limitation in this study is that the gene expression of important ECM proteins such as collagen and decorin was not assessed. This is of interest particularly to the wound healing experiments as increased ECM protein in the wound does not necessarily represent reduced degradation. Indeed, chronic wounds have been shown to have reduced ECM proteins while exhibiting increased protein expression due to the subsequent increase in proteolysis [134-138].

The use of GzmB KO mice to study GzmB in aging and disease is a useful tool, but also has important limitations. GzmB is expressed by many different immune and non-immune cell types and has a wide variety of functionalities from apoptosis to ECM remodeling, including inflammation through cytokine processing, and suppressing inflammation via Tregs. It is this diversity in activity that makes results obtained using a global knockout of GzmB potentially difficult to interpret. Protection or worsening of a particular disease phenotype may be due to a

lack of direct GzmB activity, or through indirect mechanisms such as a lack of GzmB-mediated cytokine processing or immune suppression. Although we found evidence of ECM degradation of substrates known to be cleaved by GzmB, the possibility still remains that the protective effects seen in GzmB KO mice are due at least partially to other mechanisms such as a reduction in cytokine activation. Knocking out GzmB from specific cell types or in specific tissues would provide important solutions to circumventing these limitations.

Much of what we know regarding the extracellular role of GzmB in disease comes from studies using GzmB knockout mice. For example, in a model of abdominal aortic aneurysm, GzmB knockout mice have a reduced incidence of aneurysm rupture while perforin knockout mice do not, suggesting extracellular GzmB activity is contributing to disease pathogenesis [13, 72]. GzmB knockout mice, while useful in modeling the role of GzmB in disease, do have limitations however. While most established GzmB expressing cells in humans also express GzmB in mice, certain cell types such as B cells show differences in expression patterns between the two species [28, 220]. Mice are also known to possess several granzymes not present in humans, whose functions have not been well studied and the disruption of the GzmB gene in mice could affect the activity of other nearby genes (eg. GzmC, GzmD, GzmF, and GzmG) [221]. Some differences also exist in the substrate specificity of mouse GzmB compared to humans [216]. Despite this, GzmB knockout mice provide an invaluable tool for elucidating important roles for GzmB in disease and many observations made in this model offer important rationale for examining GzmB further in human pathologies.

8.3 Future directions

In this dissertation, I have described the high fat diet-fed ApoE-KO mouse as a model of accelerated skin aging and impaired wound healing. The serine protease GzmB was found to contribute to these phenotypes, likely through the degradation of ECM proteins and proteoglycans such as fibronectin and decorin. Future work is required to further the characterization this model and the additional roles of ApoE and GzmB on the phenotypes observed and mechanisms involved.

The exact link between ApoE and GzmB in this model is currently unknown. Although ApoE has known roles in suppressing immune cell activation and proliferation, experiments designed to examine the effect of ApoE on GzmB expression in these cells would provide useful mechanistic insight towards a better understanding of the ApoE-KO model. As a number of different immune cells, when activated, are known to express GzmB, ApoE suppression of these cells could represent a possible explanation for increased GzmB-mediated tissue damage in ApoE-KO mice fed a high fat diet.

Further characterization and identification of the different cell types expressing GzmB in ApoE-KO mouse skin would also benefit our understanding of the role of GzmB in this model. In this study, mast cells were identified as potentially a key source of extracellular GzmB due to the fact that mast cell-derived GzmB is likely to function in an extracellular fashion due to the lack of perforin expression. GzmB expression was also observed in the skin of ApoE-KO mice by cell types that did not stain positive as mast cells and it is not surprising that additional cell types (T cells, NK cells, macrophages) could also be responsible for the presence of GzmB in the

skin. Further dual staining or flow cytometry experiments would help to identify all GzmB-expressing cells in this model.

DKO mice were used in this study to examine the role of GzmB in ApoE-KO mouse skin aging and impaired wound healing. Although knockout mice provide a useful tool to study the role of GzmB, the alternative use of a GzmB-inhibitor would help to confirm these results. Particularly, in high fat diet-fed ApoE-KO mice undergoing wound healing, the use of a GzmB inhibitor, rather than DKO mice, would reveal if GzmB deficiency is protective in ApoE-KO mice due to reduced GzmB activity during wound healing, or because of improved/healthier skin as a starting material. Although we did observe differences in DKO mouse skin compared to ApoE-KO mice, it is not clear if these differences are what accounts for the improved healing, or if it is primarily the result of a reduction in the amount of GzmB activity in response to injury. Either way, the role of GzmB in this process would be elucidated further through inhibitor studies.

The role of GzmB in the skin of ApoE-KO mice was examined however the role of GzmB in regular WT mouse aging and wound healing was not looked at in this study. Future work using GzmB single knockout mice would help decipher the potential detrimental or beneficial effects of GzmB deficiency during healthy aging and wound healing. Perforin knockout mice have also been used to differentiate between intracellular and extracellular GzmB activity in disease. Future experiments using perforin knockout mice would help decipher the relative contribution of intra-versus extracellular GzmB activity to skin aging and impaired healing in ApoE-KO mice.

As wound healing in humans occurs primarily through re-epithelialization, rather than contraction, an improved/optimized ApoE-KO mouse model would potentially help examine the role of GzmB in this process. Wound healing procedures using splints have been shown to be an effective way to limit wound contraction and promote wound closure in mice through re-epithelialization. Future experiments using ApoE-KO mice fitted with a splint would provide valuable information into the usefulness of this model to study re-epithelialization, and the possible role of GzmB in this process.

Finally, in order to translate these findings to humans, future work aimed at examining GzmB activity in human skin aging and wound healing is essential. GzmB has been implicated in human skin diseases associated with age as well as photoaging. However, analysis into GzmB activity in chronic wounds has yet to be examined. Chronic wound fluid from non-healing ulcers have shown increased fragments of the GzmB substrates fibronectin and vitronectin [134, 135]. Investigation into the presence and activity of GzmB in these wound fluids would greatly assist in our understanding of the role of GzmB in human chronic wounds.

9. Conclusions

Much progress has been made over the last decade in uncovering novel substrates for the serine protease GzmB. Perhaps the most ground-breaking findings have been those identifying previously unknown extracellular substrates. This has led to a renewed awareness that GzmB is more than simply a cytotoxic protease acting intracellularly to induce apoptosis. To date, extracellular GzmB substrates include a number of different ECM proteins and proteoglycans, as well as multiple pro-inflammatory cytokines. GzmB-mediated cleavage of these substrates during aging and disease has important implications on our understanding of mechanisms behind these processes.

Of the many extracellular GzmB substrates identified *in vitro*, much work remains to be done to determine the exact role of GzmB-mediated substrate cleavage during aging and disease *in vivo*. So far, the role of GzmB-mediated ECM degradation in disease has been investigated in only a few disease models. GzmB-mediated degradation of decorin and fibrillin-1 were both found to be potentially critical ECM substrates of GzmB whose degradation contributes to abdominal aortic aneurysm. In this dissertation, GzmB exerted a significant impact on skin aging and wound healing in ApoE-KO mice, likely through degradation of the ECM.

ApoE-KO mice have been studied extensively in the context of hyperlipidemia and atherosclerosis. We have shown that ApoE-KO mice fed a high fat diet, in addition to developing atherosclerosis, display a phenotype indicative of premature skin aging. The skin of ApoE-KO mice is susceptible to chronic inflammation, ECM remodeling that features collagen disorganization, skin thinning and impaired wound healing. ApoE-KO mice should therefore be considered as a potentially useful model to study skin aging and impaired wound healing, and the

ECM changes that characteristically occur. Evidence was given to suggest that GzmB is present in the skin of ApoE-KO mice, expressed by mast cells and acting extracellularly by degrading and remodeling components of the ECM. Both decorin and fibronectin remodeling by GzmB is suggested to contribute to accelerated skin aging and impaired wound healing in the inflamed skin of ApoE-KO mice. Taken together, the results of this dissertation suggests that GzmB contributes to aging and impaired wound healing in skin through excessive degradation of ECM proteins.

Bibliography

1. Pasternack, M.S. and Eisen, H.N. (1985) A novel serine esterase expressed by cytotoxic T lymphocytes. *Nature* 314, 743-745
2. Simon, M.M., Hoschutzky, H., Fruth, U., Simon, H.G., and Kramer, M.D. (1986) Purification and characterization of a T cell specific serine proteinase (TSP-1) from cloned cytolytic T lymphocytes. *The EMBO journal* 5, 3267-3274
3. Brunet, J.F., Dosseto, M., Denizot, F., Mattei, M.G., Clark, W.R., Haqqi, T.M., Ferrier, P., Nabholz, M., Schmitt-Verhulst, A.M., Luciani, M.F., and Golstein, P. (1986) The inducible cytotoxic T-lymphocyte-associated gene transcript CTLA-1 sequence and gene localization to mouse chromosome 14. *Nature* 322, 268-271
4. Masson, D., Nabholz, M., Estrade, C., and Tschopp, J. (1986) Granules of cytolytic T-lymphocytes contain two serine esterases. *The EMBO journal* 5, 1595-1600
5. Young, J.D., Leong, L.G., Liu, C.C., Damiano, A., Wall, D.A., and Cohn, Z.A. (1986) Isolation and characterization of a serine esterase from cytolytic T cell granules. *Cell* 47, 183-194
6. Bleackley, R.C., Duggan, B., Ehrman, N., and Lobe, C.G. (1988) Isolation of two cDNA sequences which encode cytotoxic cell proteases. In *FEBS Lett*, pp. 153-159
7. Smyth, M.J. and Trapani, J.A. (1995) Granzymes: exogenous proteinases that induce target cell apoptosis. *Immunol Today* 16, 202-206
8. Barry, M. and Bleackley, R.C. (2002) Cytotoxic T lymphocytes: all roads lead to death. *Nat Rev Immunol* 2, 401-409
9. Boivin, W.A., Cooper, D.M., Hiebert, P.R., and Granville, D.J. (2009) Intracellular versus extracellular granzyme B in immunity and disease: challenging the dogma. *Lab Invest* 89, 1195-1220
10. Metkar, S.S., Menea, C., Pardo, J., Wang, B., Wallich, R., Freudenberg, M., Kim, S., Raja, S.M., Shi, L., Simon, M.M., and Froelich, C.J. (2008) Human and mouse granzyme A induce a proinflammatory cytokine response. *Immunity* 29, 720-733
11. Froelich, C.J., Zhang, X., Turbov, J., Hudig, D., Winkler, U., and Hanna, W.L. (1993) Human granzyme B degrades aggrecan proteoglycan in matrix synthesized by chondrocytes. *J Immunol* 151, 7161-7171
12. Buzza, M.S., Zamurs, L., Sun, J., Bird, C.H., Smith, A.I., Trapani, J.A., Froelich, C.J., Nice, E.C., and Bird, P.I. (2005) Extracellular matrix remodeling by human granzyme B via cleavage of vitronectin, fibronectin, and laminin. *J Biol Chem* 280, 23549-23558

13. Chamberlain, C.M., Ang, L.S., Boivin, W.A., Cooper, D.M., Williams, S.J., Zhao, H., Hendel, A., Folkesson, M., Swedenborg, J., Allard, M.F., McManus, B.M., and Granville, D.J. (2010) Perforin-independent extracellular granzyme B activity contributes to abdominal aortic aneurysm. *Am J Pathol* 176, 1038-1049
14. Hatcher, V.B., Oberman, M.S., Lazarus, G.S., and Grayzel, A.I. (1978) A cytotoxic proteinase isolated from human lymphocytes. *J Immunol* 120, 665-670
15. Klein, J.L., Shows, T.B., Dupont, B., and Trapani, J.A. (1989) Genomic organization and chromosomal assignment for a serine protease gene (CSPB) expressed by human cytotoxic lymphocytes. *Genomics* 5, 110-117
16. Murphy, M.E., Moulton, J., Bleackley, R.C., Gershensfeld, H., Weissman, I.L., and James, M.N. (1988) Comparative molecular model building of two serine proteinases from cytotoxic T lymphocytes. *Proteins* 4, 190-204
17. Poe, M., Blake, J.T., Boulton, D.A., Gammon, M., Sigal, N.H., Wu, J.K., and Zweerink, H.J. (1991) Human cytotoxic lymphocyte granzyme B. Its purification from granules and the characterization of substrate and inhibitor specificity. *J Biol Chem* 266, 98-103
18. Waugh, S.M., Harris, J.L., Fletterick, R., and Craik, C.S. (2000) The structure of the pro-apoptotic protease granzyme B reveals the molecular determinants of its specificity. *Nat Struct Biol* 7, 762-765
19. Namekawa, T., Wagner, U.G., Goronzy, J.J., and Weyand, C.M. (1998) Functional subsets of CD4 T cells in rheumatoid synovitis. *Arthritis Rheum* 41, 2108-2116
20. Rissoan, M.C., Duhon, T., Bridon, J.M., Bendriss-Vermare, N., Peronne, C., de Saint Vis, B., Briere, F., and Bates, E.E. (2002) Subtractive hybridization reveals the expression of immunoglobulin-like transcript 7, Eph-B1, granzyme B, and 3 novel transcripts in human plasmacytoid dendritic cells. *Blood* 100, 3295-3303
21. Grossman, W.J., Verbsky, J.W., Tollefsen, B.L., Kemper, C., Atkinson, J.P., and Ley, T.J. (2004) Differential expression of granzymes A and B in human cytotoxic lymphocyte subsets and T regulatory cells. *Blood* 104, 2840-2848
22. Wagner, C., Iking-Konert, C., Deneffle, B., Stegmaier, S., Hug, F., and Hansch, G.M. (2004) Granzyme B and perforin: constitutive expression in human polymorphonuclear neutrophils. *Blood* 103, 1099-1104
23. Baba, T., Ishizu, A., Iwasaki, S., Suzuki, A., Tomaru, U., Ikeda, H., Yoshiki, T., and Kasahara, M. (2006) CD4⁺/CD8⁺ macrophages infiltrating at inflammatory sites: a population of monocytes/macrophages with a cytotoxic phenotype. *Blood* 107, 2004-2012
24. Tschopp, C.M., Spiegl, N., Didichenko, S., Lutmann, W., Julius, P., Virchow, J.C., Hack, C.E., and Dahinden, C.A. (2006) Granzyme B, a novel mediator of allergic inflammation: its induction and release in blood basophils and human asthma. *Blood* 108, 2290-2299

25. Kim, W.J., Kim, H., Suk, K., and Lee, W.H. (2007) Macrophages express granzyme B in the lesion areas of atherosclerosis and rheumatoid arthritis. *Immunol Lett* 111, 57-65
26. Pardo, J., Wallich, R., Ebnet, K., Iden, S., Zentgraf, H., Martin, P., Ekiciler, A., Prins, A., Mullbacher, A., Huber, M., and Simon, M.M. (2007) Granzyme B is expressed in mouse mast cells in vivo and in vitro and causes delayed cell death independent of perforin. *Cell Death Differ* 14, 1768-1779
27. Strik, M.C., de Koning, P.J., Kleijmeer, M.J., Bladergroen, B.A., Wolbink, A.M., Griffith, J.M., Wouters, D., Fukuoka, Y., Schwartz, L.B., Hack, C.E., van Ham, S.M., and Kummer, J.A. (2007) Human mast cells produce and release the cytotoxic lymphocyte associated protease granzyme B upon activation. *Mol Immunol* 44, 3462-3472
28. Hagn, M., Schwesinger, E., Ebel, V., Sontheimer, K., Maier, J., Beyer, T., Syrovets, T., Laumonnier, Y., Fabricius, D., Simmet, T., and Jahrsdorfer, B. (2009) Human B cells secrete granzyme B when recognizing viral antigens in the context of the acute phase cytokine IL-21. *J Immunol* 183, 1838-1845
29. Hirst, C.E., Buzza, M.S., Sutton, V.R., Trapani, J.A., Loveland, K.L., and Bird, P.I. (2001) Perforin-independent expression of granzyme B and proteinase inhibitor 9 in human testis and placenta suggests a role for granzyme B-mediated proteolysis in reproduction. *Mol Hum Reprod* 7, 1133-1142
30. Choy, J.C., McDonald, P.C., Suarez, A.C., Hung, V.H., Wilson, J.E., McManus, B.M., and Granville, D.J. (2003) Granzyme B in atherosclerosis and transplant vascular disease: association with cell death and atherosclerotic disease severity. *Mod Pathol* 16, 460-470
31. Horiuchi, K., Saito, S., Sasaki, R., Tomatsu, T., and Toyama, Y. (2003) Expression of granzyme B in human articular chondrocytes. *J Rheumatol* 30, 1799-1810
32. Sasson, R., Dantes, A., Tajima, K., and Amsterdam, A. (2003) Novel genes modulated by FSH in normal and immortalized FSH-responsive cells: new insights into the mechanism of FSH action. *FASEB J* 17, 1256-1266
33. Hernandez-Pigeon, H., Jean, C., Charruyer, A., Haure, M.J., Titeux, M., Tonasso, L., Quillet-Mary, A., Baudouin, C., Charveron, M., and Laurent, G. (2006) Human keratinocytes acquire cellular cytotoxicity under UV-B irradiation. Implication of granzyme B and perforin. *J Biol Chem* 281, 13525-13532
34. Vernooij, J.H., Moller, G.M., van Suylen, R.J., van Spijk, M.P., Cloots, R.H., Hoet, P.H., Pennings, H.J., and Wouters, E.F. (2007) Increased granzyme A expression in type II pneumocytes of patients with severe chronic obstructive pulmonary disease. *Am J Respir Crit Care Med* 175, 464-472
35. Babichuk, C.K., Duggan, B.L., and Bleackley, R.C. (1996) In vivo regulation of murine granzyme B gene transcription in activated primary T cells. *J Biol Chem* 271, 16485-16493

36. Fregeau, C.J. and Bleackley, R.C. (1991) Transcription of two cytotoxic cell protease genes is under the control of different regulatory elements. *Nucleic Acids Res* 19, 5583-5590
37. Wargnier, A., Lafaurie, C., Legros-Maida, S., Bourge, J.F., Sigaux, F., Sasportes, M., and Paul, P. (1998) Down-regulation of human granzyme B expression by glucocorticoids. Dexamethasone inhibits binding to the Ikaros and AP-1 regulatory elements of the granzyme B promoter. *J Biol Chem* 273, 35326-35331
38. Haddad, P., Wargnier, A., Bourge, J.F., Sasportes, M., and Paul, P. (1993) A promoter element of the human serine esterase granzyme B gene controls specific transcription in activated T cells. *Eur J Immunol* 23, 625-629
39. Hernandez-Pigeon, H., Jean, C., Charruyer, A., Haure, M.J., Baudouin, C., Charveron, M., Quillet-Mary, A., and Laurent, G. (2007) UVA induces granzyme B in human keratinocytes through MIF: implication in extracellular matrix remodeling. *J Biol Chem* 282, 8157-8164
40. Fehniger, T.A., Cai, S.F., Cao, X., Bredemeyer, A.J., Presti, R.M., French, A.R., and Ley, T.J. (2007) Acquisition of murine NK cell cytotoxicity requires the translation of a pre-existing pool of granzyme B and perforin mRNAs. *Immunity* 26, 798-811
41. Griffiths, G.M. and Isaaz, S. (1993) Granzymes A and B are targeted to the lytic granules of lymphocytes by the mannose-6-phosphate receptor. *J Cell Biol* 120, 885-896
42. Smyth, M.J., McGuire, M.J., and Thia, K.Y. (1995) Expression of recombinant human granzyme B. A processing and activation role for dipeptidyl peptidase I. *J Immunol* 154, 6299-6305
43. Grujic, M., Braga, T., Lukinius, A., Eloranta, M.L., Knight, S.D., Pejler, G., and Abrink, M. (2005) Serglycin-deficient cytotoxic T lymphocytes display defective secretory granule maturation and granzyme B storage. *J Biol Chem* 280, 33411-33418
44. Bird, C.H., Sutton, V.R., Sun, J., Hirst, C.E., Novak, A., Kumar, S., Trapani, J.A., and Bird, P.I. (1998) Selective regulation of apoptosis: the cytotoxic lymphocyte serpin proteinase inhibitor 9 protects against granzyme B-mediated apoptosis without perturbing the Fas cell death pathway. *Mol Cell Biol* 18, 6387-6398
45. Sun, J., Bird, C.H., Sutton, V., McDonald, L., Coughlin, P.B., De Jong, T.A., Trapani, J.A., and Bird, P.I. (1996) A cytosolic granzyme B inhibitor related to the viral apoptotic regulator cytokine response modifier A is present in cytotoxic lymphocytes. *J Biol Chem* 271, 27802-27809
46. Darmon, A.J., Nicholson, D.W., and Bleackley, R.C. (1995) Activation of the apoptotic protease CPP32 by cytotoxic T-cell-derived granzyme B. *Nature* 377, 446-448

47. Adrain, C., Murphy, B.M., and Martin, S.J. (2005) Molecular ordering of the caspase activation cascade initiated by the cytotoxic T lymphocyte/natural killer (CTL/NK) protease granzyme B. *J Biol Chem* 280, 4663-4673
48. Medema, J.P., Toes, R.E., Scaffidi, C., Zheng, T.S., Flavell, R.A., Melief, C.J., Peter, M.E., Offringa, R., and Krammer, P.H. (1997) Cleavage of FLICE (caspase-8) by granzyme B during cytotoxic T lymphocyte-induced apoptosis. *Eur J Immunol* 27, 3492-3498
49. Sutton, V.R., Davis, J.E., Cancilla, M., Johnstone, R.W., Ruefli, A.A., Sedelies, K., Browne, K.A., and Trapani, J.A. (2000) Initiation of apoptosis by granzyme B requires direct cleavage of bid, but not direct granzyme B-mediated caspase activation. *J Exp Med* 192, 1403-1414
50. Heibein, J.A., Goping, I.S., Barry, M., Pinkoski, M.J., Shore, G.C., Green, D.R., and Bleackley, R.C. (2000) Granzyme B-mediated cytochrome c release is regulated by the Bcl-2 family members bid and Bax. *J Exp Med* 192, 1391-1402
51. Pinkoski, M.J., Waterhouse, N.J., Heibein, J.A., Wolf, B.B., Kuwana, T., Goldstein, J.C., Newmeyer, D.D., Bleackley, R.C., and Green, D.R. (2001) Granzyme B-mediated apoptosis proceeds predominantly through a Bcl-2-inhibitable mitochondrial pathway. *J Biol Chem* 276, 12060-12067
52. Li, P., Nijhawan, D., Budihardjo, I., Srinivasula, S.M., Ahmad, M., Alnemri, E.S., and Wang, X. (1997) Cytochrome c and dATP-dependent formation of Apaf-1/caspase-9 complex initiates an apoptotic protease cascade. *Cell* 91, 479-489
53. Jiang, X. and Wang, X. (2000) Cytochrome c promotes caspase-9 activation by inducing nucleotide binding to Apaf-1. *J Biol Chem* 275, 31199-31203
54. Han, J., Goldstein, L.A., Gastman, B.R., Froelich, C.J., Yin, X.M., and Rabinowich, H. (2004) Degradation of Mcl-1 by granzyme B: implications for Bim-mediated mitochondrial apoptotic events. *J Biol Chem* 279, 22020-22029
55. McIlroy, D., Cartron, P.F., Tuffery, P., Dudoit, Y., Samri, A., Autran, B., Vallette, F.M., Debre, P., and Theodorou, I. (2003) A triple-mutated allele of granzyme B incapable of inducing apoptosis. *Proc Natl Acad Sci U S A* 100, 2562-2567
56. Sun, J., Bird, C.H., Thia, K.Y., Matthews, A.Y., Trapani, J.A., and Bird, P.I. (2004) Granzyme B encoded by the commonly occurring human RAH allele retains pro-apoptotic activity. *J Biol Chem* 279, 16907-16911
57. Gaafar, A., Aljurf, M.D., Al-Sulaiman, A., Iqniebi, A., Manogaran, P.S., Mohamed, G.E., Al-Sayed, A., Alzahrani, H., Alsharif, F., Mohareb, F., Ajarim, D., Tabakhi, A., and Al-Hussein, K. (2009) Defective gammadelta T-cell function and granzyme B gene polymorphism in a cohort of newly diagnosed breast cancer patients. *Exp Hematol* 37, 838-848

58. Girnita, D.M., Webber, S.A., Brooks, M.M., Ferrell, R., Girnita, A.L., Burckart, G.J., Chinnock, R., Canter, C., Addonizio, L., Bernstein, D., Kirklin, J.K., Naftel, D., and Zeevi, A. (2009) Genotypic variation and phenotypic characterization of granzyme B gene polymorphisms. *Transplantation* 87, 1801-1806
59. Espinoza, L.J., Takami, A., Nakata, K., Yamada, K., Onizuka, M., Kawase, T., Sao, H., Akiyama, H., Miyamura, K., Okamoto, S., Inoue, M., Fukuda, T., Morishima, Y., Kodera, Y., and Nakao, S. (2011) Genetic variants of human granzyme B predict transplant outcomes after HLA matched unrelated bone marrow transplantation for myeloid malignancies. *PLoS One* 6, e23827
60. Stepp, S.E., Dufourcq-Lagelouse, R., Le Deist, F., Bhawan, S., Certain, S., Mathew, P.A., Henter, J.I., Bennett, M., Fischer, A., de Saint Basile, G., and Kumar, V. (1999) Perforin gene defects in familial hemophagocytic lymphohistiocytosis. *Science* 286, 1957-1959
61. Stepp, S.E., Mathew, P.A., Bennett, M., de Saint Basile, G., and Kumar, V. (2000) Perforin: more than just an effector molecule. *Immunol Today* 21, 254-256
62. Buzza, M.S. and Bird, P.I. (2006) Extracellular granzymes: current perspectives. *Biol Chem* 387, 827-837
63. Choy, J.C., Hung, V.H., Hunter, A.L., Cheung, P.K., Motyka, B., Goping, I.S., Sawchuk, T., Bleackley, R.C., Podor, T.J., McManus, B.M., and Granville, D.J. (2004) Granzyme B induces smooth muscle cell apoptosis in the absence of perforin: involvement of extracellular matrix degradation. *Arterioscler Thromb Vasc Biol* 24, 2245-2250
64. Hiebert, P.R., Boivin, W.A., Abraham, T., Pazooki, S., Zhao, H., and Granville, D.J. (2011) Granzyme B contributes to extracellular matrix remodeling and skin aging in apolipoprotein E knockout mice. *Exp Gerontol* 46, 489-499
65. Boivin, W.A., Shackelford, M., Vanden Hoek, A., Zhao, H., Hackett, T.L., Knight, D.A., and Granville, D.J. (2012) Granzyme B Cleaves Decorin, Biglycan and Soluble Betaglycan, Releasing Active Transforming Growth Factor-beta1. In *PLoS One*, pp. e33163
66. Boivin, W.A., Shackelford, M., Vanden Hoek, A., Zhao, H., Hackett, T.L., Knight, D.A., and Granville, D.J. (2012) Granzyme B cleaves decorin, biglycan and soluble betaglycan, releasing active transforming growth factor-beta1. *PLoS One* 7, e33163
67. Loeb, C.R., Harris, J.L., and Craik, C.S. (2006) Granzyme B proteolyzes receptors important to proliferation and survival, tipping the balance toward apoptosis. *J Biol Chem* 281, 28326-28335
68. Gahring, L., Carlson, N.G., Meyer, E.L., and Rogers, S.W. (2001) Granzyme B proteolysis of a neuronal glutamate receptor generates an autoantigen and is modulated by glycosylation. *J Immunol* 166, 1433-1438

69. Casciola-Rosen, L., Miagkov, A., Nagaraju, K., Askin, F., Jacobson, L., Rosen, A., and Drachman, D.B. (2008) Granzyme B: evidence for a role in the origin of myasthenia gravis. *J Neuroimmunol* 201-202, 33-40
70. Afonina, I.S., Tynan, G.A., Logue, S.E., Cullen, S.P., Bots, M., Luthi, A.U., Reeves, E.P., McElvaney, N.G., Medema, J.P., Lavelle, E.C., and Martin, S.J. (2011) Granzyme B-dependent proteolysis acts as a switch to enhance the proinflammatory activity of IL-1alpha. *Mol Cell* 44, 265-278
71. Omoto, Y., Yamanaka, K., Tokime, K., Kitano, S., Kakeda, M., Akeda, T., Kurokawa, I., Gabazza, E.C., Tsutsui, H., Katayama, N., Yamanishi, K., Nakanishi, K., and Mizutani, H. (2010) Granzyme B is a novel interleukin-18 converting enzyme. *J Dermatol Sci* 59, 129-135
72. Ang, L.S., Boivin, W.A., Williams, S.J., Zhao, H., Abraham, T., Carmine-Simmen, K., McManus, B.M., Bleackley, R.C., and Granville, D.J. (2011) Serpina3n attenuates granzyme B-mediated decorin cleavage and rupture in a murine model of aortic aneurysm. *Cell Death Dis* 2, e209
73. Weismann, A. (1889) *Essays upon Heredity and Kindred Biological Problems*. Oxford: Clarendon Press 1
74. Medawar, P. (1952) *An Unsolved Problem of Biology*. H.K. Lewis & Co, London
75. Hayflick, L. (2007) Biological aging is no longer an unsolved problem. *Ann N Y Acad Sci* 1100, 1-13
76. Weinert, B.T. and Timiras, P.S. (2003) Invited review: Theories of aging. *J Appl Physiol* 95, 1706-1716
77. Harman, D. (1956) Aging: a theory based on free radical and radiation chemistry. *J Gerontol* 11, 298-300
78. Chung, H.Y., Cesari, M., Anton, S., Marzetti, E., Giovannini, S., Seo, A.Y., Carter, C., Yu, B.P., and Leeuwenburgh, C. (2009) Molecular inflammation: underpinnings of aging and age-related diseases. *Ageing Res Rev* 8, 18-30
79. Chung, H.Y., Kim, H.J., Kim, J.W., and Yu, B.P. (2001) The inflammation hypothesis of aging: molecular modulation by calorie restriction. *Ann N Y Acad Sci* 928, 327-335
80. Libby, P. (2002) Inflammation in atherosclerosis. *Nature* 420, 868-874
81. McGeer, P.L. and McGeer, E.G. (2002) Local neuroinflammation and the progression of Alzheimer's disease. *J Neurovirol* 8, 529-538
82. Sansoni, P., Vescovini, R., Fagnoni, F., Biasini, C., Zanni, F., Zanlari, L., Telera, A., Lucchini, G., Passeri, G., Monti, D., Franceschi, C., and Passeri, M. (2008) The immune system in extreme longevity. *Exp Gerontol* 43, 61-65

83. Dorshkind, K., Montecino-Rodriguez, E., and Signer, R.A. (2009) The ageing immune system: is it ever too old to become young again? *Nat Rev Immunol* 9, 57-62
84. Sansoni, P., Cossarizza, A., Brianti, V., Fagnoni, F., Snelli, G., Monti, D., Marcato, A., Passeri, G., Ortolani, C., Forti, E., and et al. (1993) Lymphocyte subsets and natural killer cell activity in healthy old people and centenarians. *Blood* 82, 2767-2773
85. McGrath, J.A. and Uitto, J. (2010) *"Anatomy and Organization of Human Skin". Rook's Textbook of Dermatology. (8th Ed).* Wiley-Blackwell
86. Gilchrist, B.A. and Krutmann, J. (2006) *Skin aging.* Heidelberg: Springer
87. Chung, J.H., Seo, J.Y., Choi, H.R., Lee, M.K., Youn, C.S., Rhie, G., Cho, K.H., Kim, K.H., Park, K.C., and Eun, H.C. (2001) Modulation of skin collagen metabolism in aged and photoaged human skin in vivo. *J Invest Dermatol* 117, 1218-1224
88. Rabe, J.H., Mamelak, A.J., McElgunn, P.J., Morison, W.L., and Sauder, D.N. (2006) Photoaging: mechanisms and repair. *J Am Acad Dermatol* 55, 1-19
89. Leiter, U. and Garbe, C. (2008) Epidemiology of melanoma and nonmelanoma skin cancer--the role of sunlight. *Adv Exp Med Biol* 624, 89-103
90. Kwon, O.S., Hwang, E.J., Bae, J.H., Park, H.E., Lee, J.C., Youn, J.I., and Chung, J.H. (2003) Seborrheic keratosis in the Korean males: causative role of sunlight. *Photodermatol Photoimmunol Photomed* 19, 73-80
91. Varani, J., Warner, R.L., Gharaee-Kermani, M., Phan, S.H., Kang, S., Chung, J.H., Wang, Z.Q., Datta, S.C., Fisher, G.J., and Voorhees, J.J. (2000) Vitamin A antagonizes decreased cell growth and elevated collagen-degrading matrix metalloproteinases and stimulates collagen accumulation in naturally aged human skin. *J Invest Dermatol* 114, 480-486
92. To, W.S. and Midwood, K.S. (2011) Plasma and cellular fibronectin: distinct and independent functions during tissue repair. *Fibrogenesis Tissue Repair* 4, 21
93. Asaga, H., Kikuchi, S., and Yoshizato, K. (1991) Collagen gel contraction by fibroblasts requires cellular fibronectin but not plasma fibronectin. *Exp Cell Res* 193, 167-174
94. Scott, J.E. and Orford, C.R. (1981) Dermatan sulphate-rich proteoglycan associates with rat tail-tendon collagen at the d band in the gap region. *Biochem J* 197, 213-216
95. Danielson, K.G., Baribault, H., Holmes, D.F., Graham, H., Kadler, K.E., and Iozzo, R.V. (1997) Targeted disruption of decorin leads to abnormal collagen fibril morphology and skin fragility. *J Cell Biol* 136, 729-743
96. Carrino, D.A., Mesiano, S., Barker, N.M., Hurd, W.W., and Caplan, A.I. (2012) Proteoglycans of uterine fibroids and keloid scars: similarity in their proteoglycan composition. In *Biochem J*

97. Honardoust, D., Varkey, M., Marcoux, Y., Shankowsky, H.A., and Tredget, E.E. (2011) Reduced Decorin, Fibromodulin, and Transforming Growth Factor-beta3 in Deep Dermis Lead to Hypertrophic Scar. *Journal of burn care & research : official publication of the American Burn Association*
98. Hildebrand, A., Romaris, M., Rasmussen, L.M., Heinegard, D., Twardzik, D.R., Border, W.A., and Ruoslahti, E. (1994) Interaction of the small interstitial proteoglycans biglycan, decorin and fibromodulin with transforming growth factor beta. *Biochem J* 302 (Pt 2), 527-534
99. Kolb, M., Margetts, P.J., Galt, T., Sime, P.J., Xing, Z., Schmidt, M., and Gauldie, J. (2001) Transient transgene expression of decorin in the lung reduces the fibrotic response to bleomycin. *American journal of respiratory and critical care medicine* 163, 770-777
100. Kolb, M., Margetts, P.J., Sime, P.J., and Gauldie, J. (2001) Proteoglycans decorin and biglycan differentially modulate TGF-beta-mediated fibrotic responses in the lung. *American journal of physiology. Lung cellular and molecular physiology* 280, L1327-1334
101. Nishiyama, T., Amano, S., Tsunenaga, M., Kadoya, K., Takeda, A., Adachi, E., and Burgeson, R.E. (2000) The importance of laminin 5 in the dermal-epidermal basement membrane. In *J Dermatol Sci*, pp. S51-59
102. Posadas, S.J., Padial, A., Torres, M.J., Mayorga, C., Leyva, L., Sanchez, E., Alvarez, J., Romano, A., Juarez, C., and Blanca, M. (2002) Delayed reactions to drugs show levels of perforin, granzyme B, and Fas-L to be related to disease severity. In *J Allergy Clin Immunol*, pp. 155-161
103. Carrino, D.A., Onnerfjord, P., Sandy, J.D., Cs-Szabo, G., Scott, P.G., Sorrell, J.M., Heinegard, D., and Caplan, A.I. (2003) Age-related changes in the proteoglycans of human skin. Specific cleavage of decorin to yield a major catabolic fragment in adult skin. *J Biol Chem* 278, 17566-17572
104. Kramer, M.D. and Simon, M.M. (1987) Are proteinases functional molecules of T lymphocytes? *Immunology Today* 8, 140-142
105. Cooper, D.M., Pechkovsky, D.V., Hackett, T.L., Knight, D.A., and Granville, D.J. (2011) Granzyme K activates protease-activated receptor-1. *PLoS One* 6, e21484
106. Sower, L.E., Klimpel, G.R., Hanna, W., and Froelich, C.J. (1996) Extracellular activities of human granzymes. I. Granzyme A induces IL6 and IL8 production in fibroblast and epithelial cell lines. *Cell Immunol* 171, 159-163
107. Irmeler, M., Hertig, S., MacDonald, H.R., Sadoul, R., Becherer, J.D., Proudfoot, A., Solari, R., and Tschopp, J. (1995) Granzyme A is an interleukin 1 beta-converting enzyme. *The Journal of experimental medicine* 181, 1917-1922

108. Anthony, D.A., Andrews, D.M., Chow, M., Watt, S.V., House, C., Akira, S., Bird, P.I., Trapani, J.A., and Smyth, M.J. (2010) A role for granzyme M in TLR4-driven inflammation and endotoxemia. *J Immunol* 185, 1794-1803
109. Vignali, D.A., Collison, L.W., and Workman, C.J. (2008) How regulatory T cells work. *Nat Rev Immunol* 8, 523-532
110. Joeckel, L.T., Wallich, R., Martin, P., Sanchez-Martinez, D., Weber, F.C., Martin, S.F., Borner, C., Pardo, J., Froelich, C., and Simon, M.M. (2011) Mouse granzyme K has pro-inflammatory potential. *Cell Death Differ* 18, 1112-1119
111. McHugh, R.S., Whitters, M.J., Piccirillo, C.A., Young, D.A., Shevach, E.M., Collins, M., and Byrne, M.C. (2002) CD4(+)CD25(+) immunoregulatory T cells: gene expression analysis reveals a functional role for the glucocorticoid-induced TNF receptor. *Immunity* 16, 311-323
112. Gondek, D.C., Lu, L.F., Quezada, S.A., Sakaguchi, S., and Noelle, R.J. (2005) Cutting edge: contact-mediated suppression by CD4+CD25+ regulatory cells involves a granzyme B-dependent, perforin-independent mechanism. *J Immunol* 174, 1783-1786
113. Norris, D.A., Clark, R.A., Swigart, L.M., Huff, J.C., Weston, W.L., and Howell, S.E. (1982) Fibronectin fragment(s) are chemotactic for human peripheral blood monocytes. *J Immunol* 129, 1612-1618
114. Clark, R.A., Wikner, N.E., Doherty, D.E., and Norris, D.A. (1988) Cryptic chemotactic activity of fibronectin for human monocytes resides in the 120-kDa fibroblastic cell-binding fragment. *J Biol Chem* 263, 12115-12123
115. Postlethwaite, A.E., Keski-Oja, J., Balian, G., and Kang, A.H. (1981) Induction of fibroblast chemotaxis by fibronectin. Localization of the chemotactic region to a 140,000-molecular weight non-gelatin-binding fragment. *The Journal of experimental medicine* 153, 494-499
116. Bowersox, J.C. and Sorgente, N. (1982) Chemotaxis of aortic endothelial cells in response to fibronectin. *Cancer research* 42, 2547-2551
117. Birdsall, H.H., Porter, W.J., Green, D.M., Rubio, J., Trial, J., and Rossen, R.D. (2004) Impact of fibronectin fragments on the transendothelial migration of HIV-infected leukocytes and the development of subendothelial foci of infectious leukocytes. In *J Immunol*, pp. 2746-2754
118. Okamura, Y., Watari, M., Jerud, E.S., Young, D.W., Ishizaka, S.T., Rose, J., Chow, J.C., and Strauss, J.F., 3rd (2001) The extra domain A of fibronectin activates Toll-like receptor 4. *J Biol Chem* 276, 10229-10233

119. Schaefer, L., Babelova, A., Kiss, E., Hausser, H.J., Baliova, M., Krzyzankova, M., Marsche, G., Young, M.F., Mihalik, D., Gotte, M., Malle, E., Schaefer, R.M., and Grone, H.J. (2005) The matrix component biglycan is proinflammatory and signals through Toll-like receptors 4 and 2 in macrophages. *J Clin Invest* 115, 2223-2233
120. Merline, R., Moreth, K., Beckmann, J., Nastase, M.V., Zeng-Brouwers, J., Tralhao, J.G., Lemarchand, P., Pfeilschifter, J., Schaefer, R.M., Iozzo, R.V., and Schaefer, L. (2011) Signaling by the matrix proteoglycan decorin controls inflammation and cancer through PDCD4 and MicroRNA-21. *Sci Signal* 4, ra75
121. Leibovich, S.J. and Ross, R. (1975) The role of the macrophage in wound repair. A study with hydrocortisone and antimacrophage serum. *Am J Pathol* 78, 71-100
122. Xue, M., Le, N.T., and Jackson, C.J. (2006) Targeting matrix metalloproteases to improve cutaneous wound healing. *Expert opinion on therapeutic targets* 10, 143-155
123. Gill, S.E. and Parks, W.C. (2008) Metalloproteinases and their inhibitors: regulators of wound healing. In *Int J Biochem Cell Biol*, pp. 1334-1347
124. Yager, D.R. and Nwomeh, B.C. (1999) The proteolytic environment of chronic wounds. In *Wound Repair Regen*, pp. 433-441
125. Wild, S., Roglic, G., Green, A., Sicree, R., and King, H. (2004) Global prevalence of diabetes: estimates for the year 2000 and projections for 2030. *Diabetes care* 27, 1047-1053
126. Ramsey, S.D., Newton, K., Blough, D., McCulloch, D.K., Sandhu, N., Reiber, G.E., and Wagner, E.H. (1999) Incidence, outcomes, and cost of foot ulcers in patients with diabetes. *Diabetes care* 22, 382-387
127. Bank, D. and Nix, D. (2006) Preventing skin tears in a nursing and rehabilitation center: an interdisciplinary effort. *Ostomy/wound management* 52, 38-40, 44, 46
128. Baumgarten, M., Margolis, D.J., Orwig, D.L., Shardell, M.D., Hawkes, W.G., Langenberg, P., Palmer, M.H., Jones, P.S., McArdle, P.F., Sterling, R., Kinoshian, B.P., Rich, S.E., Sowinski, J., and Magaziner, J. (2009) Pressure ulcers in elderly patients with hip fracture across the continuum of care. *J Am Geriatr Soc* 57, 863-870
129. Buzza, M.S., Dyson, J.M., Choi, H., Gardiner, E.E., Andrews, R.K., Kaiserman, D., Mitchell, C.A., Berndt, M.C., Dong, J.F., and Bird, P.I. (2008) Antihemostatic activity of human granzyme B mediated by cleavage of von Willebrand factor. In *J Biol Chem*, pp. 22498-22504
130. Mulligan-Kehoe, M.J., Drinane, M.C., Mollmark, J., Casciola-Rosen, L., Hummers, L.K., Hall, A., Rosen, A., Wigley, F.M., and Simons, M. (2007) Antiangiogenic plasma activity in patients with systemic sclerosis. *Arthritis Rheum* 56, 3448-3458

131. Barone, E.J., Yager, D.R., Pozez, A.L., Olutoye, O.O., Crossland, M.C., Diegelmann, R.F., and Cohen, I.K. (1998) Interleukin-1alpha and collagenase activity are elevated in chronic wounds. *Plastic and reconstructive surgery* 102, 1023-1027; discussion 1028-1029
132. Yagisawa, M., Yuo, A., Kitagawa, S., Yazaki, Y., Togawa, A., and Takaku, F. (1995) Stimulation and priming of human neutrophils by IL-1 alpha and IL-1 beta: complete inhibition by IL-1 receptor antagonist and no interaction with other cytokines. *Exp Hematol* 23, 603-608
133. Clark, R.A. (1990) Fibronectin matrix deposition and fibronectin receptor expression in healing and normal skin. *J Invest Dermatol* 94, 128S-134S
134. Grinnell, F., Ho, C.H., and Wysocki, A. (1992) Degradation of fibronectin and vitronectin in chronic wound fluid: analysis by cell blotting, immunoblotting, and cell adhesion assays. *J Invest Dermatol* 98, 410-416
135. Wysocki, A.B. and Grinnell, F. (1990) Fibronectin profiles in normal and chronic wound fluid. *Lab Invest* 63, 825-831
136. Stanley, C.M., Wang, Y., Pal, S., Klebe, R.J., Harkless, L.B., Xu, X., Chen, Z., and Steffensen, B. (2008) Fibronectin fragmentation is a feature of periodontal disease sites and diabetic foot and leg wounds and modifies cell behavior. *Journal of periodontology* 79, 861-875
137. Ongenaes, K.C., Phillips, T.J., and Park, H.Y. (2000) Level of fibronectin mRNA is markedly increased in human chronic wounds. *Dermatol Surg* 26, 447-451
138. Herrick, S.E., Ireland, G.W., Simon, D., McCollum, C.N., and Ferguson, M.W. (1996) Venous ulcer fibroblasts compared with normal fibroblasts show differences in collagen but not fibronectin production under both normal and hypoxic conditions. *J Invest Dermatol* 106, 187-193
139. Upton, Z., Cuttle, L., Noble, A., Kempf, M., Topping, G., Malda, J., Xie, Y., Mill, J., Harkin, D.G., Kravchuk, O., Leavesley, D.I., and Kimble, R.M. (2008) Vitronectin: growth factor complexes hold potential as a wound therapy approach. In *J Invest Dermatol*, pp. 1535-1544
140. Preissner, K.T. and Reuning, U. (2011) Vitronectin in vascular context: facets of a multitasking matricellular protein. *Seminars in thrombosis and hemostasis* 37, 408-424
141. To, W.S. and Midwood, K.S. (2011) Plasma and cellular fibronectin: distinct and independent functions during tissue repair. In *Fibrogenesis Tissue Repair*, pp. 21
142. Usui, M.L., Mansbridge, J.N., Carter, W.G., Fujita, M., and Olerud, J.E. (2008) Keratinocyte migration, proliferation, and differentiation in chronic ulcers from patients with diabetes and normal wounds. *J Histochem Cytochem* 56, 687-696

143. Jarvelainen, H., Puolakkainen, P., Pakkanen, S., Brown, E.L., Hook, M., Iozzo, R.V., Sage, E.H., and Wight, T.N. (2006) A role for decorin in cutaneous wound healing and angiogenesis. *Wound Repair Regen* 14, 443-452
144. Mietz, H., Chevez-Barrios, P., Lieberman, M.W., Wendt, M., Gross, R., and Basinger, S.F. (1997) Decorin and suramin inhibit ocular fibroblast collagen production. *Graefes Arch Clin Exp Ophthalmol* 235, 399-403
145. Shimizukawa, M., Ebina, M., Narumi, K., Kikuchi, T., Munakata, H., and Nukiwa, T. (2003) Intratracheal gene transfer of decorin reduces subpleural fibroproliferation induced by bleomycin. In *American journal of physiology. Lung cellular and molecular physiology*, pp. L526-532
146. Westergren-Thorsson, G., Sime, P., Jordana, M., Gauldie, J., Sarnstrand, B., and Malmstrom, A. (2004) Lung fibroblast clones from normal and fibrotic subjects differ in hyaluronan and decorin production and rate of proliferation. In *Int J Biochem Cell Biol*, pp. 1573-1584
147. Wu, J., Utani, A., Endo, H., and Shinkai, H. (2001) Deficiency of the decorin core protein in the variant form of Ehlers-Danlos syndrome with chronic skin ulcer. *J Dermatol Sci* 27, 95-103
148. Bernstein, E.F., Fisher, L.W., Li, K., LeBaron, R.G., Tan, E.M., and Uitto, J. (1995) Differential expression of the versican and decorin genes in photoaged and sun-protected skin. Comparison by immunohistochemical and northern analyses. *Lab Invest* 72, 662-669
149. Zhang, Z., Garron, T.M., Li, X.J., Liu, Y., Zhang, X., Li, Y.Y., and Xu, W.S. (2009) Recombinant human decorin inhibits TGF-beta1-induced contraction of collagen lattice by hypertrophic scar fibroblasts. *Burns* 35, 527-537
150. Mukhopadhyay, A., Wong, M.Y., Chan, S.Y., Do, D.V., Khoo, A., Ong, C.T., Cheong, H.H., Lim, I.J., and Phan, T.T. Syndecan-2 and decorin: proteoglycans with a difference--implications in keloid pathogenesis. *J Trauma* 68, 999-1008
151. Aso, Y., Fujiwara, Y., Tayama, K., Inukai, T., and Takemura, Y. (2002) Elevation of von Willebrand factor in plasma in diabetic patients with neuropathic foot ulceration. *Diabet Med* 19, 19-26
152. Murakami, M., Fukaya, S., Furuya, M., and Hyakusoku, H. (2010) A case of von Willebrand disease discovered during treatment of a sacral pressure ulcer. *J Nippon Med Sch* 77, 325-327
153. Herouy, Y., Trefzer, D., Hellstern, M.O., Stark, G.B., Vanscheidt, W., Schopf, E., and Norgauer, J. (2000) Plasminogen activation in venous leg ulcers. *Br J Dermatol* 143, 930-936

154. Browse, N.L. and Burnand, K.G. (1982) The cause of venous ulceration. In *Lancet*, pp. 243-245
155. Amadeu, T.P., Braune, A.S., Porto, L.C., Desmouliere, A., and Costa, A.M. (2004) Fibrillin-1 and elastin are differentially expressed in hypertrophic scars and keloids. *Wound Repair Regen* 12, 169-174
156. Ikeda, M., Naitoh, M., Kubota, H., Ishiko, T., Yoshikawa, K., Yamawaki, S., Kurokawa, M., Utani, A., Nakamura, T., Nagata, K., and Suzuki, S. (2009) Elastic fiber assembly is disrupted by excessive accumulation of chondroitin sulfate in the human dermal fibrotic disease, keloid. *Biochem Biophys Res Commun* 390, 1221-1228
157. Ashcroft, G.S., Kielty, C.M., Horan, M.A., and Ferguson, M.W. (1997) Age-related changes in the temporal and spatial distributions of fibrillin and elastin mRNAs and proteins in acute cutaneous wounds of healthy humans. *J Pathol* 183, 80-89
158. Utermann, G., Kindermann, I., Kaffarnik, H., and Steinmetz, A. (1984) Apolipoprotein E phenotypes and hyperlipidemia. *Hum Genet* 65, 232-236
159. Rubinsztein, D.C. and Easton, D.F. (1999) Apolipoprotein E genetic variation and Alzheimer's disease. a meta-analysis. *Dement Geriatr Cogn Disord* 10, 199-209
160. Ang, L.S., Cruz, R.P., Hendel, A., and Granville, D.J. (2008) Apolipoprotein E, an important player in longevity and age-related diseases. *Exp Gerontol* 43, 615-622
161. Schachter, F., Faure-Delanef, L., Guenot, F., Rouger, H., Froguel, P., Lesueur-Ginot, L., and Cohen, D. (1994) Genetic associations with human longevity at the APOE and ACE loci. *Nat Genet* 6, 29-32
162. Schumacher, K., Maerker-Alzer, G., and Wehmer, U. (1974) A lymphocyte-inhibiting factor isolated from normal human liver. *Nature* 251, 655-656
163. Hui, D.Y., Harmony, J.A., Innerarity, T.L., and Mahley, R.W. (1980) Immunoregulatory plasma lipoproteins. Role of apoprotein E and apoprotein B. *J Biol Chem* 255, 11775-11781
164. Pepe, M.G. and Curtiss, L.K. (1986) Apolipoprotein E is a biologically active constituent of the normal immunoregulatory lipoprotein, LDL-In. *J Immunol* 136, 3716-3723
165. Mistry, M.J., Clay, M.A., Kelly, M.E., Steiner, M.A., and Harmony, J.A. (1995) Apolipoprotein E restricts interleukin-dependent T lymphocyte proliferation at the G1A/G1B boundary. *Cell Immunol* 160, 14-23
166. Fujii, D.K. and Edgington, T.S. (1980) Direct suppression of lymphocyte induction by the immunoregulatory human serum low density lipoprotein, LDL-In. *J Immunol* 124, 156-160

167. Hui, D.Y. and Harmony, J.A. (1980) Phosphatidylinositol turnover in mitogen-activated lymphocytes. Suppression by low-density lipoproteins. *Biochem J* 192, 91-98
168. Getz, G.S. and Reardon, C.A. (2009) Apoprotein E as a lipid transport and signaling protein in the blood, liver, and artery wall. *J Lipid Res* 50 Suppl, S156-161
169. Laurat, E., Poirier, B., Tupin, E., Caligiuri, G., Hansson, G.K., Bariety, J., and Nicoletti, A. (2001) In vivo downregulation of T helper cell 1 immune responses reduces atherogenesis in apolipoprotein E-knockout mice. *Circulation* 104, 197-202
170. Ali, K., Middleton, M., Pure, E., and Rader, D.J. (2005) Apolipoprotein E suppresses the type I inflammatory response in vivo. *Circ Res* 97, 922-927
171. Ophir, G., Amariglio, N., Jacob-Hirsch, J., Elkon, R., Rechavi, G., and Michaelson, D.M. (2005) Apolipoprotein E4 enhances brain inflammation by modulation of the NF-kappaB signaling cascade. *Neurobiol Dis* 20, 709-718
172. Terkeltaub, R.A., Dyer, C.A., Martin, J., and Curtiss, L.K. (1991) Apolipoprotein (apo) E inhibits the capacity of monosodium urate crystals to stimulate neutrophils. Characterization of intraarticular apo E and demonstration of apo E binding to urate crystals in vivo. *J Clin Invest* 87, 20-26
173. Tenger, C. and Zhou, X. (2003) Apolipoprotein E modulates immune activation by acting on the antigen-presenting cell. *Immunology* 109, 392-397
174. Werb, Z. and Chin, J.R. (1983) Apoprotein E is synthesized and secreted by resident and thioglycollate-elicited macrophages but not by pyran copolymer- or bacillus Calmette-Guerin-activated macrophages. *J Exp Med* 158, 1272-1293
175. Saura, J., Petegnief, V., Wu, X., Liang, Y., and Paul, S.M. (2003) Microglial apolipoprotein E and astroglial apolipoprotein J expression in vitro: opposite effects of lipopolysaccharide. *J Neurochem* 85, 1455-1467
176. Maezawa, I., Nivison, M., Montine, K.S., Maeda, N., and Montine, T.J. (2006) Neurotoxicity from innate immune response is greatest with targeted replacement of E4 allele of apolipoprotein E gene and is mediated by microglial p38MAPK. *FASEB J* 20, 797-799
177. Feingold, K.R., Elias, P.M., Mao-Qiang, M., Fartasch, M., Zhang, S.H., and Maeda, N. (1995) Apolipoprotein E deficiency leads to cutaneous foam cell formation in mice. *J Invest Dermatol* 104, 246-250
178. Bonomini, F., Filippini, F., Hayek, T., Aviram, M., Keidar, S., Rodella, L.F., Coleman, R., and Rezzani, R. (2010) Apolipoprotein E and its role in aging and survival. *Exp Gerontol* 45, 149-157

179. Hafezi-Moghadam, A., Thomas, K.L., and Wagner, D.D. (2007) ApoE deficiency leads to a progressive age-dependent blood-brain barrier leakage. *Am J Physiol Cell Physiol* 292, C1256-1262
180. Masliah, E., Samuel, W., Veinbergs, I., Mallory, M., Mante, M., and Saitoh, T. (1997) Neurodegeneration and cognitive impairment in apoE-deficient mice is ameliorated by infusion of recombinant apoE. *Brain Res* 751, 307-314
181. Moghadasian, M.H., McManus, B.M., Nguyen, L.B., Shefer, S., Nadji, M., Godin, D.V., Green, T.J., Hill, J., Yang, Y., Scudamore, C.H., and Frohlich, J.J. (2001) Pathophysiology of apolipoprotein E deficiency in mice: relevance to apo E-related disorders in humans. *FASEB J* 15, 2623-2630
182. Hiebert, P.R. and Granville, D.J. (2012) Granzyme B in injury, inflammation, and repair. *Trends Mol Med*
183. Kurschus, F.C., Kleinschmidt, M., Fellows, E., Dornmair, K., Rudolph, R., Lilie, H., and Jenne, D.E. (2004) Killing of target cells by redirected granzyme B in the absence of perforin. In *FEBS Lett*, pp. 87-92
184. Tremblay, G.M., Wolbink, A.M., Cormier, Y., and Hack, C.E. (2000) Granzyme activity in the inflamed lung is not controlled by endogenous serine proteinase inhibitors. *J Immunol* 165, 3966-3969
185. Prakash, M.D., Bird, C.H., and Bird, P.I. (2009) Active and zymogen forms of granzyme B are constitutively released from cytotoxic lymphocytes in the absence of target cell engagement. In *Immunol Cell Biol*, pp. 249-254
186. McElhaney, J.E., Zhou, X., Talbot, H.K., Soethout, E., Bleackley, R.C., Granville, D.J., and Pawelec, G. (2012) The unmet need in the elderly: How immunosenescence, CMV infection, co-morbidities and frailty are a challenge for the development of more effective influenza vaccines. *Vaccine* 30, 2060-2067
187. Junqueira, L.C., Bignolas, G., and Brentani, R.R. (1979) Picrosirius staining plus polarization microscopy, a specific method for collagen detection in tissue sections. *Histochem J* 11, 447-455
188. Kligman, L.H. (1981) Luna's technique. A beautiful stain for elastin. *Am J Dermatopathol* 3, 199-201
189. Abraham, T., Carthy, J., and McManus, B. (2009) Imaging of collagen matrix remodeling in three-dimensional space using second harmonic generation and two photon excitation fluorescence. *Proc. SPIE* 7183, 71831Z
190. Willoughby, C.A., Bull, H.G., Garcia-Calvo, M., Jiang, J., Chapman, K.T., and Thornberry, N.A. (2002) Discovery of potent, selective human granzyme B inhibitors that inhibit CTL mediated apoptosis. *Bioorg Med Chem Lett* 12, 2197-2200

191. Chang, S., Multani, A.S., Cabrera, N.G., Naylor, M.L., Laud, P., Lombard, D., Pathak, S., Guarente, L., and DePinho, R.A. (2004) Essential role of limiting telomeres in the pathogenesis of Werner syndrome. *Nat Genet* 36, 877-882
192. Kuro-o, M., Matsumura, Y., Aizawa, H., Kawaguchi, H., Suga, T., Utsugi, T., Ohyama, Y., Kurabayashi, M., Kaname, T., Kume, E., Iwasaki, H., Iida, A., Shiraki-Iida, T., Nishikawa, S., Nagai, R., and Nabeshima, Y.I. (1997) Mutation of the mouse *klotho* gene leads to a syndrome resembling ageing. *Nature* 390, 45-51
193. Bhattacharyya, T.K. and Thomas, J.R. (2004) Histomorphologic changes in aging skin: observations in the CBA mouse model. *Arch Facial Plast Surg* 6, 21-25
194. Baumann, L. (2007) Skin ageing and its treatment. *J Pathol* 211, 241-251
195. Lovell, C.R., Smolenski, K.A., Duance, V.C., Light, N.D., Young, S., and Dyson, M. (1987) Type I and III collagen content and fibre distribution in normal human skin during ageing. *Br J Dermatol* 117, 419-428
196. Uitto, J. (2008) The role of elastin and collagen in cutaneous aging: intrinsic aging versus photoexposure. *J Drugs Dermatol* 7, s12-16
197. Zipfel, W.R., Williams, R.M., Christie, R., Nikitin, A.Y., Hyman, B.T., and Webb, W.W. (2003) Live tissue intrinsic emission microscopy using multiphoton-excited native fluorescence and second harmonic generation. *Proc Natl Acad Sci U S A* 100, 7075-7080
198. Palero, J.A., de Bruijn, H.S., van der Ploeg van den Heuvel, A., Sterenborg, H.J., and Gerritsen, H.C. (2007) Spectrally resolved multiphoton imaging of in vivo and excised mouse skin tissues. *Biophys J* 93, 992-1007
199. Kligman, L.H. (1996) The hairless mouse model for photoaging. *Clin Dermatol* 14, 183-195
200. Miyata, M. and Smith, J.D. (1996) Apolipoprotein E allele-specific antioxidant activity and effects on cytotoxicity by oxidative insults and beta-amyloid peptides. *Nat Genet* 14, 55-61
201. Zechner, R., Moser, R., Newman, T.C., Fried, S.K., and Breslow, J.L. (1991) Apolipoprotein E gene expression in mouse 3T3-L1 adipocytes and human adipose tissue and its regulation by differentiation and lipid content. *J Biol Chem* 266, 10583-10588
202. Wassef, H., Bernier, L., Davignon, J., and Cohn, J.S. (2004) Synthesis and secretion of apoC-I and apoE during maturation of human SW872 liposarcoma cells. *J Nutr* 134, 2935-2941
203. Kinoshita, M., Kawamura, M., Maeda, T., Fujimaki, Y., Fujita, M., Kojima, K., and Teramoto, T. (2000) Apolipoprotein E accelerates the efflux of cholesterol from macrophages: mechanism of xanthoma formation in apolipoprotein E deficiency. *J Atheroscler Thromb* 6, 22-27

204. Zhang, W.Y., Gaynor, P.M., and Kruth, H.S. (1996) Apolipoprotein E produced by human monocyte-derived macrophages mediates cholesterol efflux that occurs in the absence of added cholesterol acceptors. *J Biol Chem* 271, 28641-28646
205. Kruth, H.S., Skarlatos, S.I., Gaynor, P.M., and Gamble, W. (1994) Production of cholesterol-enriched nascent high density lipoproteins by human monocyte-derived macrophages is a mechanism that contributes to macrophage cholesterol efflux. *J Biol Chem* 269, 24511-24518
206. Trapani, J.A. and Sutton, V.R. (2003) Granzyme B: pro-apoptotic, antiviral and antitumor functions. *Curr Opin Immunol* 15, 533-543
207. Granville, D.J. (2010) Granzymes in disease: bench to bedside. *Cell Death Differ* 17, 565-566
208. Hendel, A., Hiebert, P.R., Boivin, W.A., Williams, S.J., and Granville, D.J. (2010) Granzymes in age-related cardiovascular and pulmonary diseases. *Cell Death Differ* 17, 596-606
209. Fleischmajer, R., Fisher, L.W., MacDonald, E.D., Jacobs, L., Jr., Perlish, J.S., and Termine, J.D. (1991) Decorin interacts with fibrillar collagen of embryonic and adult human skin. *J Struct Biol* 106, 82-90
210. Berthou, C., Michel, L., Soulie, A., Jean-Louis, F., Flageul, B., Dubertret, L., Sigaux, F., Zhang, Y., and Sasportes, M. (1997) Acquisition of granzyme B and Fas ligand proteins by human keratinocytes contributes to epidermal cell defense. *J Immunol* 159, 5293-5300
211. Zhang, H.L., Wu, J., and Zhu, J. (2010) The immune-modulatory role of apolipoprotein E with emphasis on multiple sclerosis and experimental autoimmune encephalomyelitis. *Clin Dev Immunol* 2010, 186813
212. Wong, V.W., Sorkin, M., Glotzbach, J.P., Longaker, M.T., and Gurtner, G.C. (2011) Surgical approaches to create murine models of human wound healing. *J Biomed Biotechnol* 2011, 969618
213. Cybulsky, M.I. and Gimbrone, M.A., Jr. (1991) Endothelial expression of a mononuclear leukocyte adhesion molecule during atherogenesis. *Science* 251, 788-791
214. Li, H., Cybulsky, M.I., Gimbrone, M.A., Jr., and Libby, P. (1993) An atherogenic diet rapidly induces VCAM-1, a cytokine-regulatable mononuclear leukocyte adhesion molecule, in rabbit aortic endothelium. *Arterioscler Thromb* 13, 197-204
215. Libby, P. (2007) Inflammatory mechanisms: the molecular basis of inflammation and disease. *Nutr Rev* 65, S140-146
216. Kaiserman, D., Bird, C.H., Sun, J., Matthews, A., Ung, K., Whisstock, J.C., Thompson, P.E., Trapani, J.A., and Bird, P.I. (2006) The major human and mouse granzymes are structurally and functionally divergent. *J Cell Biol* 175, 619-630

217. Froelich, C.J., Pardo, J., and Simon, M.M. (2009) Granule-associated serine proteases: granzymes might not just be killer proteases. *Trends Immunol* 30, 117-123
218. Beresford, P.J., Xia, Z., Greenberg, A.H., and Lieberman, J. (1999) Granzyme A loading induces rapid cytolysis and a novel form of DNA damage independently of caspase activation. *Immunity* 10, 585-594
219. Casciola-Rosen, L., Garcia-Calvo, M., Bull, H.G., Becker, J.W., Hines, T., Thornberry, N.A., and Rosen, A. (2007) Mouse and human granzyme B have distinct tetrapeptide specificities and abilities to recruit the bid pathway. *J Biol Chem* 282, 4545-4552
220. Hagn, M., Belz, G.T., Kallies, A., Sutton, V.R., Thia, K.Y., Tarlinton, D.M., Hawkins, E.D., and Trapani, J.A. (2012) Activated mouse B cells lack expression of granzyme B. *J Immunol* 188, 3886-3892
221. Pham, C.T., MacIvor, D.M., Hug, B.A., Heusel, J.W., and Ley, T.J. (1996) Long-range disruption of gene expression by a selectable marker cassette. *Proc Natl Acad Sci U S A* 93, 13090-13095